

Fundamentals aspects of crosslinking control of PDMS rubber at high temperatures using TEMPO nitroxide

Skander Mani

▶ **To cite this version:**

Skander Mani. Fundamentals aspects of crosslinking control of PDMS rubber at high temperatures using TEMPO nitroxide. Other. Université Claude Bernard - Lyon I; Université Laval (Québec, Canada). Faculté des sciences et de génie, 2011. English. NNT : 2011LYO10002 . tel-00839605

HAL Id: tel-00839605

https://theses.hal.science/tel-00839605

Submitted on 28 Jun 2013

HAL is a multi-disciplinary open access archive for the deposit and dissemination of scientific research documents, whether they are published or not. The documents may come from teaching and research institutions in France or abroad, or from public or private research centers.

L'archive ouverte pluridisciplinaire **HAL**, est destinée au dépôt et à la diffusion de documents scientifiques de niveau recherche, publiés ou non, émanant des établissements d'enseignement et de recherche français ou étrangers, des laboratoires publics ou privés.

SKANDER MANI

FUNDAMENTALS ASPECTS OF CROSSLINKING CONTROL OF PDMS RUBBER AT HIGH TEMPERATURES USING TEMPO NITROXIDE

Thèse de doctorat en cotutelle présentée
à la Faculté des études supérieures de l'Université Laval, Québec
dans le cadre du programme de doctorat en Génie Chimique
pour l'obtention du grade de Philosophiae Doctor (Ph.D)

DEPARTEMENT DE GÉNIE CHIMIQUE
FACULTÉ DES SCIENCES ET DE GÉNIE
UNIVERSITÉ LAVAL
QUÉBEC

et

UNIVERSITÉ CLAUDE BERNARD LYON 1
LYON, FRANCE
pour l'obtention du grade de Docteur

04 JANVIER 2011

© Skander Mani, 2011

Résumé

Cette thèse présente une contribution originale à la compréhension et la maîtrise des mécanismes physico-chimiques qui contrôlent l'élaboration d'un nouveau matériau polymère biphasique de type Super-TPV (thermoplastique vulcanisé) contenant une phase réticulée par le procédé d'extrusion réactive. La phase caoutchoutique est constituée d'un Vinyl-Polydiméthylsiloxane (vinyl-PDMS) de haute masse molaire (gomme silicone) qui est réticiluée dynamiquement avec une matrice thermoplastique PA12 lors du procédé de mise en œuvre à l'état fondu (T≈200℃). Le premier des quatre chapitres de ce mémoi re est consacré à une étude bibliographique des différents aspects fondamentaux de la réticulation radicalaire des silicones. Dans le chapitre 2, nous avons étudié le processus de réticulation radicalaire du PDMS en fonction de la température (T>160℃). Le peroxyde de dicumyle (DCP) a été utilisé comme amorceur de la réaction. L'effet de la température et de la concentration en DCP sur la cinétique de réticulation et les propriétés viscoélastiques finales du matériau ont été étudiées. Pour tenter de contrôler cette réaction de réticulation à ces températures élevées, le tétraméthylpipéridyloxyde (TEMPO) a été utilisé. Nous avons ainsi montré que le temps à la transition sol-gel viscoélastique augmente en fonction de la concentration de l'inhibiteur. La variation du rapport molaire DCP/TEMPO a permis de définir un rapport molaire optimal et ainsi de contrôler le temps d'inhibition et la densité de réticulation finale. Des études en RMN, DSC et TGA-MS ont montré que le mécanisme à l'origine de ce temps d'inhibition est le greffage des radicaux nitroxyles sur la chaine polymère silicone. Dans le chapitre 3, un modèle original a été développé avec succès pour décrire la rhéocinétique de la réticulation radicalaire contrôlée du PDMS. Cette modélisation est basée sur le couplage de la cinétique des macro-radicaux PDMS recombinés [$R_{cc}(t)$] et la variation des modules complexes de cisaillement (G'(t) et de G''(t)). Notre modèle rhéocinétique tient compte de la décomposition de l'initiateur (DCP) et des macro-radicaux PDMS piégés en présence d'un inhibiteur tel que le TEMPO. Finalement, dans le chapitre 4 ces études fondamentales ont été développées à l'élaboration d'un TPV basé sur la réticulation radicalire de la gomme silicone dans une matrice PA12. Nous avons alors montré que l'addition du TEMPO permet d'élaborer par un procédé dynamique un nouveau Super-TPV ayant une structure et une morphologie contrôlée.

Abstract

The control of macromolecular structure has recently become an important topic of polymer science from both an academic and an industrial point of view. Indeed, free-radical crosslinking of Polydimethyl-vinylmethyl-siloxane (vinyl-PDMS) rubber by organic peroxide suffers from premature crosslinking at high temperatures, which is called scorching. Consequently, the basic aim of the investigations described in this thesis is to widen and explore the network topology–crosslinking kinetics relationships and find a novel way to control free-radical crosslinking chemistry and topological parameters of final PDMS networks. The work is primarily focused on the extensive study of the crosslinking control of PDMS rubber at high temperatures. A novel composition using 2,2,6,6-tetramethylpiperidinyloxyl (TEMPO) and dicumyl peroxide (DCP) for scorch delay and control of the final network topology of the PDMS has been proposed. The work specified in this thesis is therefore directed to find a proper [TEMPO]/[DCP] ratio provided the development of a new biphasic material such as PA12/PDMS blend type TPV (Thermoplastic Vulcanizated). For this purpose a new method based on the relationship between the kinetics of the macro-radicals coupling [Rcc(t)] was derived from a fundamental kinetic model and the viscoelastic changes of the complex shear modulus (G'(t)ω and G"(t)ω). The kinetic model takes into account the initiator (DCP) decomposition and the trapped PDMS macro-radicals in the presence of a radical scavenger such as TEMPO. As a main result, the rheological modelling shows that this new method accurately predicts the time variation of complex shear modulus at any temperature and [TEMPO]/[DCP] ratio. Interestingly, addition of TEMPO to the TPV novel composition provided the PA12/PDMS blend compatibilization in the dynamic process and gives a new material having a controlled structure and morphology. A better insight in understanding the blend composition and the morphology development relationships is aimed at.

Remerciements

Je tiens à exprimer ma profonde gratitude à mon directeur de thèse en France, Prof. Philippe Cassagnau et mon co-directeur Prof. Philippe Chaumont, qui m'ont enseigné les bases de cette science, pour leur hospitalité particulière, et pour l'opportunité qu'ils m'ont donnée pour approfondir mes connaissances dans le monde fascinant des matériaux polymères. Également, de la façon gentille, généreuse et bien française avec laquelle ils m'ont soutenu pendant les périodes très difficiles au cours de cette thèse. J'ai trouvé en eux la France, sa civilisation et son humanisme, que j'ai appris sur les bancs des écoles françaises. Les nombreuses discussions que nous avons eues ont été, et seront toujours pour moi une source inépuisable d'inspiration. Je tiens à leur témoigner de ma profonde reconnaissance pour m'avoir inculqué la rigueur scientifique, le goût du travail minutieux, l'esprit critique de même que toutes les valeurs qui sont de mise dans l'exercice de ce noble métier qu'est la recherche scientifique.

Je tiens à remercier mon directeur de thèse au Canada, Prof. Mosto Bousmina, de m'avoir accepté au sein de son groupe et de m'avoir offert non seulement son soutien moral et financier, mais surtout sa confiance qui ne s'est jamais démentie.

Je tiens à exprimer mes remerciements aux membres du jury, qui ont accepté d'évaluer mon travail de thèse. Merci au Prof. René Muller de l'école Européenne de Chimie Polymères et Matériaux (ECPM) et le Prof. Jean Jacques Robin de l'institut Charles

Gerhardt de Montpellier, d'avoir accepté d'être les rapporteurs de ce manuscrit. Merci également au Prof. Serge Kaliaguine du département génie chimique et le Prof. Freddy Kleitz du département de chimie de l'université Laval, pour avoir accepté d'examiner mon mémoire et de faire partie de mon jury de thèse.

Mes remerciements vont également aux personnes ayant participé de près ou de loin à l'accomplissement de ce travail, en particulier à Mme. Agnès Crepet et M. flavien Mélis deux ingénieurs de recherche à l'IMP@LYON1, aussi Mme Marlaine Rousseau et à M. Steve Pouliot qui sont tous deux professionnels de recherche dans le groupe du Prof. Mosto Bousmina.

Je souhaite également exprimer ma plus vive reconnaissance à l'égard de mes très chers parents Habiba et Slah, de ma femme Hikmet, de mes deux frères Nizar et Elies pour leur soutien et leurs encouragements sans lesquels il m'aurait été très difficile de mener à terme mes projets.

Je tiens enfin à remercier les amis, thésards ou non, en France et au Canada, qui m'ont aidé au cours des trois ans de cette Cotutelle de thèse.

Skander MANI

To my wife, Hikmet,
whose support and perseverance
is greatly appreciated;
to my mother Habiba and my father Slah
who installed into me the importance
of education at an early age
to my brothers Nizar and Elies,
and my childhood friend Wissem Chemsi
for their encouragement,

To my son Amine…

……(Then a ploughman said, ***"Speak to us of Work."***

“Work is love made visible. And if you cannot work with love but only with distaste, it is better that you should leave your work and sit at the gate of the temple and take alms of those who work with joy. ”

And a man said, ***"Speak to us of Self-Knowledge."***

Say not, "I have found the truth," but rather, "I have found a truth." Say not, "I have found the path of the soul." Say rather, "I have met the soul walking upon my path." For the soul walks upon all paths. The soul walks not upon a line, neither does it grow like a reed. The soul unfolds itself, like a lotus of countless petals.

Then said a teacher, ***"Speak to us of Teaching."***

*And he said: "No man can reveal to you aught but that which already lies half asleep in the dawning of your knowledge. The teacher who walks in the shadow of the temple, among his followers, gives not of his wisdom but rather of his faith and his lovingness. If he is indeed wise he does not bid you enter the house of his wisdom, but rather leads you to the threshold of your own mind. The astronomer may speak to you of his under standing of space, but he cannot give you his under standing. The musician may sing to you of the rhythm which is in all space, but he cannot give you the ear which arrests the rhythm, nor the voice that echoes it. And he who is versed in the science of numbers can tell of the regions of weight and measure, but he cannot conduct you thither. "****)***

Gibran Khalil Gibran (1883-1931), “The prophet”, 1923 United States.

Table of Contents

Introduction		**9**
Chapter 1	Free Radical Crosslinking Control: The State of the Art	**10**
Chapter 2	Crosslinking Control of PDMS Rubber at High Temperatures Using TEMPO Nitroxide	**32**
Chapter 3	Rheological Modelling of the Free-Radical Crosslinking of PDMS Rubber in the Presence of TEMPO Nitroxide	**60**
Chapter 4	Morphology Development in Novel Composition of Thermoplastic Vulcanizates Based on PA12/PDMS Reactive Blends	**92**
Summary		**122**

Introduction

1.1 The research programme

The investigations of this thesis have been carried out in the framework of “co-tutelle of thesis” between the Claude Bernard Lyon 1 University (FRANCE) and the Laval University (CANADA).

1.2 Aim of the project

In the case of free-radical crosslinking of rubbers and/or thermoplastics by organic peroxide, scorching at high temperatures still a problem of major concern. This is the main reason, which limits the applicability of peroxides-crosslinking, in spite of all their potential benefits.

Therefore, the basic aim of the investigations described in this thesis is to find a novel way to control free-radical crosslinking chemistry and topological parameters of final networks such as the length of the network strands, functionality of cross-links, the amounts of entanglements and dangling chains. Moreover, the PDMS will be crosslinked by Dicumyl peroxide (DCP). The advantage of this free radical crosslinking reaction that it is can be well controlled at the mixing step and at higher temperatures using an appropriate inhibitor. Furthermore, addition of inhibitor to a new biphasic material such as PA12/PDMS blend type TPV (Thermoplastic Vulcanizated) provided the compatibilization in the dynamic process and gives a new material having a controlled structure and morphology.

Chapter 1

Free radical Crosslinking Control:

The state of the art

The present chapter introduces various topics and aspects which are relevant for the work described in this thesis. Free radical crosslinking of polymers and the control at high temperatures of this complex chemical process are reviewed in this chapter. The PDMS rubbers and their typical end-use applications are also touched upon.

1.1 Introduction

Rubbers exhibit large reversible deformabilities with distinctly low elastic modulus which are incomparable in solid materials due to the entropic elasticity. Such unique mechanical properties of rubbers originate from the network structure comprising long and flexible polymer chains obtained by crosslinking reaction [1]. Furthermore, crosslinking is an exothermic and irreversible chemical process, able to convert a viscous entanglement of long-chain molecules of polymer into three-dimensional elastic network [2]. Therefore, the mechanical properties of the networks are drastically depending on the crosslinking mode [3]. One reason for that is the nature of the chemical bonds formed between the chains and the functionality of the crosslinks [4]. The other is attributed to the several topological parameters such as the length of the network strands, the distribution of crosslinks and defects in the amorphous network structure [5].

1.2 PDMS Rubber

The polydimethylsiloxane (PDMS) is the basic silicone polymer with a backbone of silicon-oxygen linkages and two methyl groups on each silicon. PDMS is known as one of the most flexible polymers [6]. The high flexibility of PDMS originates from the structural features of the Si–O bonds; they have a longer bond length, larger bond angle, and significantly lower torsional potential than C–C bonds. This leads to a very low glass transition temperature (-120℃) for PDMS [7].

In addition, the polysiloxane molecules can be tailor-made by the chemist to optimise some properties required by particular applications. Furthermore, the basic polymer properties are modified by replacing minor amounts of the methyl substituents with phenyls and/or vinyls. Phenyl groups improve low temperature flexibility without sacrificing high temperature properties [8]. The incorporation of vinyl groups (less than 1 mol %) as lateral chemical groups in VMQ significantly increases the crosslinking efficiency with organic peroxides resulting in elastomers with low compression set and

improved hot oil resistance as compared to polydimethylsiloxanes (MQ) [9]. The vinyl sites can be placed at predetermined selected positions within the polymer molecules so that the chemical crosslinks of the network can be controlled. This in turn influences the mechanical behaviour in beneficial ways such as allowing tougher products to be made.

Of the available silicone elastomers, methyl silicone (MQ), methyl-vinyl silicone (VMQ), methyl-phenylsilicone (PMQ), methyl-phenyl-vinyl silicone (PVMQ), and fluoro-vinyl-methyl silicone (FVMQ); the methyl-vinyl types are most widely used. Depending on the chemical side groups in polysiloxane, silicone rubbers as classified by ASTM D1418 [10] are shown in Figure 1.

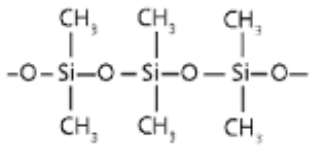
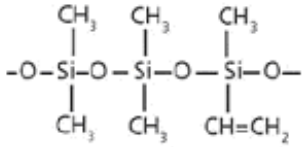
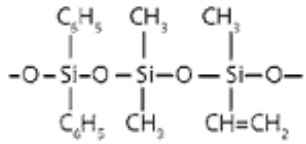
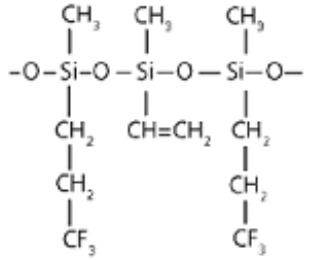
Type	Structure	ASTM D1418 Classification [8]
Dimethyls		MQ
Methyl vinyls		VMQ
Methyl phenyl vinyls		PVMQ
Methyl vinyls fluoroalkyls (Fluorosilicone)		FVMQ

Figure 1. Type and structure of silicones

The use of vinyl groups in PDMS rubber opened the door for new applications requiring improved performance and long-term reliability [11]. These features of PDMS are beneficial for fundamental studies of the free radical crosslinking control.

The unique balance of mechanical and chemical properties of PDMS rubber have already given it a good position in the market place due to its:

- High temperature resistance,
- Low temperature flexibility,
- Excellent electrical and thermal insulation properties,
- Excellent mechanical properties over a wide range of temperature, and
- Excellent bio-compatibility and chemical inertness.

Therefore, they are used for the production of seals in the automotive and aerospace industry, packaging in the food industry and implants and devices for medical purposes [12].

1.3 Characteristics of crosslinking by organic peroxide

The most important characteristics of crosslinking peroxide are its crosslinking efficiency, f, and its decomposition rate, which is generally expressed by half-life time ($t_{1/2}$) at a particular temperature. The crosslinking efficiency of peroxide is defined as the number of moles of chemical crosslinks formed per mole of reacted peroxide. The efficiency of the total crosslinking reaction depends mainly on the type of peroxide and polymer radicals formed during the process. The relationship between peroxide structure and crosslinking efficiency has been described by Endstra [13].

The half-life time is the time required for one half of the molecules of a given amount of peroxide to decompose at a certain temperature. Commonly, the half-life time is determined by differential scanning calorimetry-thermal activity monitoring (DSC-TAM)

of a dilute solution of the peroxide in monochlorobenzene [14]. The dependence of the half-life time on temperature can theoretically be described by an Arrhenius equation [15]:

$$k_d = A_0 \exp(-E_a / RT) \quad (1)$$

$$t_{1/2} = \frac{Ln(2)}{k_d} \quad (2)$$

where, k_d = rate constant for the peroxide decomposition (s^{-1})

A_0 = the collision frequency factor (s^{-1})

E_a = activation energy for the peroxide decomposition ($J.mol^{-1}$)

R = 8.3142, gas constant, ($J.mol^{-1}.K^{-1}$)

T = temperature (K) and

$t_{1/2}$ = half-life time (s)

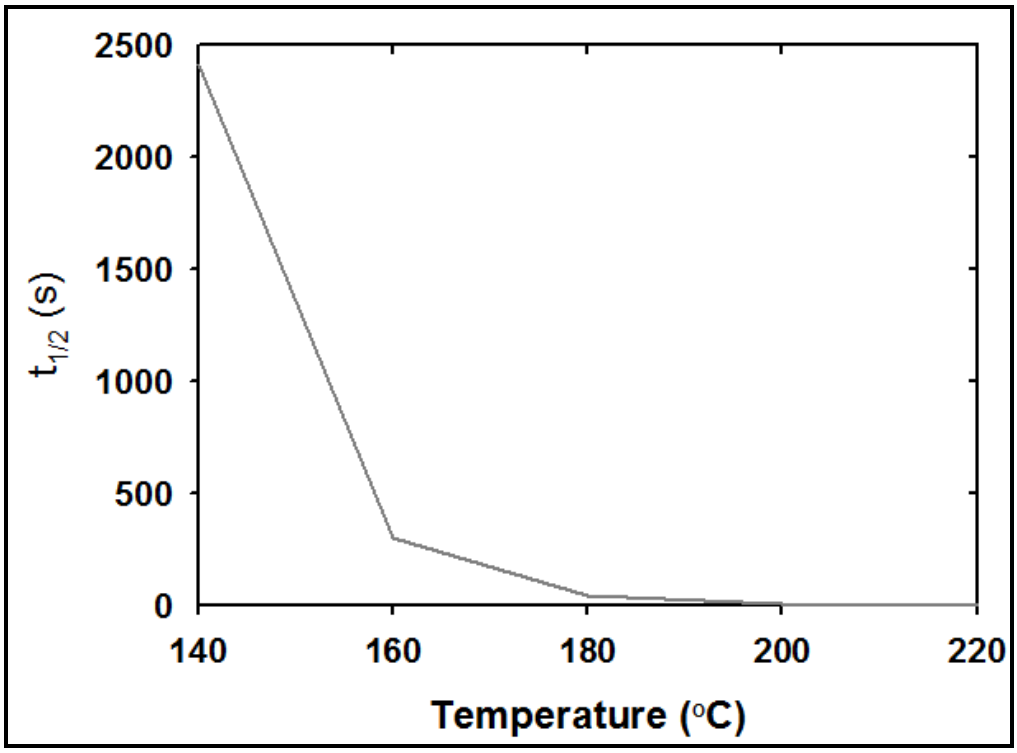


Figure 2. Temperature effect on the half-time $t_{1/2}$

With: A_0 = 7.47 x 10^{15} s^{-1} and E_a = 153.5 kJ.mol^{-1} for the dicumyl peroxide (DCP) [16].

At higher temperatures (T=200℃) the thermal decomp osition of DCP is fast according to high activation energy (Figure 2). Indeed, according to Equation 2, $t_{1/2}$(T=140℃)= 2411s and $t_{1/2}$(T=200℃)= 8s.

1.4 Free radical crosslinking of PDMS

PDMS productions have increased drastically since their discovery in the late 1940s because of their unique properties [17]. Typically PDMS are produced as linear macromolecules, which are later crosslinked to get elastomeric materials. Since the discovery of Wright and Oliver [18] in 1948, the main process to realize such a transformation involves the decomposition of peroxides in linear PDMS. To achieve this process, a number of peroxide types and formulations were developed, which overcame the drawbacks in thermal stability, crosslinking efficiency and handling and safety aspects of the few existing peroxide types [19]. However, the performance and level of each peroxide in a particular compound will depend on its decomposition temperature, level of peroxide used in composition, percentage of active oxygen, half-life and so on [20]. Generally, the higher the active oxygen in the peroxide, the lower the amount required to be added in the compound formulation and vice versa.

The most frequently used peroxides (Figure 3) bis-2,4-dichlorobenzoyl peroxide (ClBP), dicumyl peroxide (DCP) and 2,5-dimethyl-2,5-bis-(tert-butylperoxy)hexane (DBPH) are classified in two families [21] according to their ability to crosslink just vinyl groups (called ‘vinyl’ specific peroxides) or both methyl and vinyl groups (called ‘general purpose’ peroxides) [22]. The dialkyl peroxides, e.g., dicumyl peroxide, fall into the former category, while the diaroyl peroxides such as benzoyl peroxide fall in the latter category [23]. These peroxides generate acidic decomposition products, and a relatively long post-cure treatment is required for thick-sectioned articles.

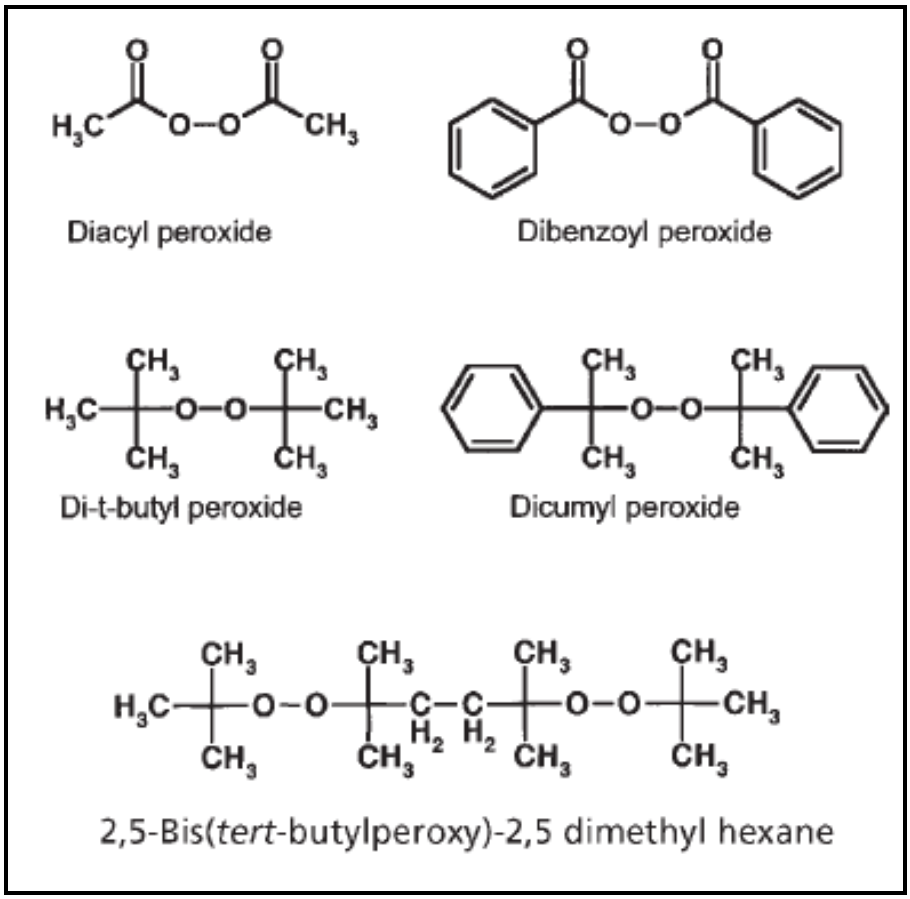


Figure 3. Structures of organic peroxides [24]

The 'vinyl specific' peroxides are not acidic, and as a result, post-cure treatment is relatively short or even not done at all. Thus, for the vinyl specific peroxides, satisfactory cure density is obtained in vinyl containing silicone rubber (150-200℃) [25]. For vinyl containing polymers, the free radical adds to the vinyl group, while in the case of the methyl group, a hydrogen atom is abstracted, leaving the free radical attachment to the silicone [26].

1.5 Mechanism of the PDMS free radical crosslinking

The crosslinking process is based on the fact that the polymeric radicals generated by the peroxide combine to form carbon-carbon bonds [27]. Different mechanisms have

been proposed to explain the 'peroxidic' crosslinking of the PDMS [28]. In particular, Dluzneski [29] attributed the difference of reactivity of these two families cited above, to the inability of alkoxy radicals to abstract a hydrogen from a methyl of the PDMS for thermodynamic reasons. Therefore, the presence of vinyl functional groups in the polymer chain enables the free-radical cross-linking of PDMS by dialkyl peroxides [30].

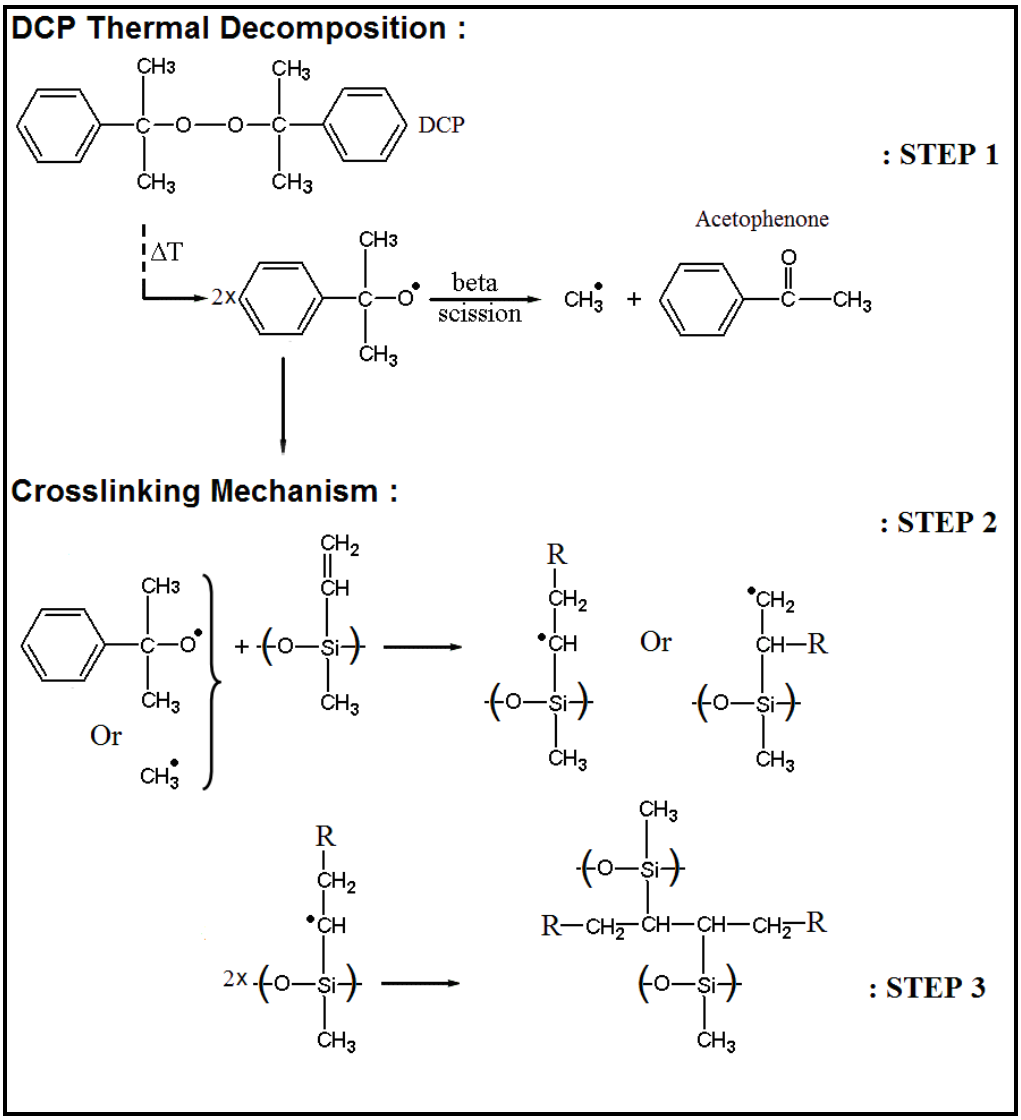


Figure 4. DCP decomposition and free-radical crosslinking mechanism of vinyl-PDMS

In this case, the generated peroxide radicals initiate cross-linking by addition to the double bonds [31].

The different steps of this chemical mechanism are shown in Figure 4. The initiation step in DCP-induced crosslinking is the thermal decomposition of the initiator to give two cumyloxyl free-radicals (step 1). Therefore, next step is the addition of cumyloxyl radicals to a double bond of the polymer molecule (step 2). Two of these polymeric radicals then combine to form a cross-link that is a more stable bond (higher bonding energy 347 kJ.mol^{-1}) with superior heat aging and oxidation resistance (step 3) [32]. Sometimes, undesired side reactions like disproportionation or β-chain scission can also take place during the crosslinking process, also shown in Figure 4.

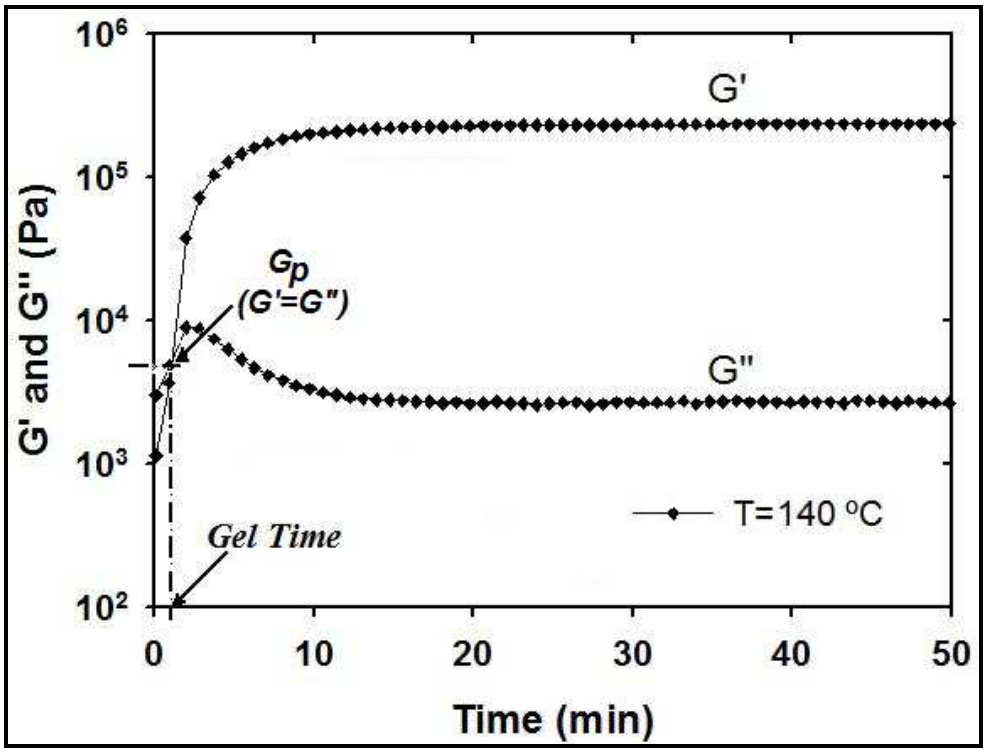


Figure 5. Radical crosslinking of vinyl-PDMS initiated by 36 mol.m^{-3} of DCP. Variation of the storage G' and loss G'' modulus versus reaction time. T=140℃ and ω=1rad. s^{-1} [33]

From a rheological point of view, during the initial stages of the PDMS crosslinking, branched molecules of widely distribution sizes and of various architectures are formed [34]. Their average molecular weight increases with increasing extent of the crosslinking density (ν). The system reaches its gel point (G_P) at a critical extent of reaction at witch either the weight average molecular weight diverges to infinity (infinite sample) or a first macromolecular cluster extends across the entire sample (finite sample size) [35]. Consequently, the system loses its solubility, the steady-shear viscosity diverges to infinity, and the equilibrium modulus starts to rise to finite value. The newly formed macroscopic network structure starts to coexist with the remaining branched molecules which are not yet attached. Beyond G_P, the network stiffness continues to increase steadily with increasing crosslink density until the system reaches completion of the chemical reaction, showed in Figure 5.

1.6 Free radical Crosslinking Control: Fundamentals Aspects

1.6.1 Scorch delay in free radical crosslinking

Typically, free radical crosslinking of rubbers and thermoplastics shows an increase in Young's modulus, the resulting cured materials should have a good compression set and high processing temperature [36]. However, one difficulty in using thermally activated free radical initiators, such as organic peroxides, is scorching [37] during compounding and/or processing prior to the actual phase in the overall process in which curing is desired. Premature crosslinking, which is called, scorching, usually occurs in a mold, autoclave or die head of the extruder in which the compositions containing peroxide is being processed, at elevated temperatures [38]. High temperatures leads to the partial decomposition of peroxide, thus inducing to the imperfections in the form (inhomogeneity) and roughness in the surface of the final product caused by gel particles in the body of the crosslinked product [39]. In addition, excessive scorching may cause enough of pressure build-up in the process device to require a cessation of the processing operation entirely. Thus, control of crosslinking reaction cannot be

overemphasized. To overcome this disadvantage, several solutions have been proposed have been discussed and reviewed in literature [40].

For scorch delay, one widely accepted method for minimizing scorch is to choose a free radical initiator that has a sufficiently high activation temperature so that compounding and/or other processing steps can be successfully completed prior to the final curing step [41]. Typical of this class of initiators are those with a high 10-hour half-life temperature. The disadvantages of this method are longer cure times, and thus lower throughput. Another method of minimizing scorch is to lower the compounding and/or processing temperature to improve the scorch safety margin of the crosslinking agent. This method, however, may have limited scope depending upon the polymer and/or process involved. In addition, here too curing at a lower temperature requires a longer cure time and results in lower throughput. Lower temperatures can also increase the viscosity of the material which in turn can make mixing more difficult, and can increase the risk of running up against the cristallisation point of the polymer [42].

1.6.2 Nitroxides: How They Work

Since 1980 several researchers [43] have introduced a new concept in the field of free radical polymerization which can be called the ''living character''. To achieve such a ''living character'' the classical termination (disproportion or combination) and side reactions such as transfers must be inhibited while, of course, the propagation is still occurring. This concept is based on the thermally labile bond in the *N*-alkoxyamine, formed between the growing polymer chain and the nitroxide (Figure 6). The controlled free radical polymerization as first introduced by Otsu et al. [44] is an established way to prepare polymers with a narrow molecular weight distribution and block copolymer structure.

It is well documented that carbon-centered radicals can be effectively trapped by free radical species such as molecular oxygen [45] or nitric oxide [46], with rate constants

near the diffusion controlled limit, i.e., beyond 10^9 $M^{-1}.s^{-1}$. By way of contrast, the recombination rates with persistent sterically hindered organic nitroxides are significantly slower. The kinetic behavior of carbon-centered radicals ($R^{\bullet}$) with 2,2,6,6-tetramethylpiperidin-1-oxyl (TEMPO) has been studied in quite some detail [47]. The variation in rate constants can be associated with the structure of ($R^{\bullet}$), ranging from 10^9 (1-nonyl) to as low as 10^6 $M^{-1}.s^{-1}$ for sterically hindered species such as triphenylmethyl. The reversible thermal bond homolysis the chain-propagating carbon centered radical is released allowing the addition of the next monomer to the chain. At the same time, the radical concentration is kept low, preventing random termination.

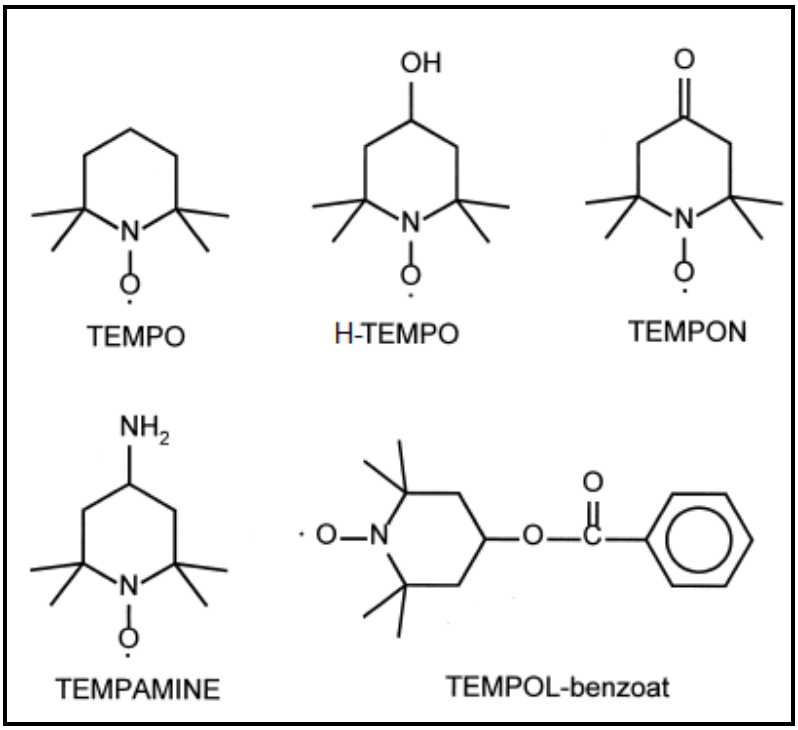


Figure 6. Structural formula of different piperidine Nitroxides [48]

In 1986, Solomon et al. [49] used nitroxides as stable free radicals in order to react reversibly with the growing polymeric chain. Since nitroxides cannot initiate the polymerization an initiator was needed to start the polymerization. Furthermore, the polymers obtained exhibit a narrow polymolecularity: this is due to high rate constants of

the coupling reaction between a nitroxide radical and the corresponding intermediate polymeric radical [50].

The general mechanism of Nitroxyl-mediated free radical polymerization (NMP) is shown in Figure 7. The key to the success is a reversible thermal C-O-bond cleavage of a polymeric alkoxyamine to generate the corresponding polymeric radical and a nitroxide. Monomer insertion with subsequent nitroxide trapping leads to chain-extended polymeric alkoxyamine. The whole process is controlled by the so called Persistent Radical Effect (PRE) [51]. The PRE is a general principle that explains the highly specific formation of the cross-coupling product (R^1-R^2) between two radicals R^1 and R^2 when one species is persistent (in NMP the nitroxide) and the other transient (in NMP the polymeric radical), and the two radicals are formed at equal rates (guaranteed in NMP by thermal C-O-bond homolysis). The initial build up in concentration of the persistent nitroxide, caused by the self termination of the transient polymeric radical, steers the reaction subsequently to follow a single pathway, namely the coupling of the nitroxide with the polymeric radical.

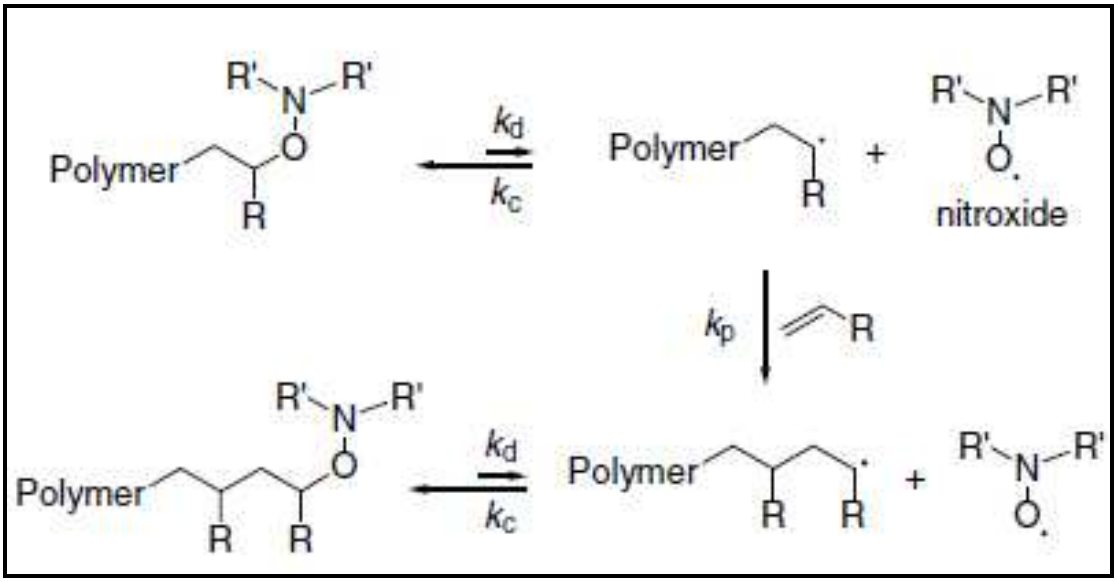


Figure 7. Mechanism of NMP [52]

First, nitroxide mediated polymerizations of styrene were conducted using conventional free radical initiators in the presence of free nitroxide and monomer [53]. The TEMPO

radical was used as the nitroxide component in these initial studies. The alkoxyamine is formed in situ during the polymerization process. Based on the mechanism depicted in Figure 7 it is obvious that the equilibrium constant K between the dormant alkoxyamine and the polymeric radical and nitroxide is a key parameter of the polymerization process. The equilibrium constant *K* is defined as k_d/k_c (k_d = rate constant for alkoxyamine C-O-bond homolysis; k_c = rate constant for trapping of the polymeric radical with the given nitroxide). Various parameters such as steric effects, H-bonding and polar effects influence the K-value [54]. Solomon and al. [55] demonstrate that at the low temperatures typically associated with standard free radical polymerizations (40-60℃); TEMPO reacted at near diffusion controlled rates with carbon-centered free radicals, generated from the addition of initiating radicals to vinyl monomers. The resulting alkoxyamine derivatives were essentially stable at these temperatures, thus acting as radical traps.

In addition, the nitroxide radicals have been used for the inhibition of the peroxidative processes [56]. All radicals taking part in this process may be inactivated by coupling reactions with the nitroxide radicals.

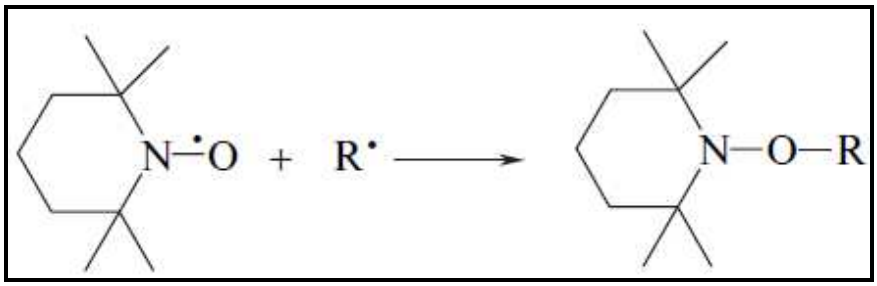


Figure 8. Formation of alkoxyamines

These reactions have very low activation energies therefore their rates are almost diffusion controlled [57]. Nitroxide radicals can deactivate radicals also through this mechanism thereby acting as chain-breaking antioxidants. These compounds, similarly

to phenoxy radicals, are very unreactive towards non-radical molecules, but they react with carbon-centred radicals leading to the formation of alkoxyamines as shown in Figure 8 for TEMPO, one of the most widely studied aliphatic nitroxides.

1.6.3 Nitroxides for free radical crosslinking control

The control of macromolecular structure has recently become an important facet of polymer science from both an academic and an industrial viewpoint. This interest is governed by the realization that control of macromolecular architecture can lead to the development of new polymeric materials with improved and/or new mechanical and physical properties. The control of free radical crosslinking reaction provides the mechanism to fabricate rubbers and/or thermoplastics with a rich variety of topological characteristics.

Recently, Chaudhary et al. [58] showed that the reaction of carbon-centered radicals with nitroxides and its derivatives can be a novel means for scorch delay and cure control in peroxide crosslinking of polyethylene thermoplastic. Moreover, TEMPO derivatives having functional groups (such as hydroxyl) may be used to introduce desired attributes into the polymer. The results show that when the 4-hydroxy TEMPO (h-TEMPO) derivative is used for scorch suppression in peroxide crosslinking of polyethylene, there may be a loss in ultimate degree of crosslinking. However, stable organic free radicals comprising more than one nitroxyl not only suppress scorch, but also enhance the ultimate degree of crosslinking. Furthermore, the addition of 0.25 wt% of bis(1-oxyl-2,2,6,6-tetramethylpiperidine-4-yl)sebacate (bis-TEMPO) resulted in increased scorch at 140℃ and increased cure at 182 ℃, in contrast to the use of h-TEMPO. However, increasing the amount of bis-TEMPO from 0.25 to 1 wt% resulted in decreased rate and degree of crosslinking at both 140 and 182℃. The gel contents of the samples crosslinked at 182℃ were as follows, a nd generally increased with higher ultimate torque: 78 wt% gels without bis-TEMPO; 84 wt% gels with 0.25 wt% bis-TEMPO; 80 wt% gels with 0.5 wt% bis-TEMPO; and 74 wt% gels with 1 wt% bis-

TEMPO. It is hypothesized that one end of bis-TEMPO molecules first trapped polymer radicals (as well as methyl radicals from peroxide decomposition) followed by radical-trapping with the pendant nitroxyls. At low concentrations of bis-TEMPO, the pendant nitroxyls were used efficiently, resulting in increased crosslinking of the polymer. At increased concentrations of bis-TEMPO, the mobility of the polymer-bound nitroxyl was restricted such that radical trapping was increasingly due to the ‘‘free’’ bis-TEMPO, with the pendant nitroxyls being used less efficiently, there by resulting in decreased crosslinking (compared with 0.25 wt% bis-TEMPO). Be that as it may, the use of 1 wt% bis-TEMPO still yielded the desired combination of fast and high degree of crosslinking at 182℃, and increased scorch protection at 140℃ (unlike h-TEMPO). It is possible that the amount of peroxide could be decreased in combination with 1 wt% bis-TEMPO, in order to achieve a fixed degree of crosslinking, which in turn would further enhance scorch protection at 140℃.

In addition, a model study in hexadecane was conducted to understand the mechanism of TEMPO effect on free radical crosslinking of LDPE. Figure 9 showed that the mechanism involves the selectivity of TEMPO for radical termination with carbon-centered radicals formed after peroxide homolysis and propagation steps before peroxide-initiated crosslinking. The build up of radical concentration is controlled through the introduction of the nitroxyls, which are able to trap the early forming radicals from the peroxide, such as methyl radical. Theoretically, alkyl radical concentrations are kept low by the TEMPO and propagation is stopped before crosslinking can occur. Once the TEMPO is consumed, crosslinking proceeds as usual.

Likewise, Robert [59] described in his patent a process for grafting a functional monomer, in particular maleic anhydride, onto a thermoplastic polymer in presence of a nitroxide such as TEMPO, the role of which is to avoid crosslinking during the grafting operation. Moreover, Debaud et al. [60] relates to scorch prevention and, more specifically, to a composition which comprises a nitroxide and organic peroxide and which can be used to delay scorching prior to crosslinking of ethylene-propylene-diene terpolymer (EPDM rubber).

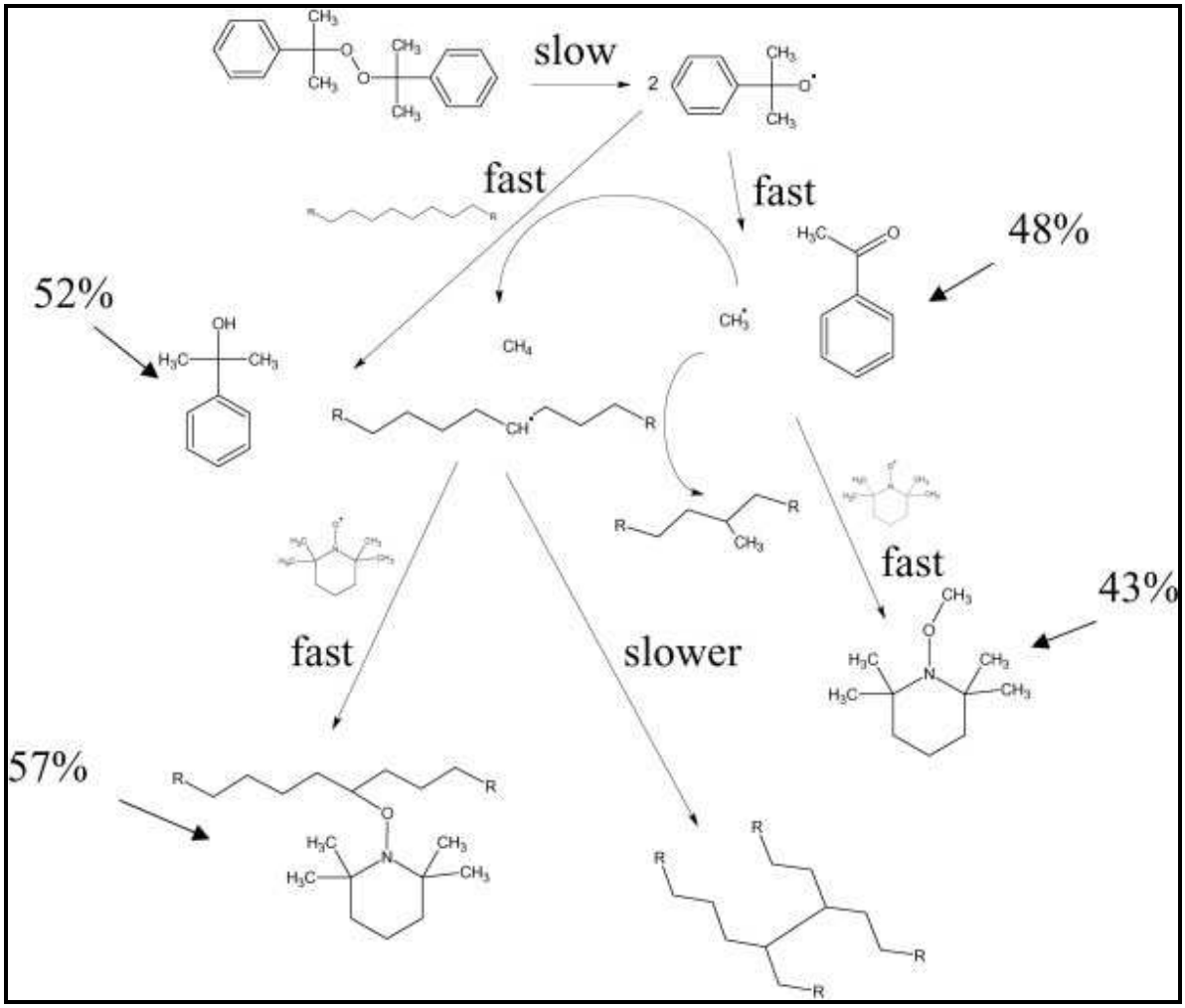


Figure 9. Reactions of TEMPO in the presence of DCP and an alkane substrate.

1.6.4 Stability of the Alkoxyamine

The thermal stability of bonds formed between the nitroxyl and carbon-centered radicals has been studied extensively in model systems [61]. The results presented in the Chaudhary et al. [58] studies indicate that primary and secondary alkoxyamines should be robust enough to withstand processing and testing conditions at elevated temperatures for many hours to several days or longer, such that the integrity of grafts to primary and secondary polymeryl carbons will be maintained. In contrast, grafts to

tertiary carbons are predicted to be unstable with respect to alkene elimination and this reaction will occur relatively rapidly under testing/processing conditions. Thus, the fraction of grafts that occur to tertiary positions will be important in determining the thermal stability of the alkoxyamine. The primary/secondary/tertiary selectivity will be strongly dependent on the relative abundance of each type of C-H bond (statistics) as well as the choice of peroxide used. For polymers with low branching, stable TEMPO grafts should still be possible. Since tertiary C-H bonds are the weakest, increasing ‘‘selectivity’’ will enhance the fraction of tertiary-centered grafts. Using an unselective peroxide (e.g., a fast-acting one that acts mostly through oxy radicals) and polymers, which are statistically biased toward primary and secondary hydrogen abstraction, may be beneficial.

1.7 Summary and considerations for our research plan

This survey of the available literature reveals that free-radical crosslinking of rubbers and/or thermoplastics by organic peroxide suffer from premature crosslinking at high temperatures. High temperatures lead to the faster decomposition of peroxide. Indeed, several solutions have been discussed in literature to prevent scorching. Nevertheless, the control of free-radical crosslinking of the PDMS rubber materials has never been resolved. Consequently, the molecular understanding of the network topology–crosslinking kinetics relationships still remains incompletely understood. This is primarily because conventional rubbers formed by random cross-linking methods have very obscure structure with a broad network strand length distribution and an unknown number of dangling chains [62]. The ultimate objective of this part is to find a novel way to control free-radical crosslinking chemistry and topological parameters of final networks such as the length of the network strands, functionality of cross-links, the amounts of entanglements and dangling chains. Moreover, the PDMS will be crosslinked by Dicumyl peroxide (DCP). The advantage of this free radical crosslinking reaction that it is can be well controlled at the mixing step and at higher temperatures using an appropriate inhibitor. Furthermore, addition of inhibitor to a new biphasic

material such as PA12/PDMS blend type TPV (Thermoplastic Vulcanizated) provided the compatibilization in the dynamic process and gives a new material having a controlled structure and morphology.

While TEMPO has been extensively studied as an initiator for living free radical polymerizations, the use of TEMPO to control free radical crosslinking and that control of macromolecular architecture to the development of new biphasic polymeric materials with improved and/or new mechanical and physical properties has never been studied. Based on these conclusions, the original research described in this thesis will basically focus on:

1- Exploring the potentiality of TEMPO nitroxide in cross-Linking control of PDMS rubber at high temperatures (Chapter II)

2- An experimental and modelling study of rheological behaviour of the free-radical crosslinking of PDMS rubber in the presence of TEMPO nitroxide (Chapter III)

3- To observe the effects of novel composition like DCP/TEMPO, Lotader and Silica nanoparticles to influence the crosslinking, compatibilization and morphology development of new TPV based on PA12/PDMS reactive blends (Chapter IV)

References

[1] Mark, J. E.; Erman. B. ‘Rubberlike elasticity: a molecular primer’ 2nd ed. Cambridge University Press, 2007.

[2] Ignatz-Hoover, F.; To, B. H. ‘Rubber Compounding’ Brendan Rodgers, New York, 2004.

[3] Akiba, M.; Hashim, A. S. Prog. Polym. Sci. 1997, 22, 421-75.

[4] Grobler, J. H. A.; McGill, W. J. J. Polym. Sci. B 1994, 32, 287-95.

[5] Mark, H. F. Rubber Chem. Technol. 1988, 61-73.

[6] Stepto, R. F. T; Clarson, S. J; Semlyen, J. A. editors. ‘Siloxane polymers’, New Jersey: Prentice Hall, 1993, p. 373-414.

[7] Datta, S. ‘Rubber Compounding’ Chap. 3, Brendan Rodgers: New York, 2004.

[8] Polmanteer, K. E.; Hunter, M. J. J. Appl. Polym. Sci. 1959,1, 1-3.

[9] Ciullo, P. A.; Hewitt, N. ‘The Rubber Formulary’ Noyes Publication: New York, 1999.

[10] ASTM D1418, ‘Standard Practice for Rubber and Rubber Latices-Nomenclature’, 2006.

[11] Lucas, P.; Robin, J. J. Adv. Polym. Sci. 2007, 209, 111-147.

[12] Lynch, W.; ‘Handbook of Silicone Rubber Fabrication’, Van Nostrand Reinhold Company, New York, 1978.

[13] Endstra, W. C. Proceedings of SRC Conference on "Organic peroxides for Crosslinking applications", Copenhagen, Denmark, 1985.

[14] Akzo Nobel Company: “Crosslinking Peroxides and Co-agents”: A/06-91.

[15] Msakni, A.; Chaumont, P.; Cassagnau, P. Rheol. Acta. 2007, 46, 933-943.

[16] Flat, J. J. Private communication. Internal report from Arkema Company, 2004.

[17] Rhône-Poulenc Département Silicones In Les silicones, Production et Application, Techno-Nathan, 1988.

[18] Wright, J. G. E.; Oliver, S. G. US Patent 2.448.565, 1948.

[19] Keller, R. C. Rubber Chemistry and Technology, 1988, 61, 2, 238.

[20] Endstra, W. C.; Wreesmann, C. T. J. In Elastomer Technology Handbook, Eds., N. P. Cheremisinoff and P. N. Cheremisnoff, CRC Press, NJ, USA, 1993, Chap. 12.

[21] Caprino, J. C.; Macander R. F. In Rubber Technology, 3rd ed., Reinhold: New York, 1987, p. 375.

[22] Nijhof, L.; Cubera, M. In Rubber Chem. Technol. 2001, 74, 181.

[23] Thomas, D. R. Siloxane polymers. In: Clarson S. J; Semlyen J. A, editors, New Jersey: Prentice Hall, 1993, p. 567.

[24] Datta, R. N.; Ingham, F. A. A. Rubber Technologist's Handbook, Rapra Technology, 2001, Chap. 6.

[25] Sarkar, A. Rubber Technologist's Handbook volume 2, Rapra Technology, 2009, Chap. 11.

[26] Dunham, M. L.; Bailey, D. L.; Mixer, R. Y. Ind Eng. Chem. 1957, 49, 1373.

[27] Baquey, G.; Moine, L.; Degueil-Castaing, M.; Lartigue, J. C.; Maillard, B. Macromolecules 2005, 38(23), 9571-9583.

[28] Brooke, M. R. In: Silicon in organic, organometallic and polymer chemistry. New York: Wiley, 2000, p.282.

[29] Dluzneski, P. R. Rubber Chem Technol 2001, 74, 451.

[30] Baquey, G; Moine, L.; Babot, O.; Degueil, M.; Maillard, B. Polymer 2005, 46, 6283-6292.

[31] Lopez, L. M.; Cosgrove, A. B.; Hernandez-Ortiz, J. P.; Osswald, T. A. Polym. Eng. Sci. 2007, 47, 675–683.

[32] Vollhardt, K.; Schore, N. E. Traite de chimie organique, 4th ed., De Boeck Université, 2004.

[33] Mani, S.; Cassagnau, P.; Bousmina, M.; Chaumont, P. Macromolecules 2009, 42, 8460-8467.

[34] Tanaka, F.; Edwards, S. F. Macromolecules 1992, 25, 1516-1523.

[35] Chambon, F.; Winter, H. H. Journal of Rheology 1987, 31(8), 683-697.

[36] Heiner, J.; Stenberg, B.; Persson,M. Polym Test. 2003, 22, 253–257.

[37] Dorn, M. Adv. Polym. Technol. 1985, 5, 87–91.

[38] Alvarez-Grima, M. M.; Talma, A. G.; Datta, R. N.; Noordermeer, J. W. M. PCT/EP WO2006;100214; A1, 2006.

[39] Gulmine, J. V.; Akcelrud, L. J. Appl. Polym. Sci. 2004, 94, 222–230.

[40] Ghosh,P.;Katare,S.;Patkar,P.;Caritjers, J.M.;Venkatasubramanian V.;Walker, K. A. Rubber Chem. Technol. 2003, 76, 592.

[41] Schober, D. L. U. S. Patent 4,015,058, 1977.

[42] Esseghir, M. M.; Chaudhary, B. I.; Cogen, J. M.; Klier, J.; Jow, J.; Eaton, R. F.; Guerra, S. M. U. S. Patent 7,465,769, B2, 2008.
[43] Bledzki, A.; Braun, K. Makromol Chem. 1983, 184, 745.
[44] Otsu, T.; Yoshida, M. Makromol Chem. Rapid Commun 1982, 3, 127-133.
[45] Neta, P.; Grodkowski, J.; Ross, A. B. J. Phys. Chem. Ref. Data 1996, 25, 709-1050.
[46] Mallard, W. G.; Westley, F.; Herron, J. T.; Hampson, R. F.; Frizzell, D. H. NIST Chemical Kinetics Database, version 2Q98; NIST Standard Reference Data; Gaithersburg, MD, 1998.
[47] Beckwith, A. L. J.; Bowry, V. W.; Ingold, K. U. J. Am. Chem. Soc. 1992, 114, 4983-4992.
[48] Kroll, C.; Langner, A.; and Borchert, H. H. Free Radical Biology & Medicine 1999, 26, 850-857.
[49] Solomon, D.; Rizzardo, E.; Cacioli, P. U.S. Patent 4,581,429, 1986.
[50] Moad, G.; Solomon, D.; Rizzardo, E. Polym. Bull. 1992, 29, 647.
[51] Fischer, H. J. Polym. Sci. Part A: Polym. Chem. 1999, 37, 1885.
[52] Studer, A.; Schulte, T. The Chemical Record 2005, 5, 27-35.
[53] Georges, M. K.; Veregin, R. P. N.; Kazmaier, P. M.; Hamer, G. K. Macromolecules 1993, 26, 2987.
[54] Marque, S. J. Org. Chem. 2003, 68, 7582.
[55] Moad, G.; Rizzardo, E.; Solomon, D. H. Macromolecules 1982, 15, 909-914.
[56] Chateauneuf, J.; Lusztyk, J.; Ingold, K. U. J. Org. Chem. 1988, 53(8), 1629-1632.
[57] Ingold, K. U. “Rate constants for free radical reactions in solution.” In Free Radicals, J. K. Kochi, New York, Interscience, 1973, p. 37-112.
[58] Chaudhary, B. I.; Chopin, L.; Klier, J. J. Polym. Sci. 2007, 47, 50-61.
[59] Robert, P. M. EP 0,837,080, A1; 1997.
[60] Debaud, F.; Kervennal, J.; Defrancisci, A.; Guerret, O. U.S. Patent 0051496A1, 2008.
[61] Ciriano, M. V.; Korth, H. G.; Van Scheppingen, W. B.; Mulder, P. J. Am. Chem. Soc., 1999, 121, 6375.
[62] Gottlieb, M.; Macosko, C. W.; Benjamin, G. S.; Meyers, K. O.; Merrill, E. W. Macromolecules 1981, 14, 1039-1046.

Chapter 2

Crosslinking Control of PDMS Rubber at High Temperatures Using TEMPO Nitroxide

ABSTRACT:

A novel composition using 2,2,6,6-tetramethylpiperidinyloxyl (TEMPO) and dicumyl peroxide (DCP) for scorch delay and control of the final network topology of polydimethylvinylmethylsiloxane (vinyl-PDMS) at high temperatures has been proposed. The evolution of linear viscoelasticity during crosslinking reaction was carried out on parallel plate geometry rheometer. The rubber was cross-linked with different ratios of [TEMPO]/[DCP] in order to control scorch time, which is defined as the time during which the PDMS rubber can be worked at a given temperature before cross-linking begins (i.e., the time at which the complex shear modulus suddenly increases). We showed that scorch delay increases according to the amount of TEMPO acting as an inhibitor. Nuclear magnetic resonance spectroscopy (^{1}H NMR) has been used to investigate the effect of TEMPO. This study reveals that the delayed action is the result of a TEMPO-grafted polymer action formed by reaction between TEMPO and polymer radicals. Furthermore, polymeric radicals are rapidly trapped by a grafting reaction

before they are able to form cross-links. The cross-linking density (ν) and the number of junctions (μ) have been obtained from the phenomenological network model of Langley and Dossin and Graessley. In addition, a differential scanning calorimeter (DSC) was used to characterize the cross-linking reaction. Specific heat data show two exothermic reactions. These reactions may be associated on one hand to the decomposition of DCP and TEMPO grafting in vinyl-PDMS and on the other hand to the C-C covalent bonds creation. The DSC results indicate that the variation of scorch time with the [TEMPO]/[DCP] ratio is in reasonable agreement with those obtained from rheological measurements. Finally, an original method based on DSC experiments was derived to estimate the density of chemical junctions in PDMS networks. This method is based on the balance between the enthalpy of created crosslinked bonds and the standard enthalpy for one covalent carbon-carbon bond. Interestingly, predicted numbers of chemical junctions are in close agreement with those calculated using viscoelastic data.

This chapter 2 was published in ***Macromolecules 2009, 42, 8460-8467***

1. Introduction

PDMS rubbers or silicone products maintain its mechanical and electrical properties over a wide range of temperatures [1]. They are used for the production of seals in the automotive and aerospace industry, implants and devices for medical purposes, and packaging in the food industry [2]. PDMS rubbers are made by crosslinking functionalized polydimethylsiloxane. Commonly, a major curing mechanism frequently used for PDMS is the generation of polymer radicals through the use of organic peroxides that subsequently combine to form carbon-carbon bonds [3]. This exothermic and irreversible chemical process converts a viscous entanglement of long-chain molecules of polymer into three-dimensional elastic network [4]. The most frequently used organic peroxides are dialkyl peroxides, such as dicumyl peroxide. Different mechanisms have been proposed to explain the crosslinking of the PDMS by dialkyl peroxides [5]. Dluzneski has proved the inability of alkoxy radicals to abstract hydrogen from a methyl of the PDMS for thermodynamic reasons [6]. Therefore, the presence of vinyl functional groups in the polymer chain enables the free-radical crosslinking of PDMS [7]. In this case, the generated peroxide radicals initiate crosslinking by addition to the double bonds [8]. With this curing mode stable carbon–carbon bonds are formed [9].

Typically, peroxide-cured PDMS rubbers shows an increase in Young's modulus, the resulting cured rubber should have a good compression set and high processing temperature [10]. However, free-radical crosslinking by peroxide suffers from premature cross-linking at high temperatures, which is called scorching [11]. High temperatures leads to the partial decomposition of peroxide, thus inducing to the imperfections in the form (inhomogeneity) and roughness in the surface of the final product caused by gel particles in the body of the cross-linked product [12]. Thus, control of crosslinking reaction cannot be overemphasized. Delayed mechanisms and reactions kinetics have been discussed and reviewed in literature [13]. In his patent, Robert [14] described a process for grafting a functional monomer, in particular maleic anhydride, onto a thermoplastic polymer in presence of a nitroxide such as TEMPO, the role of which is to

avoid crosslinking during the grafting operation. It should be noted that nitroxides are mostly used like stable free radicals in the controlled radical polymerization [15]. Nitroxyl-mediated free radical polymerization (NMP) techniques are valued for their reported ability to prepare polymers with a narrow molecular weight distribution [16] and block copolymer structure [17]. Solomon and al. [18] demonstrate that at the low temperatures typically associated with standard free radical polymerizations (40-60℃) TEMPO reacted at near diffusion-controlled rates with carbon-centered free radicals, generated from the addition of initiating radicals to vinyl monomers. The resulting alkoxyamine derivatives were essentially stable at these temperatures, thus acting as radical traps.

Recently, Chaudhary et al. [19] showed that the reaction of carbon-centered radicals with nitroxides and its derivatives can be a novel means for scorch time and cure control in peroxide cross-linking of polyethylene thermoplastics. Although, several solutions have been proposed in the literature to control scorching and cure process of thermoplastics. In contrast, control of free-radical cross-linking of rubber materials has never been discussed. Consequently, the molecular understanding of the network topology–crosslinking kinetics relationships still remains incompletely understood. This is primarily because conventional elastomers formed by random cross-linking methods have very obscure structure with a broad network strand length distribution and an unknown number of dangling chains [20].

The ultimate objective of this work is to propose a novel way using of nitroxides to control free-radical cross-linking chemistry and topological parameters of final networks such as the length of the network strands, functionality of cross-links, the amounts of entanglements, and dangling chains. A complete investigation about the effect of TEMPO in this free-radical mechanism is described in this paper.

2. Experimental materials and procedures

PDMS. PDMS of high molecular weight (PDMS gum) from ABCR was used. The number-average ($\overline{M}_n = 300,000 g.mol^{-1}$) and weight-average ($\overline{M}_w = 650,000 g.mol^{-1}$) were determined by size exclusion chromatography (SEC). This PDMS contains 0.2% mol of vinyl groups. The molar weight of molecular segment between two consecutive reactive sites, i.e. between two vinyl sites, is therefore $M_0 = 37,000 g.mol^{-1}$.

Free-Radical Crosslinking. Dicumyl peroxide (DCP, $M = 270 g.mol^{-1}$) was used as the free-radical initiator of the crosslinking reaction, and the nitroxide 2,2,6,6-tetramethylpiperidinyloxyl (TEMPO, $M = 156 g.mol^{-1}$) was used as the scorch reactant. Both products were purchased from Aldrich and used without any further purification. All experiments were carried out with an identical concentration in DCP: [DCP]=*36 mol.m*$^{-3}$. The concentration of TEMPO was calculated in order to have the following molar ratios (r=[TEMPO]/[DCP]): r=1.2, 1.6, 1.8, 2 and 2.4.

Rheological Measurements. The rheological experiments were carried out on a rheometrics mechanical spectrometer (RMS800) using a parallel-plate geometry (R=12.5 mm). The parallel plate system was preheated at the temperature of the experiment. Then, the sample was put between the plates once the temperature of regulation was reached. The rheological kinetics of cross-linking were carried out in real time at only one pulsation (ω=1 rad.s^{-1}) and at different temperatures T=140, 160, 180 and 200 °C. At the end of this crosslinking process , a frequency sweep experiment ($10^{-2}<\omega$ (rad s^{-1})$<10^{2}$) was performed on the same sample at the same temperature to determine the equilibrium modulus ($G_e = \lim_{\omega \to 0} G'(\omega)$). In all experiments, sample response linearity with respect to strain amplitude was verified, and nitrogen gas was used to prevent thermal oxidation. In this type of experiment, we assumed that DCP and TEMPO were perfectly dispersed in molten polymer at a molecular scale (homogeneous conditions of reaction).

Network Characterization. The PDMS network was characterized by the soluble fraction (ω_s) only. Tetrahydrofuran (THF) was used as good solvent at room temperature. Specimens taken from the vulcanized sheet were immersed in THF for 72 h at 25 °C. Swollen samples at equilibrium were taken out from the solvent, blotted with filter paper, and weighed immediately. Samples were subsequently dried in a vacuum oven for 24 h at 70 °C and reweighed. The soluble fraction was then be directly measured.

Dynamic Scanning Calorimetry (DSC). Differential scanning calorimeter equipment manufactured by TA Instruments (Q100 system), equipped with Sealed aluminium pans, was used to measure the heat of crosslinking reactions. The mass of the samples ranged from 20 to 23 mg. A sealed empty pan was used as a reference. The total heats of reactions were obtained from isothermal conditions (T=160 °C) or nonisothermal method (Heating rate: $\dot{T} = 2.5°\mathrm{C.min^{-1}}$). All experiments were performed under nitrogen purge.

NMR. As previously explained, samples with different molar ratio [TEMPO]/[DCP]) were prepared at 160 °C in a rheometer oven. First of all, uncrosslinked samples (i.e samples totally soluble) cured up to the scorch time were characterized. The stability of the TEMPO-polymer graft was studied by analysis of the soluble fraction of cross-linked sample obtained at the end of the crosslinking reaction. All these samples were dissolved in Chloroform ($CHCl_3$) for 24 h at 25 °C. ^{1}H NMR study was performed at room temperature. Spectra were obtained with an ALS Bruker 300 MHz spectrometer.

***Thermogravimetry coupled Gas Chromatogrphy/Mass spectroscopy (*TGA-GC/MS)**. TGA coupled with Gas chromatography–mass spectrometry (GC–MS) was performed with an Agilent 6890 series GC system equipped with an HP-5 ms (5% phenyl)methylpolysiloxane, ref 19091S-433. Injection and detection by MS were carried out at 200 °C. The degradation was measured from the TGA results.

3. Results and discussion

3.1. Rheology

Cross-linking of vinyl-PDMS by organic peroxide is believed to be achieved via a free-radical mechanism, which involves three key steps as shown in Figure 1: (Step 1) the generation of two cumyloxy radicals by thermal decomposition of the peroxide,

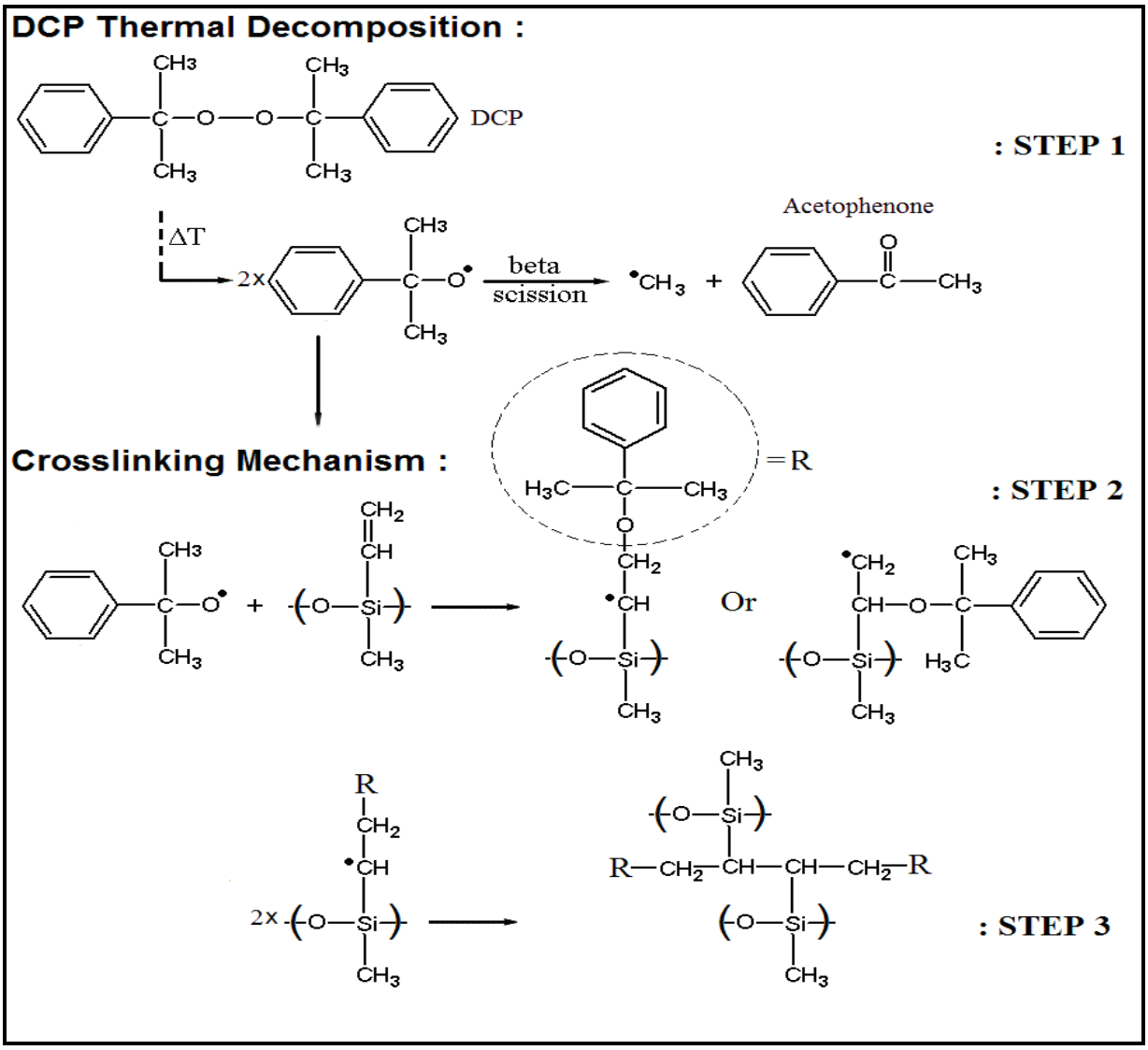


Figure 1. DCP decomposition and free-radical cross-linking mechanisms of vinyl-PDMS.

(Step 2) cumyloxyl radicals attack the unsaturated pendant groups (vinyls) in the polymer chain via addition reaction to generate polymer radicals, and (Step 3) the polymer radicals produced are quite reactive, so that they can add to another polymer radicals to form a covalent carbon–carbon crosslink. As a result, the molecular chain mobility is strongly affected and the storage and loss moduli increase with time as shown in Figure 2 for T=140 ℃. At a particular point, the storage and loss moduli cross each other. It was shown [21] that the gel point of a crosslinking polymer coincides with the G'-G'' crossover only if the power law on both storage and loss moduli followed the power law $G' \propto G'' \propto \omega^n$ with n=1/2. According to our previous results, it can be assumed in the present study that the crossover between G'(t) and G″(t) defines the gel point of a network based on polymer precursor of high molecular weight. In other words, we admit the storage and loss moduli are equal over the whole spectrum of frequencies and proportional to the square of the frequency. Reaching this critical point, named gel point, the PDMS chains form a three dimensional network. Above the gel point, the density of the network increases and the storage modulus reaches a steady-state value (G_e= 2.6 x 10^5 Pa) corresponding to the end of the cross-linking reaction. Interestingly, the loss modulus passes through a maximum (just above the gel point) and decreases to a constant value ($\tan\delta = \frac{G''}{G'} = 8.0x10^{-3}$). A possible explanation of this behavior stands from the fact that, thanks to the crosslinking reaction, high molar masses polymers are first formed which results in increases of both the storage and loss moduli. However, beyond the gel point, the increase of the elasticity is the leading factor, and the network tends to be more and more perfect so that $\tan\delta$ decreases with higher density network to finally reach an equilibrium value.

At higher temperatures (T=160 ℃) the thermal decom position of DCP is fast according to the high-energy activation of DCP decomposition (E≈156 $kJ.mol^{-1}$). Therefore, the curves at these temperatures cannot capture the initial stage of cross-linking (gelation process) as one part of DCP is already decomposed during the preparation of the sample between the plates of the rheometer, estimated to be around 30 s.

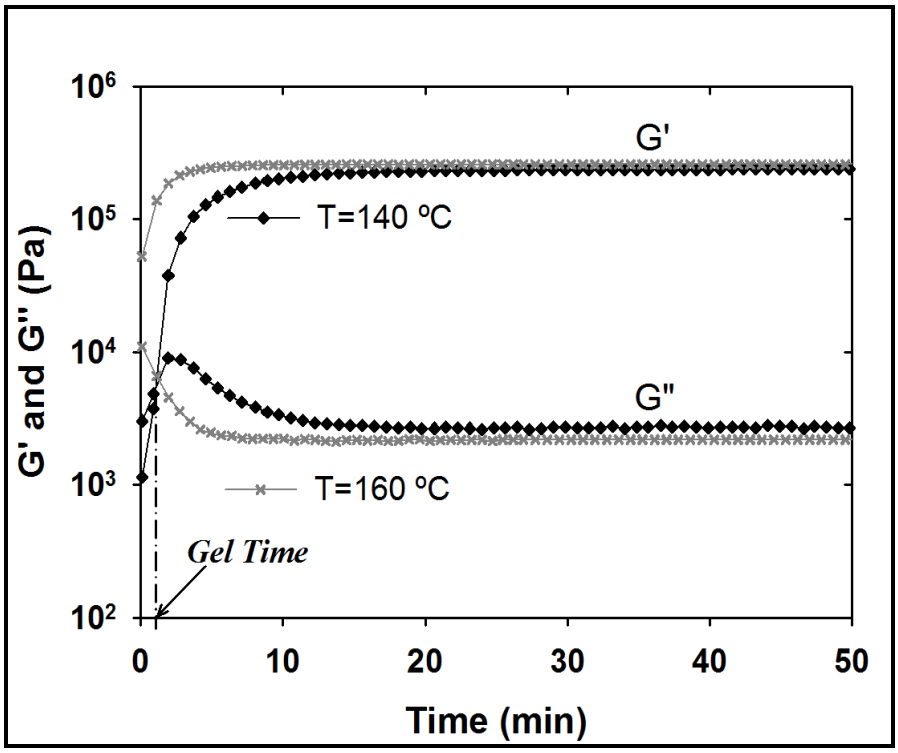


Figure 2. Radical cross-linking of vinyl-PDMS initiated by 36 mol.m^{-3} of DCP. Variation of the storage G' and loss G" modulus vs reaction time. T=140 and 160 ℃. ω=1 rad. s^{-1}.

However, it can be qualitatively observed that the same cross-link density has been obtained after reaction completion. According to our previous works [22] the present work shows that the efficiency of DCP does not depend on temperature, at least for temperature lower than 160 ℃. Obviously, it is clear that the time needed by the modulus to reach a plateau gets longer as the temperature is lower (Kinetic effect).

The influence of the TEMPO concentration, via the ratio r=[TEMPO]/[DCP], on scorch time and crosslinking density of PDMS network is shown in Figure 3a,b. From a qualitative point of view, Figure 3a (r=1.8 for illustrative example) shows that the cross-linking process is delayed by few minutes. The scorch time is defined in Figure 3b as the time at which the storage modulus suddenly increases. At 160 ºC, the addition of TEMPO results in an increase of the scorch time from 7.2 min (r = 1.2) to 16.9 min (r= 2.0). Surprisingly, the cross-linking reaction is totally inhibited at higher amount of

TEMPO (r = 2.4). Although the scorch mechanism has been reported in the literature [19, 23], such quantitative experiments from TEMPO addition have been never shown in literature.

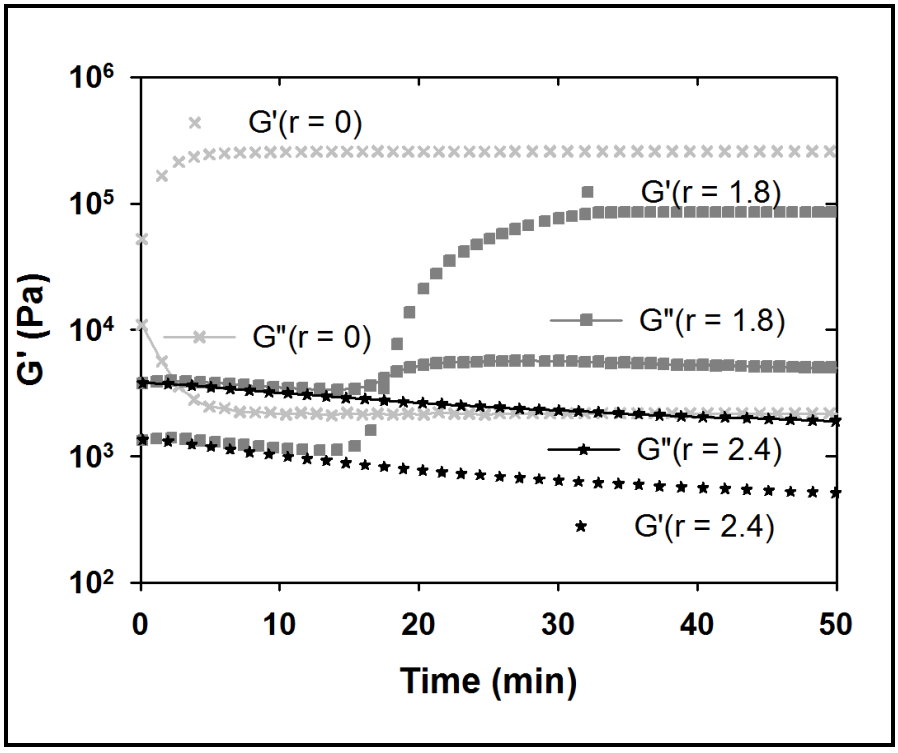


Figure 3a. Variation of the storage and loss modus at the following ratio: r = 0, 1.8 and 2.4

According to a free radical crosslinking mechanism, it can be hypothesized that crosslinking delay is the result of a TEMPO-grafted polymer action formed by reaction between TEMPO and the polymer radical. Furthermore, polymeric radicals are rapidly trapped by a grafting reaction with TEMPO before they are able to form crosslinks by combination. NMR techniques were employed to clarify chemical bond formation involved during PDMS crosslinking controlled by TEMPO. Figure 4 compares the NMR spectrum of virgin PDMS (Figure 4a) and reactive samples (Figure 4b,c). Reactive sample (Figure 4b) has been obtained upon the following reactive conditions between

the plates of the rheometer: r = 1.8, curing time= 15 min. From Figure 3a,b (T=160℃) this sample has not reached its gel point and is still soluble.

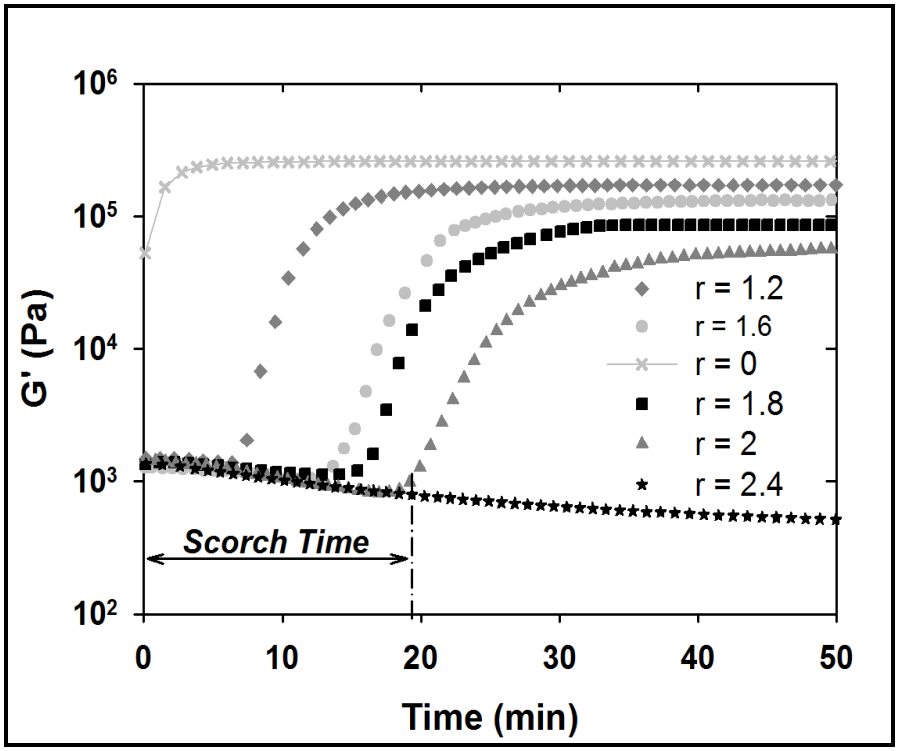


Figure 3b. Variation of the storage modulus (r = 0, 1.2, 1.6, 1.8, 2 and 2.4). Definition of the scorch time.

Finally, Figure 4c shows the NMR spectrum of the soluble fraction of the same sample (r = 1.8) but cross-linked in a Rheometer for 30min. The ^{1}H spectrum of the virgin PDMS sample (Figure 4a) exhibits the expected signals at 7.2 ppm of the chloroform ($CHCl_3$) and 0 ppm of the tetramethylsilane (TMS). The chemical shifts at 0.2 and 0.8 ppm can be assigned to Si-CH_3 resonance. The strong peak at 1.5 ppm shows the presence of water residue in the sample. Moreover, a broad signal around 2.1 ppm can be observed and is attributed to CH groups. However, in the ^{1}H NMR spectra the peaks for the terminal (-CH_2=CH) double bond should be observed at 5.8 and 6.7ppm [24]; the absence of this peak is due to the low molar concentration of vinyl groups in the PDMS sample. The comparison of the ^{1}H spectrum (Figure 4b, c) with the spectrum of the

reference sample (Figure 4a) shows evidence of the TEMPO grafting onto the polymer chains. Additional resonances can be found in spectrum b and c.

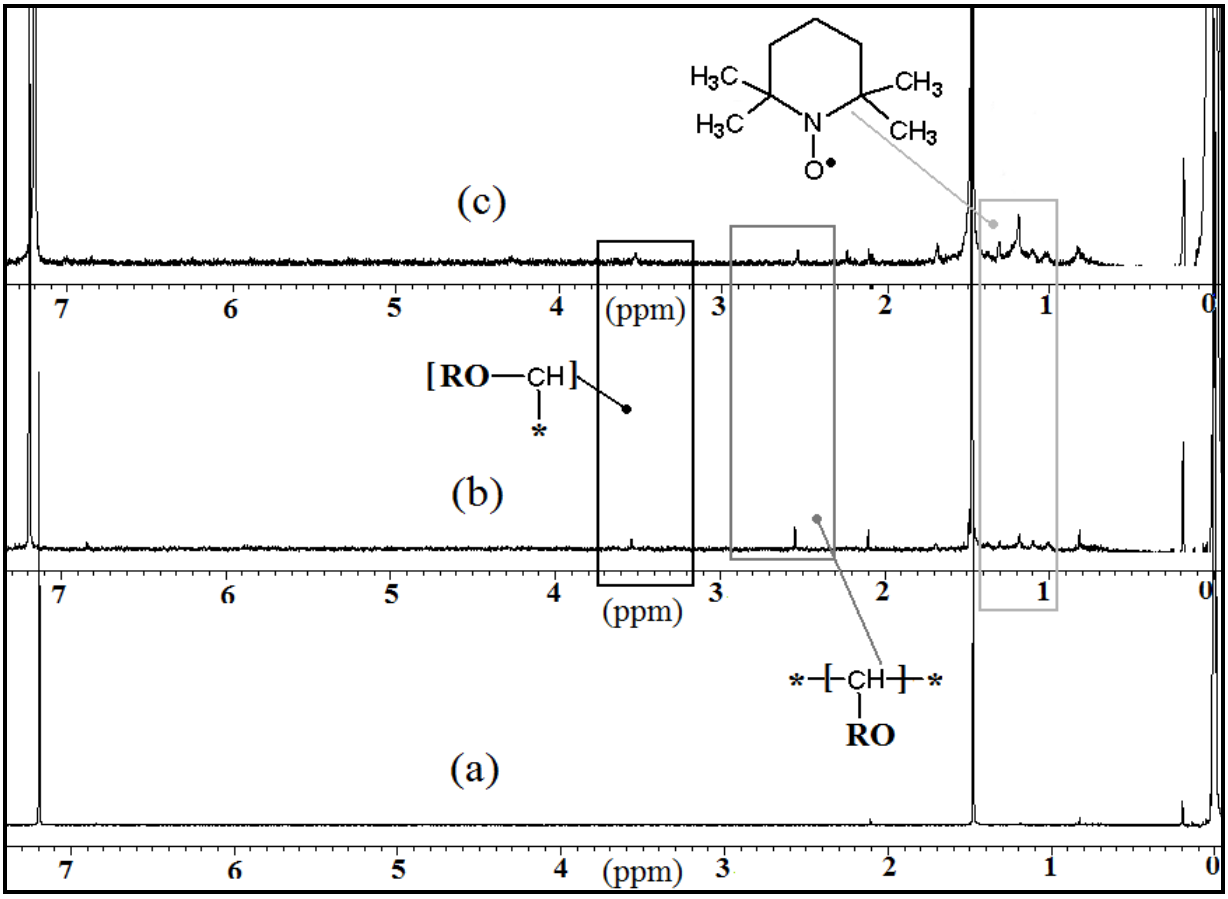


Figure 4. ^{1}H NMR spectrum proving TEMPO grafting onto PDMS (r = 1.8, T = 160 ℃).
a) Virgin vinyl-PDMS.
b) Reactive vinyl-PDMS sample: curing time 15min, the sample is totally soluble.
c) Reactive vinyl-PDMS sample: curing time 30min. The spectrum corresponds to the soluble fraction.

The primary indication for grafting in presence of TEMPO is the existence of new peaks at 2.55 and 3.55 ppm which are attributed to the formation of C-O bonds (-i.e R-O-CH- and R-O-CH_2 species). However, the most significant modification is the presence of oxygen–carbon bonds formed by the addition of the cumyloxyl radicals after

the peroxide decomposition. The ^{1}H spectrum (Figure 4b, c) shows the additional resonances in the range from 1 to 1.3 ppm witch are typical of the CH_2 and CH_3 groups of TEMPO [25]. Therefore, the present ^{1}H NMR results prove the presence of TEMPO onto PDMS chains of reactive samples. Furthermore, these results indicate also the stability of bonds formed between the nitroxyl and carbon-centered radicals at elevated temperatures of processing.

From a quantitative point of view, the phenomenological model of Langley [26] and Dossin and Graessley, [27] which takes into account the contribution of chemical crosslinks and trapped physical entanglements to prediction of the shear equilibrium modulus, can be used in the present study. According to the entanglement interpretation of the topological contributions, a portion of the restrictions on configurational rearrangements of macromolecules becomes permanently trapped when a chemical network is formed and therefore is able to contribute to the equilibrium elasticity [28]. The contributions to the modulus are given by the widely used Langley equation:

$$G_e^{Langley-Grassely} = G_{ch} + T_e G_N^0 \quad (1)$$

Here, the equilibrium modulus G_e is given as the sum of the modulus G_{ch} due to chemical crosslinks and the trapped entanglement term ($T_e G_N^0$), where T_e (called the Langley trapping factor) is the proportion of the maximum concentration of topological interactions that contribute to the modulus, and G_N^0 is the plateau modulus related to the entangled molecular weight ($G_N^0 = \rho RT / M_e$). According to the arguments based on the constrained-junction model [29], the term (G_{ch}) should equate to the phantom network modulus [30], onto which contributions from entanglements are added:

$$G_{ch} = (\nu - h\mu)RT \quad (2)$$

where h is an empirical parameter between zero and one but genarally considered to be equal to 0. The parameters ν (density of strands elastically actives), μ (density of crosslink bonds), and T_e for the phenomenological model can be calculated using the theoretical relations established by Pearson and Graessley [31, 32]. According to these equations, assuming a tetrafunctional network and from the measurement of the soluble fraction ω_s, the parameters ν, μ and T_e have been calculated (see Table 2) for the different [TEMPO]/[DCP] ratios. Furthermore, the conversion p of vinyl groups consumed by the reaction of crosslinking can also calculated by this method. The rubbery modulus G_N^0 of entangled PDMS chains has been reported in the literature by Plazek et al. [33] and Valles and Macosko [34] to be 2.0 × 10^5 Pa at room temperature. Assuming an entropic elasticity of G_N^0, we finally calculated G_N^0 = 2.9 × 10^5 Pa at T= 160 ℃. Finally, the comparison of G_e experimental (Table 1) with G_e computed (Table 2) shows very satisfactory agreement which validates our approach based on the Pearson and Graessley model.

Table 1. Kinetics and Linear Viscoelastic Parameters of PDMS Networks Cross-linked at 160 ℃ in the Presence of Different Conce ntrations of TEMPO[a]

[TEMPO] (mol.m^{-3})	r = ([TEMPO]/[DCP])	*Scorch time* (min)	*Gel time* (min)	G_e (Pa)	*tan (δ)*
0	0			2.6 × 10^5	0.008
43	1.2	7.2	8.2	1.7 × 10^5	0.012
58	1.6	13	15.6	1.3 × 10^5	0.024
65	1.8	14.1	17.7	8.6 × 10^4	0.057
72	2	16.9	21.9	5.9 × 10^4	0.1

[a]) *Initial concentration in DCP: [DCP] = 36 mol.m^{-3}*

First of all, Table 1 (r = 0, T = 160 °C) shows that the conversion of vinyl groups belonging to the network is close to 83%. Therefore, the DCP efficiency is low for the cross-linking reaction as it is about 31% (DCP efficiency = (0.83 x 27)/(36 x 2), where 27 is the molar concentration of vinyl function (expressed in $mol.m^{-3}$), 36 is the molar concentration of DCP which gives two radicals when reacting, and 0.83 is the conversion of vinyl groups). However, this DCP efficiency is in good agreement with the literature results. For example, Hulse et al. [35] prove that the overall cross-linking efficiency for LPE with DCP is between 20 and 40% (at 150 °C) of the theoretically expected value. Moreover, it has been proved that cross-linking of high-consistency silicone rubbers such as vinyl-PDMS using peroxide leads to formation of peroxide's volatile residues such as acetophenone [9]. These breakdown products explain the low efficiency of DCP. Therefore, we obtained about 62% cumyloxyl and 38% methyl reactive ($CH_3^{\bullet}$) radicals after DCP decomposition. On the other hand, Table 1 shows that in presence of TEMPO the optimal ratio (r) necessary to cross-link the vinyl-PDMS is between 2 and 2.4. Consequently, the TEMPO efficiency is about 21% at T = 160 °C. This was unsurprising result, because TEMPO could be involved in coupling reaction with $CH_3^{\bullet}$ radicals, leading to the formation of methyl-TEMPO [25]. Indeed, the grafting reaction was comparatively slow, presumably because the diffusion of polymer radicals is constrained.

Nevertheless, methyl-TEMPO formation is not the only side reaction for the present system. Figure 3b shows a slowly decreasing of the storage modulus at the earlier stage of reaction. This phenomenon is clearly shown for r = 2 and 2.4, and from our rheological investigations it results from polymer chain degradation. Furthermore, this side reaction was studied by TGA-GC/MS experiments. As a result, Figure 5 shows the mass spectra of vinyl-PDMS containing 1% wt of TEMPO and cured for 30 min at the temperature T = 200 °C. This analysis proves the formation of major degradation products of PDMS such as the cyclic volatile oligomer decamethylcyclopentasiloxane (D5) and the ion fragment trimethylsiloxane (M_3T) [36, 37].

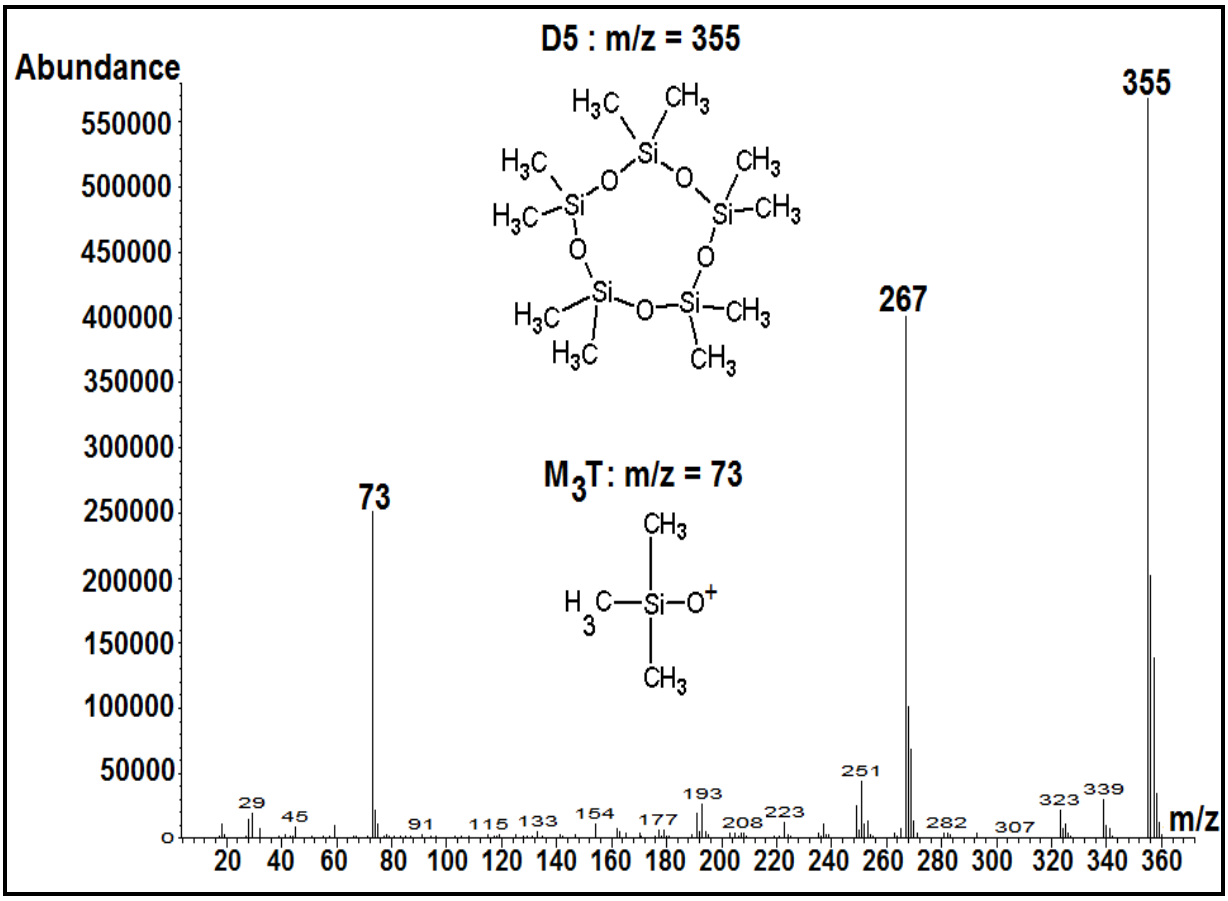


Figure 5. Overlay mass spectra of vinyl-PDMS with 1% of TEMPO at 200 ℃.

Indeed, in the presence of trace of water and metal in polymer, nitroxides can oxidize the reduced form of metal trace from the syntheses process of the polymer, while they themselves are reduced to hydroxylamines [38] as shown in Figure 6. Therefore, the change of nitroxide to a strong base due to the presence of water and catalyst residues in polymer leads to silanolate formation and depolymerisation of the PDMS chains. This depolymerisation mechanism has been already studied in the literature. Thomas [39] and Grassie and Macfarlane [40] described that cleavage of the PDMS backbone by moisture and contamination by strong bases or acids is the principal mode of depolymerisation at lower temperatures 120 to 275 °C and is of most concern in normal operating environments.

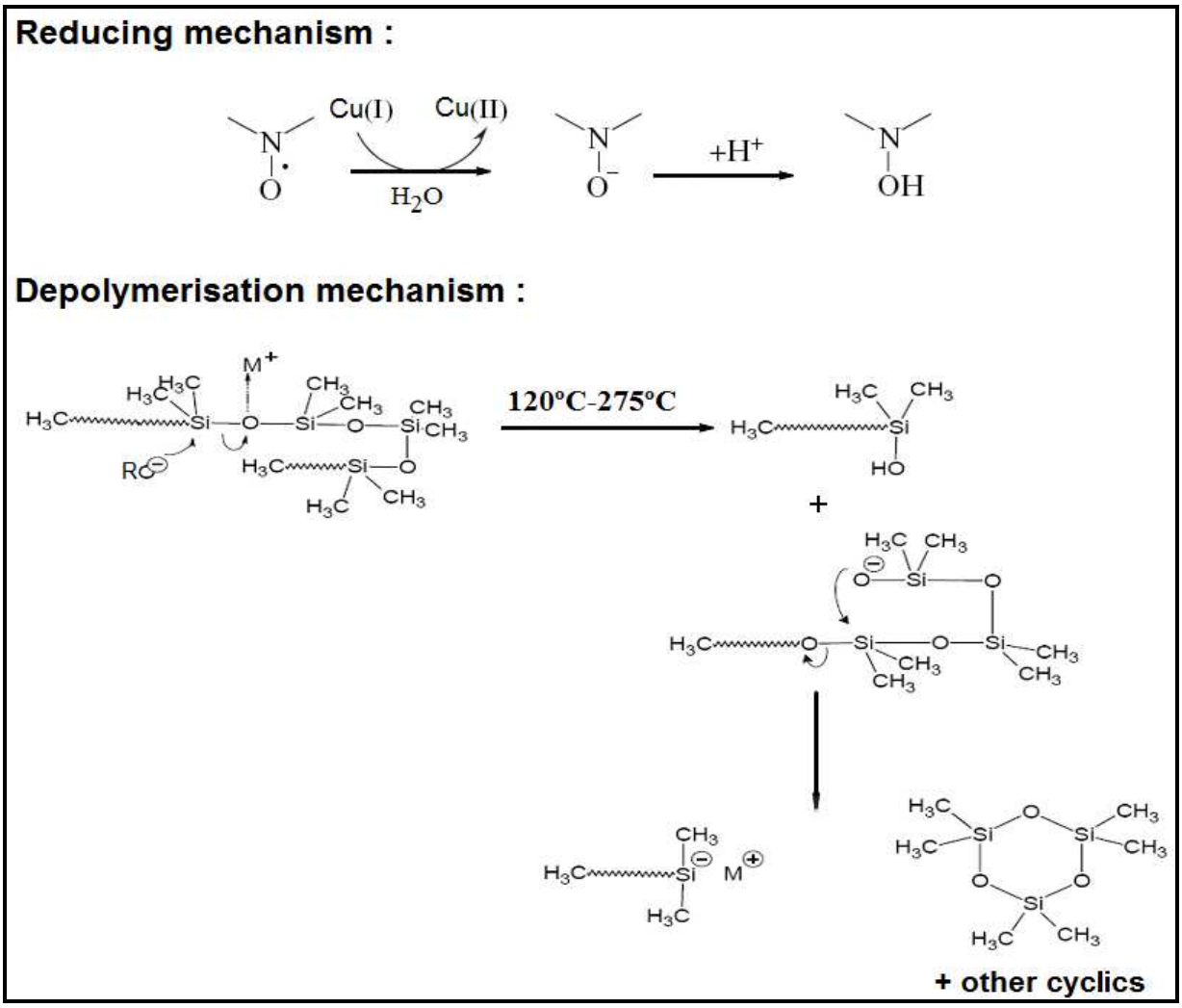


Figure 6. Proposed mechanisms for reduction of TEMPO and depolymerisation of PDMS [38-40].

Finally, Figure 7 (r= 1.6) shows that the steady-state value of the complex shear modulus does not seem to depend on the temperature (T = 160, 180 and 200 ℃) which is a balance between increase of both the modulus (entropic elasticity) and the defects with temperature. Then, temperature can be considered to have not effect in the stability of the nitroxyls graft and thus on the final cross-linking degree. In fact, the thermal stability of bonds formed between the nitroxyl and carbon-centered radicals has been studied extensively in model systems [41]. The results presented in these studies

indicate that primary and secondary alkoxyamines should be robust enough to withstand processing and testing conditions at elevated temperatures for many hours to several days or longer, such that the integrity of grafts to primary and secondary carbons will be maintained. However, it can be noted that scorch delay decreased with increasing of temperature. The scorch time shifted from 13 min at 160 ºC to 3.4 min at 180 ºC and to 1.5 min at 200 ºC. This is unsurprising results because the kinetics of TEMPO grafting and chains combination increase with temperature. However from these results, the activation energy of each process cannot be achieved.

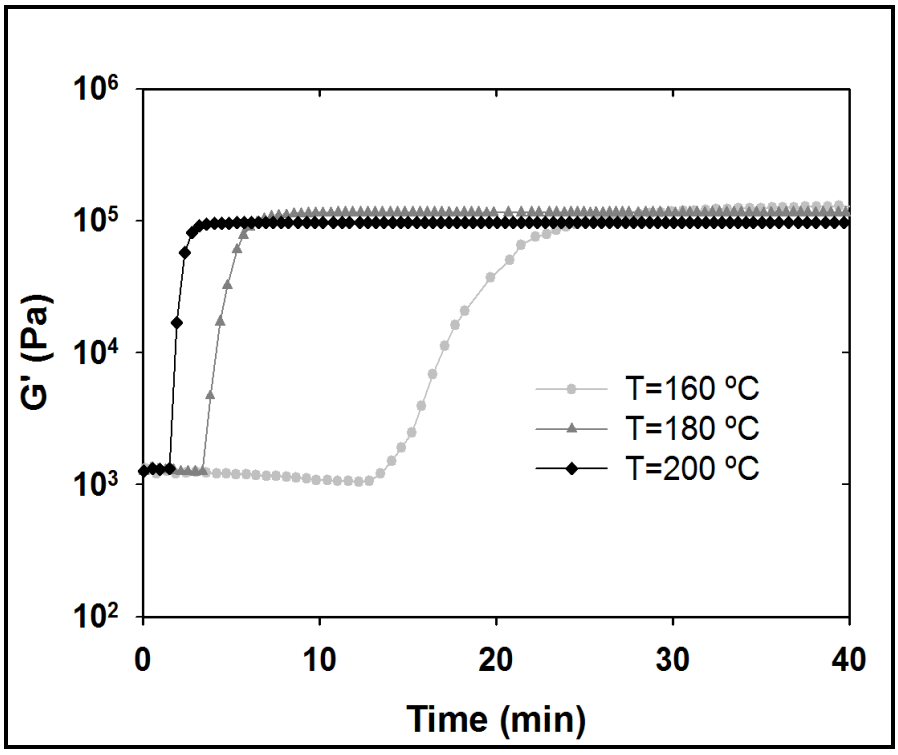


Figure 7. Temperature dependence (T= 160, 180 and 200 ℃) of the cross-linking reaction: Variation of the storage modulus vs time for r= [TEMPO]/[DCP] =1.6

3.2. DSC analysis

The crosslinking reaction consists to create covalent bonds between the macromolecular chains of polymer. These covalent bonds are obtained by reaction

between reactive sites and they are formed with releases a quantum of energy, making crosslinking an exothermic reaction. We propose hereafter to use the differential scanning calorimetry to investigate the PDMS crosslinking controlled by the addition of TEMPO. This technique is expected to study the crosslinking process at the molecular scale and to relate the variation of the crosslinked bonds formed between the macromolecular chains in presence of TEMPO with the change of the physical properties of final networks.

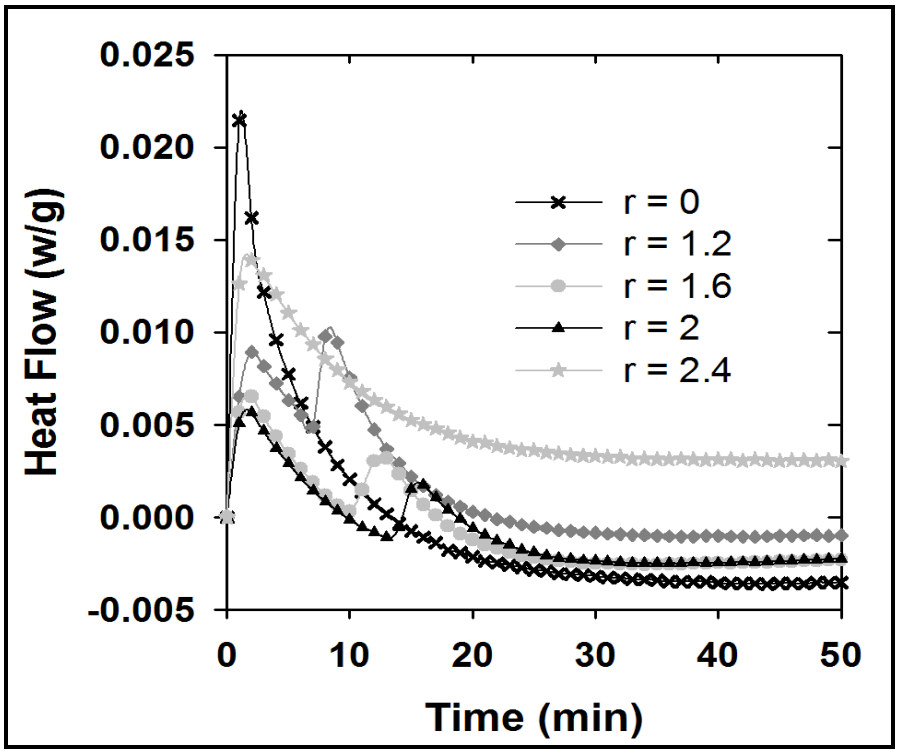


Figure 8. DSC traces showing the total heat of cross-linking reaction obtained for various r = [TEMPO]/ [DCP] ratio at 160 ℃.

The isothermal DSC scans of (PDMS/DCP/TEMPO) curing system at different amount of TEMPO (r = 0, 1.2, 1.4, 1.6, 2 and 2.4) are shown in Figure 8. Interestingly, these DSC kinetics allowed us to separate the own exothermic heat of C-C bonds creation (or quantum of energy of formed cross-linked bonds) in a complex system of the other reactions like the homolytic decomposition of the initiator (DCP) and its addition on the

polymer chains. Actually, as shown in Figure 8, the addition of TEMPO in the PDMS/DCP system results in a secondary exothermic peak. This second peak is time shifted with increasing the TEMPO concentration. Eventually at r = 2.4, this second peak disappears. These DSC results show the complexity of the present system as two exothermic phenomena with different apparent enthalpies have been revealed. These two phenomena can associated to two different reactions. In the absence of TEMPO, the global reaction is related to DCP decomposition, vinyl sites activation, and C-C bonds creation (Figure 1).

However, in the presence of TEMPO, the first exothermic peak corresponds to DCP decomposition, vinyl sites activation, and the grafting of nitroxyl radicals on the polymeric radicals as shown in Figure 9. This last mechanism prevents the formation of cross-link bonds. Once all TEMPO

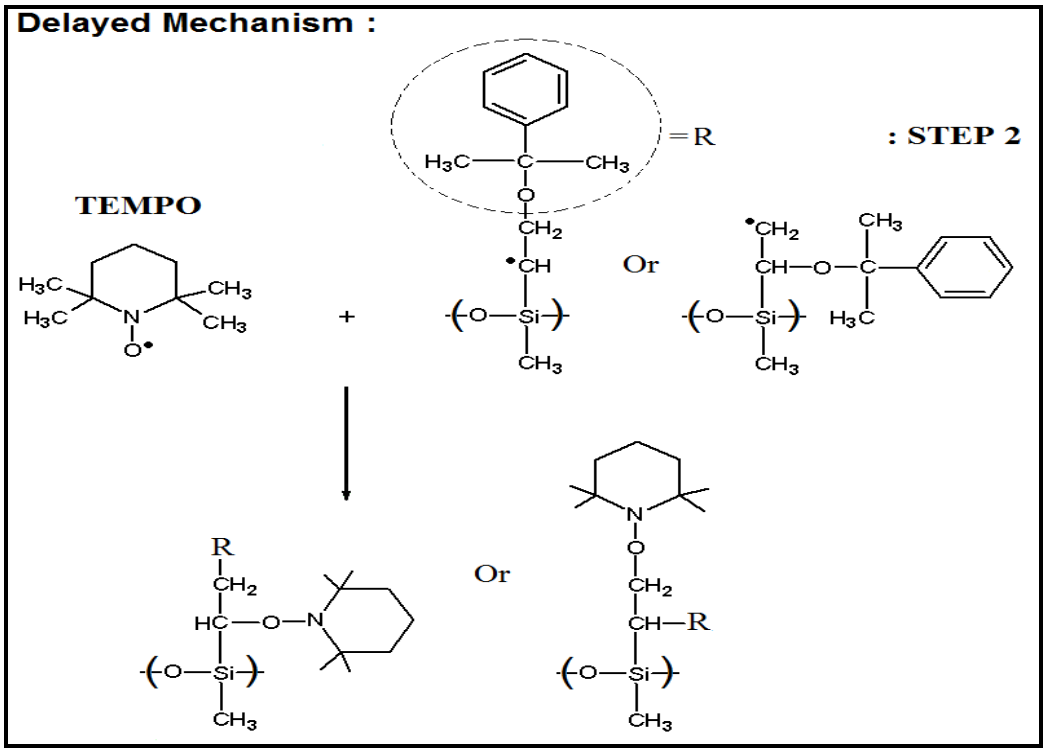


Figure 9. Mechanism for delayed-action (scorch time) of TEMPO on free-radical crosslinking of vinyl-PDMS.

molecules are consumed, the second peak can then arise. This peak is then assigned to the C-C bonds creation. This hypothesis was validated by the fact that this second peak disappears with increasing the TEMPO concentration above a critical value (r > 2) at which the crosslinking reaction is not observed anymore. Moreover, these results are in perfect agreement with rheology results. Indeed, time corresponding to the second peak (t_{picR2} from Table 3) for the various samples coincides well with the scorch time determined by rheology (Table 2). A small difference is observed between DSC and rheological data due to the temperature control between the two techniques.

Table 2. Topological Parameters for the Different Samples, as Computed from the Theoretical Relations Derived by Pearson and Graessley [32]

r	ω_s	p	T_e	ν $(mol.m^{-3})$	$\mu(mol.m^{-3})$	G_e (Pa)
0	0.018	0.83	0.58	18.3	10.1	2.3×10^5
1.2	0.04	0.513	0.43	10	5.6	1.6×10^5
1.6	0.06	0.4	0.34	6.9	4	1.2×10^5
1.8	0.095	0.3	0.24	4.3	2.6	8.5×10^4
2	0.14	0.231	0.16	2.7	1.6	5.6×10^4

More precisely, the rheology and DSC results for r = 1.2 are compared in Figure 10. Both techniques are quite complementary for the kinetic study of this complex reactive system. At the earlier stages of the reaction, the rheology does not record any variation of the viscoelastic properties since TEMPO react with polymer radical and then embed the crosslinking reaction. On the contrary, DSC analysis shows a first exothermic peak of reaction which is spread out until the starting time (scorch time) of the complex modulus variation. This result confirms our last hypothesis: the first phase corresponds to the DCP decomposition, vinyl sites activation, and the addition of nitroxyl radicals on the polymeric radicals (DSC exothermic peak and no variation of the complex shear modulus). The end of this inhibition phase is announced by both techniques: strong variation of the complex shear modulus and evidence of a second exothermic peak.

Therefore, this second peak corresponds to the network formation through to the covalent bonds formation (or chemical cross-link) between the PDMS polymer chains.

Generally speaking, DSC experiments in both isothermal and anisothermal modes have mostly used in the literature to study the kinetics of cure reactions [42]. Several alternative methods for estimating the cross-linking density with DSC has been discussed in the literature for thermosets like the epoxy-amine systems. However, in the case of elastomer cross-linking there is no a significant variation of the heat capacity during the reaction. Furthermore, the methods generally used are based on the assumption that the rate of heat generation is proportional to the rate of the cure reactions [43]. This is questionable for a complex reaction system.

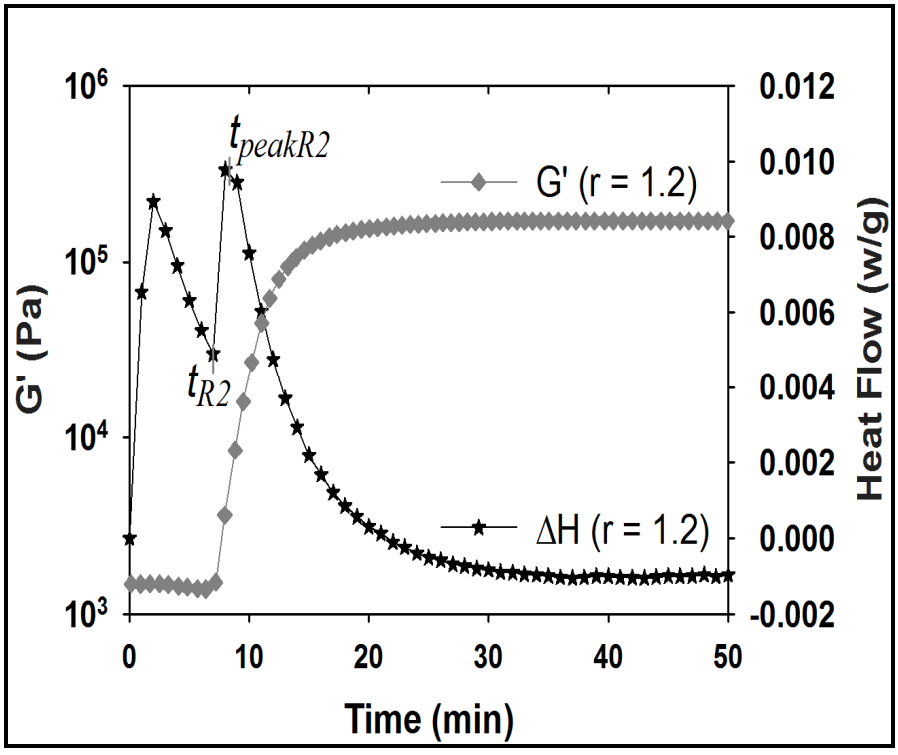


Figure 10. Comparison of the variation storage modulus and enthalpy of the reaction (r = 1.2 T = 160 ℃).

In their work on the kinetic of vulcanization of a natural rubber compound, Ding and Leonov [44] described that DSC data were found to be incompatible with the cure meter test, because the complex vulcanization reaction system is multiexothermal. Therefore, DSC analysis was never used to calculate the extent of the crosslinking reaction in terms of crosslinking density.

In the present work, it is assumed that the enthalpy of C-C covalent bonds (ΔH_{C-C}) can be separated from the other reactions and derived from the total enthalpy ΔH_T as follows:

$$\Delta H_{C-C} = \Delta H_T - \Delta H_{R1} \quad (3)$$

Where ΔH_{R1} is the enthalpy of the first reaction including DCP decomposition, vinyl sites activation, and grafting of nitroxyl radicals on the polymer chains. Therefore, the chemical crosslink density can be calculated according to the following equation:

$$\mu = \frac{\rho_{polymer}\ \Delta H_{C-C}}{\Delta H^0_{c-c}} \quad (4)$$

Where ΔH^0_{c-c} is the standard enthalpy to form one mole of C-C bonds. According to the literature [45], $\Delta H^0_{c-c} = 347 kJ.mol^{-1}$.

Experimentally, the enthalpy (ΔH_{C-C}) was derived as shown in Figure 11, and the crosslinking density was calculated according to Equ 4. These values are reported in Table 3. It should be noted that the cross-linking density for r = 0 (TEMPO free) has been calculated by a linear extrapolation of the values obtained for r = 1.2, 1.6 and 2. According to Table 2 and 3, chemical cross-link densities calculated from soluble fraction (Langley and Dossin and Graessley model) and DSC analysis are in good agreement even if the later underestimated the cross-linking density.

Table 3. DSC Results at 160 ℃ and Predicted Densit y of Chemical Junctions Using the DSC Method

r	t_{R2} *(min)*	t_{peakR2} *(min)*	$\Delta H_{C\text{-}C}$ $(J.g^{-1})$	μ $(mol.m^{-3})$
0				8.4[a]
1.2	7.1	8.4	1.71	4.8
1.6	10	12.6	1.26	3.6
2	13.4	15.7	0.87	2.5

[a]*) From extrapolation of data at r = 1.2, 1.6 and 2*

From using the same extrapolation, the total amount of TEMPO necessary to totally inhibit the cross-linking reaction is then equal to 102 $mol.m^{-3}$. Translating this value in terms of [TEMPO]/[DCP] ratio leads to r = 2.8. This result is in agreement with the value observed from rheological measurement r = 2.4 for which no cross-linking reaction was observed.

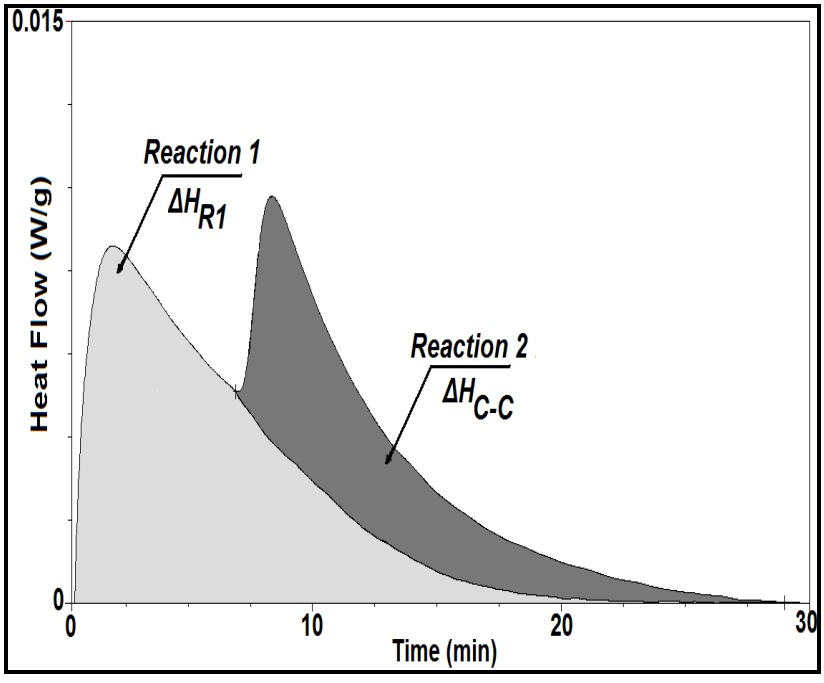


Figure 11. Principle of the experimental method to calculate the enthalpy ΔH_{C-C} of cross-link C-C bonds. r = 1.2, T = 160 ℃.

4. Conclusion

The roles of nitroxides such as TEMPO in scorch delay and crosslinking control of free-radicals cross-linking process have been demonstrated in this study. A remarkably scorch delay has been found with varying the molar ratio [TEMPO]/[DCP] in the range r = 0-2.4. First of all, rheological measurements were carried out in order to determine the linear viscoelastic properties of the PDMS networks. The scorch and gel times, the equilibrium modulus (Ge), and the soluble PDMS chains fraction were found to be a function of the concentration of TEMPO. Furthermore, the characterization of the network features based on the phenomenological model of Langley and Dossin and Graessley provided that the control of the network topology can be achieved by using nitroxide TEMPO. In agreement with rheological measurements, NMR microstructural studies revealed that the cross-linling delayed action in presence of TEMPO is the result of trapped carbon-centered polymer radicals by nitroxides. As a result, once the TEMPO is totally consumed, the crosslinking can proceed as usual.

Furthermore, DSC was used to characterize the effect of TEMPO in cross-linking reaction at the molecular scale. An original result has been shown using this technique by varying the molar ratio [TEMPO]/[DCP]. Correlation between DSC and rheometry experiments proved that the secondary exothermic enthalpy corresponds to the covalent bonds formation between only carbon-centered polymer radicals and thus the network formation. According to this result, we developed an original method to determine the chemical cross-link density in the case of complex cure reaction system which has multiexothermal heat reaction. The predicted chemical cross-link densities are in close agreement with those calculated using the phenomenological model of the viscoelasticity.

Finally, the findings of this study will be an important impact in polymer science from both an academic and an industrial viewpoint. This interest is governed by the need to control the network architecture in order to develop new class of elastomer formulations

with a rich variety of topological characteristics improved and/or new mechanical and physical properties.

References

[1] Chang, C.L.; Don, T.M.; Lee, H.S.J.; Sha, Y.O. Polym. Degra. 2004, 85, 769-777.

[2] Yoo, S.H.; Cohen, C.; Hui, C.Y. Polymer 2006, 47, 6226-6235.

[3] Baquey, G.; Moine, L.; Degueil-Castaing, M.; Lartigue, J.C.; Maillard, B. Macromolecules 2005, 38 (23), 9571–9583.

[4] Ignatz-Hoover, F.; To, B. H. ‘‘Rubber compounding’’, New York, 2004.

[5] Dunham, M.L.; Bailey, D.L.; Mixer, R.Y. Ind. Eng. Chem 1957, 49, 1373-1376.

[6] Dluzneski, P.R. Rubber Chem. Technol. 2001, 74, 451-492.

[7] Ciullo, P. A.; Hewitt, N. ‘The rubber formulary’’, New York, 1999.

[8] Lucas, P.; Robin, J.J. Adv. Polym. Sci. 2007, 209, 111-147.

[9] Vallat, M.F.; Ruch, F.; David, M.O. Eur. Polym. J. 2004, 40, 1575–1586.

[10] Heiner, J.; Stenberg, B.; Persson, M. Polym Test. 2003, 22, 253–257.

[11] Dorn, M. Adv. Polym. Technol. 1985, 5, 87-91.

[12] Gulmine, J.V.; Akcelrud, L. J. Appl. Polym. Sci. 2004, 94, 222-230.

[13] Ghosh, P.; Katare, S.; Patkar, P.; Caritjers, J.M.; Venkatasubramanian, V.; Walker, K.A. Rubber Chem. Technol. 2003, 76, 592.

[14] Robert, P.M. EP 0,837,080, A1; 1997.

[15] Lizotte, J.R.; Long, T.E. Macromol. Chem. Phys. 2003, 204, 570–576.

[16] Li, I.Q.; Howell, B.A.; Koster, R. A.; Priddy, D. B. Macromolecules 1996, 29, 8554-8555.

[17] Keoshkerian, B.; MacLeod, P. J.; Georges, M. K. Macromolecules 2001, 34, 3594-3599.

[18] Moad, G.; Rizzardo, E.; Solomon, D. H. Macromolecules 1982, 15, 909-914.

[19] Chaudhary, B.I.; Chopin, L.; Klier, J. J. Polym. Sci. 2007, 47, 50-61.

[20] Gottlieb, M.; Macosko, C.W.; Benjamin, G.S.; Meyers, K.O.; Merrill, E.W. Macromolecules 1981, 14 (4), 1039-1046.

[21] Winter, H.H.; Mours. M. Adv. Polym. Sci. 1997, 134-165.

[22] Mskani, A.; Chaumont, P.; Cassagnau, P. Rheologica Acta. 2007, 46, 933-943.

[23] Alvarez-Grima, M.M.; Talma, A.G.; Datta, R.N.; Noordermeer, J.W.M. PCT/EP WO2006;100214; A1, 2006.

[24] Birkefeld, A.B.; Bertermann, R.; Eckert, H.; Pfleiderer, B. Biomat. 2003, 24, 35-46.

[25] Baquey, G.; Moine, L.; Babot, O.; Degueil, M.; Maillard, B. Polymer 2005, 46, 6283-6292.

[26] Langley, N.R., J.D. Macromolecules 1968, 1, 348-352.

[27] Dossin, L.M.; Graessley, W.W. Macromolecules 1979, 12, 123-130.

[28] Patel, S.K.; Malone, S.; Cohen, C.; Gillmor, J.R.; Colby, R.H. Macromolecules 1992, 25, 5241-5251.

[29] Flory, P.J. J. Chem. Phys. 1977, 66, 5720-5729.

[30] James, H. M.; Guth, E. J. Chem. Phys. 1947, 15, 669-683.

[31] Pearson, D.S.; Graessley, W.W. Macromolecules 1978, 11, 528-533.

[32] Pearson, D.S.; Graessley, W.W. Macromolecules 1980, 13, 1001-1009.

[33] Plazek, D.J.; Dannhauser, W.; Ferry, J. D. J. Colloid Sci. 1961, 16, 101-126.

[34] Valles, E.M.; Macosko, C. W. Macromolecules 1979, 12, 673-679.

[35] Hulse, G. E.; Kersting, R. G; Warfel, D. R. J. Polym. Sci. 1981, 19, 655-667.

[36] Ballistreri, A.; Montaudo, G. ; Lenz, R. W. Macromolecules, 1984, 17 (9), 1848–1854.

[37] Ballistreri, A. ; Garozzo, D. ; Montaudo, G. Macromolecules, 1984, 17 (7), 1312–1315.

[38] Bar-On, P.; Mohsen, M.; Zhang, R; Feigin, E.; Chevion, M.; Samuni, A. J. Am. Chem. Soc. 1999, 121 (35), 8070–8073.

[39] Thomas, D. K. Polymer 1966, 7, 99-105.

[40] Grassie, N. ; Macfarlane, I. J. Eur. Polym. J. 1978, 14, 875-884.

[41] Wetter, C.; Jantos, K.; Woithe, K.; Studer, A. Org. Lett. 2003, 5, 2899-2902.

[42] Yousefi, A.; Lafleur, P. G. Polym. Comp. 1997, 18 (2), 157-168.

[43] Kamal, M. R; Ryan, M. E. Adv. Polym. Technol. 1984, 4, 323-327.

[44] Ding, R.; Leonov, A. L. J. Polym. Sci. 1996, 61,455-463.

[45] Vollhardt, K.; Schore, N. E. ‘‘Traité de chimie organique’’, 4 ed.; De Boeck Université, 2004.

Chapter 3

Rheological Modelling of the Free-Radical Crosslinking of PDMS Rubber in the Presence of TEMPO Nitroxide

Abstract

The aim of the present work is to study the free-radical kinetics of PDMS rubber crosslinking in the presence of 2,2,6,6-tetramethylpiperidinyloxyl (TEMPO) nitroxide. For this purpose a new method based on the relationship between the kinetics of the macro-radicals coupling [$R_{cc}(t)$] was derived from a fundamental kinetic model and the viscoelastic changes of the complex shear modulus ($G'(t)_\omega$ and $G''(t)_\omega$). The kinetic model takes into account the initiator (Dicumyl peroxide in the present study) decomposition and the trapped PDMS macro-radicals in the presence of a radical

scavenger such as TEMPO. Activation energy E_{ac} and collision frequency factor A_{0c} for the bimolecular termination reaction coefficient rate k_{cc} have been derived from the anisothermal DSC results according to the Kissinger method. Furthermore, it was observed that addition of TEMPO nitroxide can boost the initiator efficiency. The concentration variation of the active PDMS carbon-cantered radicals $[R_p^{\bullet}(t)]_{act}$ and the $[R_{cc}(t)]$ with reaction time were predicted using this kinetic model. On the other hand, the influence of TEMPO concentration in formulation ($[N]_0$) and effect of temperature on viscoelastic variations are studied. As a main result, the rheological modelling shows that this new method accurately predicts the time variation of complex shear modulus at any temperature and [TEMPO]/[DCP] ratio.

This chapter 3 was published in ***Polymer 2010, 42, 8460-8467***

1. Introduction

Modelling of crosslinking process has recently received a great deal of attention [1]. Actually, modelling of the variation of the viscoelastic properties during crosslinking is of particular importance from a processing point of view. This modelling requires in-depth study of chemistry of reaction, kinetic models [2], molecular structure, and changes in mechanical properties during crosslinking process [3]. However, free-radical crosslinking of rubber is a very complex chemical process and no known simulation techniques can directly investigate the changes in physico-chemical properties of the crosslinked network at molecular scale.

Commonly, a major curing mechanism frequently used for elastomers is the generation of polymer radicals (through the use of organic peroxides) that subsequently combine to form carbon-carbon bonds [4]. However, free-radical crosslinking by organic peroxide suffers from premature crosslinking at high temperatures, which is called scorching [5]. Chaudhary et al. [6] showed that the reaction of carbon-centred radicals with nitroxides and its derivatives can be a novel mean for scorch suppression, cure control and functionalisation in peroxide crosslinking of polyethylene thermoplastic. On the other hand, we investigated in a previous work [7] the effect of TEMPO in free-radical mechanism of vinyl-PDMS rubber crosslinking initiated by dicumyl peroxide (DCP) and noted a remarkable scorch delay by varying the molar ratio [TEMPO]/[DCP] in the range r =0 to 2.4. Furthermore, the characterisation of the network features based on the phenomenological model of Langley [8] and Dossin and Graessley [9] demonstrated that the control of the network topology can be achieved by using TEMPO nitroxide. Nitroxide chemistry has opened a new avenue in the domain of radical chemistry development for polymers. For example, Robert [10] patented a process for grafting maleic anhydride onto a thermoplastic polymer in the presence of a nitroxide such as TEMPO to avoid crosslinking during the grafting operation. More recently, Esseghir et al. [11] patented a new method of selecting a nitroxide for use as an inhibitor for free-radical crosslinking of EPDM elastomer.

The aim of the present work is to introduce a new simple modelling technique for direct investigation of the variations in viscoelastic properties during randomly crosslinking process in the presence of TEMPO. This modelling aims to predict the variation of complex shear modulus ($G'(t)_\omega$ *and* $G''(t)_\omega$) from the kinetics of macro-radicals coupling. The present study is based on free radical crosslinking of PDMS used as a model system as described in our previous work [7]. Actually, the presence of vinyl functional groups in the polymer chain enables the free-radical crosslinking of PDMS [12] with control over crosslink structure.

2. Experimental procedures

2.1 Differential Scanning Calorimetry (DSC)

Differential scanning calorimeter equipment manufactured by TA Instruments (Q100 system), equipped with Sealed aluminium pans, was used to measure the heat of crosslinking reactions. The mass of the samples ranged from 20 to 23 mg. A sealed empty pan was used as a reference. The total heats of reactions were obtained from non-isothermal method (Heating rate: $\dot{T}$ = 2.5, 5, 10, 15 and 20 °C.min^{-1}). All experiments were performed under nitrogen purge.

2.2 Rheological measurements

The rheological experiments were carried out on a rheometrics mechanical spectrometer (RMS800) using a parallel-plate geometry (R=12.5 mm). The parallel plate system was preheated at the temperature of the experiment. Then, the sample was put between the plates once the temperature of regulation was reached. The rheological kinetics of cross-linking were measured in real time at only one pulsation (ω=1 rad.s^{-1}) and at different temperatures T = 160, 180 and 200 °C. At the end of this crosslinking process, a frequency sweep experiment ($10^{-2}<\omega$ rad s$^{-1}<10^{2}$) was performed on the

same sample at the same temperature to determine the equilibrium modulus ($G_e = \lim_{\omega \to 0} G'(\omega)$).

Dynamic measurements during the non-isothermal conditions (Heating rate: $\dot{T}$ = 2.5, 5, 10, 15 and 20 °C.min^{-1}) were used to compare with the DSC kinetics results. In all experiments, sample response linearity with respect to strain amplitude was verified, and nitrogen gas was used to prevent thermal oxidation. In this type of experiment, we assumed that DCP and TEMPO were perfectly dispersed in molten polymer at a molecular scale (homogeneous conditions of reaction).

3. Kinetic modelling

3.1. Mechanism assumptions

Free radical crosslinking is a process of chemically producing network by creation of a carbon to carbon crosslinking bond between polymer chains. PDMS that contain vinyl groups can be crosslinking by dialkyl peroxides such as dicumyl peroxide. The different steps of this chemical mechanism are shown in Figure 1. The initiation step in peroxide-induced crosslinking is the thermal decomposition of the initiator to give two cumyloxyl free radicals (reaction (1)). In the case of vinyl-PDMS, the radical addition predominates over abstraction route [13]. Therefore, next step is the addition of cumyloxyl radicals to a double bond of the polymer molecule (reaction (2)). The polymer radicals hence produced are quite reactive, so that they combine to other polymer radicals to form a covalent carbon-carbon crosslinks (reaction (4)) [4]. Nevertheless, we revealed in our last study [7] that in presence of inhibitor molecule like TEMPO nitroxide, the polymer radicals are rapidly trapped by a grafting reaction before they are able to form crosslink. As shown in reaction (3), primary and secondary alkoxyamines (-C-O-N-) was formed between the nitroxyl and carbon-centered radicals (inactive PDMS macro-radical).

From a modelling point of view, several assumptions are necessary to reduce the number of parameters in the kinetic modelling of this complex crosslinking process:

1. The peroxide and nitroxide molecules are homogeneously distributed in the polymer. Furthermore, the reactions are not diffusion controlled [14]; so, the reaction rates for DCP decomposition and PDMS crosslinking were assumed constant during the course of the reaction,
2. All cumyloxyl free-radicals produced from DCP decomposition have the same dissociation energy,
3. The reactivity of cumyloxyl free-radicals on the vinyl function of the PDMS is supposed to be constant,
4. The side reactions [7] coming from the DCP molecules decomposition are negligible,
5. Inhibition involving primary radicals is negligible; i.e. TEMPO is capable of reacting and destroying only the PDMS carbon-centered radicals,
6. Side reactions in the presence of TEMPO nitroxide, such as degradation of PDMS [7] are negligible.

According to these assumptions, the experimental results are then analyzed by the simplified reactions scheme as described in Figure 1.

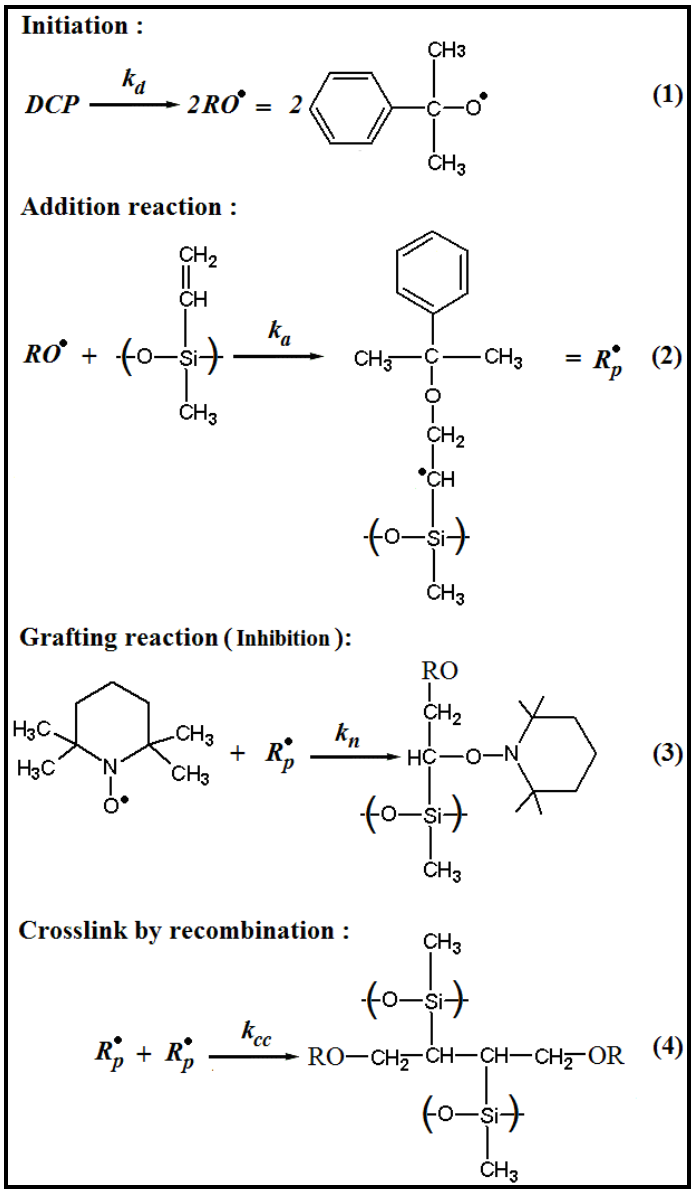


Figure 1. Controlled free-radical crosslinking mechanism of vinyl-PDMS used in this simulation.

3.2. Kinetic equations

According to Figure 1, the initiation step may include the formation of the initiated radicals and its reaction with pendent vinyl groups. Where $RO^•$ represents the cumyloxyl radicals (primary radicals) and k_d is the coefficient rate for the initiator decomposition, which governs the previous process. The factor 2 refers to the formation of two free

radicals for each decomposed molecule of initiator. For the first order kinetics, the rate of the initiator decomposition can be expressed as [15]:

$$\frac{d[DCP]}{dt} = -k_d[DCP(t)] \quad (1)$$

Where k_d can be simply derived from an empirical Arrhenius law:

$$k_d = A_0 Exp\left(-E_a/RT\right) \quad (2)$$

Where A_0 represents the collision frequency factor and E_a is the activation energy for the initiator decomposition reaction, with: $A_0 = 7.47\times10^{15}$ (s^{-1}) and $E_a = 153.5$ ($kJ.mol^{-1}$) for DCP [16].

Reordering the above equation and integrating between the time at which the initiator is added $t = 0$ and the testing time t; we obtain:

$$\left[DCP(t)\right] = \left[DCP\right]_0 exp\left(-k_d t\right) \quad (3)$$

Where $[DCP]_0$ is the initial concentration of DCP at t = 0. In the present study, $[DCP]_0 = 36 \times 10^{-3}$ ($mol.L^{-1}$). [DCP(t)] represents the residual concentration of the initiator at a reaction time t.

The coefficient rate of reaction (2), k_a, is in the range of 10^6 to 10^7 ($L.mol^{-1}.s^{-1}$) [17] which is high enough as compared with k_d (2.3×10^{-3} s^{-1} at T = 160 ℃); so it can be supposed that the primary radicals produced in reaction (1) at a time t can be transformed immediately and completely into PDMS carbon-centered radicals in reaction (2). Moreover, in the presence of inhibitor like TEMPO, we showed [7], that the polymeric radicals are rapidly trapped by a grafting reaction before they are able to form crosslinks. Assuming that TEMPO is an efficient radical scavenger, i.e TEMPO is

capable of reacting with polymer macro-radicals only, its decomposition rate can be expressed as following:

$$\frac{d[N]}{dt} = -k_n \left[R_p^{\bullet}(t)\right]_{act} [N(t)] \quad (4)$$

Where [N(t)] is TEMPO concentration, k_n is the coefficient rate of reaction (3), $[R_p^{\bullet}(t)]_{act}$ is active PDMS carbon-centered radicals' concentration and k_n is the coefficient rate of side reaction between the primary initiator radicals and TEMPO.

In addition, assuming bimolecular combination of backbone radicals [18], the rate of chain recombination (or crosslinking rate) described by reaction (4) is calculated according to the following equation:

$$\frac{d\left[R_p^{\bullet}(t)\right]_{act}}{dt} = 2\frac{d[R_{cc}(t)]}{dt} = -k_{cc}\left[R_p^{\bullet}(t)\right]_{act}^2 \quad (5)$$

Where k_{cc} is the rate for the disappearance of active PDMS macro-radicals by bimolecular termination and $[R_{cc}(t)]$ is the concentration of crosslink covalent bonds.

According to the crosslinking mechanism in Figure 1, the increases rate of active PDMS macro-radicals in the presence of TEMPO can be expressed as:

$$\frac{d\left[R_p^{\bullet}(t)\right]_{act}}{dt} = 2 f k_d \left[DCP(t)\right] - k_n \left[R_p^{\bullet}(t)\right]_{act} \left[N(t)\right] - k_{cc}\left[R_p^{\bullet}(t)\right]_{act}^2 \quad (6)$$

The parameter f in Equ 6 is called the efficiency of initiator [19].

Moreover, we assumed that during scorch phase the bimolecular termination of PDMS macro-radicals is totally quenched ($k_{cc}([R_p^{\bullet}(t)]_{act})^2 = 0$), so $[R_p^{\bullet}(t)]_{act}$ is constant; and therefore quasi-steady-state approximation (QSSA) [20] is applied to Equ 6 ($d[R_p^{\bullet}(t)]_{act}/dt = 0$) :

$$\frac{d[N]}{dt} = -k_n \left[R_p^{\bullet}(t)\right]_{act} [N(t)] = -2 f k_d [DCP(t)] \tag{7}$$

By substituting Equ 3 into Equ 7, it can be shown that the rate of inhibitor consumption is independent of the time variation of its concentration:

$$\frac{d[N]}{dt} = -2 f k_d [DCP]_0 \, exp(-k_d t) \tag{8}$$

By integrating Equ 8 with the initial conditions ($[N(t = 0)] = s \times [N]_0$); the nitroxide concentration obeys the following equation :

$$[N(t)] = \left(s \times [N]_0\right) - 2 f [DCP]_0 \left[1 - exp(-k_d t)\right] \tag{9}$$

The parameter *s* in Equ 9 is called the efficiency of nitroxide (TEMPO). It is defined as:

$$s = \frac{[\mathrm{C\text{-}O\text{-}N}]_{formed}}{[\mathrm{N}]_0} \tag{10}$$

Therefore, we can define scorch time (t_r) as the time at witch $[N(t=t_r)] = 0$. Accordingly and using Equ 9, we obtain:

$$t_r = -\frac{1}{k_d}\ln\left[1-\frac{[N]_0}{2\alpha[DCP]_0}\right] \tag{11}$$

With (α = *f*/*s*) is the initiator and inhibitor efficiency ratio. After depletion of the inhibitor ($[N(t \geq t_r)] = 0$), active PDMS macro-radicals can combine and the crosslinking reaction occurs. Under such conditions and according to Equ 6, $[R_p^{\bullet}(t)]_{act}$ increases at a rate of :

$$\frac{d\left[R_p^{\bullet}(t)\right]_{act}}{dt} = 2 f k_d \left[DCP(t)\right] - k_{cc}\left[R_p^{\bullet}(t)\right]_{act}^2 \tag{12}$$

After initiation, the active macro-radicals concentration decreases according to the termination rate law (Equ 5). According to Equ 12, the rate of active radical is not constant over the crosslinking process. Consequently, the steady state principle does not hold true ($d[R_p^{\bullet}(t)]_{act}/dt \neq 0$). In order to find the time-dependent concentration $[R_p^{\bullet}(t)]_{act}$, the non-linear differential Equ 12 was integrated with the initial value of $[R_p^{\bullet}(t = t_r)]_{act} = 0$ to finally obtain for $t \geq t_r$:

$$\left[R_p^{\bullet}(t)\right]_{act} = \left\{\left[\frac{2 f k_d \left[DCP(t)\right]}{k_{cc}}\right]^{1/2} \times \tanh\left[\left(2 f k_{cc} k_d \left[DCP(t)\right]\right)^{1/2}(t - t_r)\right]\right\} \tag{13}$$

Following this and by substituting Equ 3 into Equ 13, the general kinetic law for $[R_p^{\bullet}(t)]_{act}$ is then derived:

$$\left[R_p^{\bullet}(t)\right]_{act} = \left\{ \begin{array}{l} \left[\dfrac{2 f k_d \left[DCP\right]_0 exp\left(-k_d t\right)}{k_{cc}} \right]^{1/2} \\ \times \tanh\left[\left(2 f k_{cc} k_d \left[DCP\right]_0 exp\left(-k_d t\right) \right)^{1/2} (t - t_r) \right] \end{array} \right\} \qquad (14)$$

Finally, using the mass conservation, the concentration of chemical bonds $[R_{cc}(t)]$ is determined as :

$$\left[R_{cc}(t)\right] = 1/2\left(\left[R_p^{\bullet}(t)\right]_{tot} - \left[R_p^{\bullet}(t)\right]_{act}\right) \qquad (15)$$

With $[R_p^{\bullet}(t)]_{tot}$ is the concentration of the total macro-radicals generated without taking account the competition between initiation and chains recombination reactions. Integrating Equ 12 between t_r and t with $k_{cc}([R_p^{\bullet}(t)]_{act})^2 = 0$ gives :

$$\left[R_p^{\bullet}(t)\right]_{tot} = 2 f \left[DCP\right]_0 \left(Exp\left(-k_d t_r\right) - Exp\left(-k_d t\right)\right) \qquad (16)$$

By substituting Equ 16 and Equ 14 into Equ 15, the kinetic model for this controlled crosslinking reaction and hence for the network growth prediction at the molecular scale can be expressed as following:

$$\left[R_{cc}(t)\right]=\left\{\begin{array}{l}\left[2f\left[DCP\right]_0\left(exp\left(-k_d t_r\right)-exp\left(-k_d t\right)\right)\right]- \\ \left[\frac{2f k_d\left[DCP\right]_0 exp\left(-k_d t\right)}{k_{cc}}\right]^{1/2}\times \\ \tanh\left[\left(2f k_{cc}k_d\left[DCP\right]_0 exp\left(-k_d t\right)\right)^{1/2}(t-t_r)\right]\end{array}\right\} \quad (17)$$

4. Results and discussion

4.1. Effect of TEMPO on the initiator efficiency

The scorch time (t_r) is also defined as the time at which the active polymer macro-radicals suddenly increase. From a viscoelastic point of view, the scorch time is defined [7] as the time at which the storage modulus suddenly increases (See ahead in Figure 9). The Equ 11 was derived from the assumption that the efficiency *f* of initiator is constant, regardless of the other crosslinking conditions. However, *f* can be affected by the crosslinking conditions such as temperature, crosslinking density and concentration of initiator and/or inhibitor [21]. Reordering Equ 11, we express the variation of the initiator and inhibitor efficiency ratio ($\alpha = f/s$) *vs* $[N]_0$ and $[DCP]_0$:

$$\alpha=\frac{\left[N\right]_0}{2\left[DCP\right]_0\left[1-Exp\left(-k_d t_r\right)\right]} \quad (18)$$

Figure 2a.

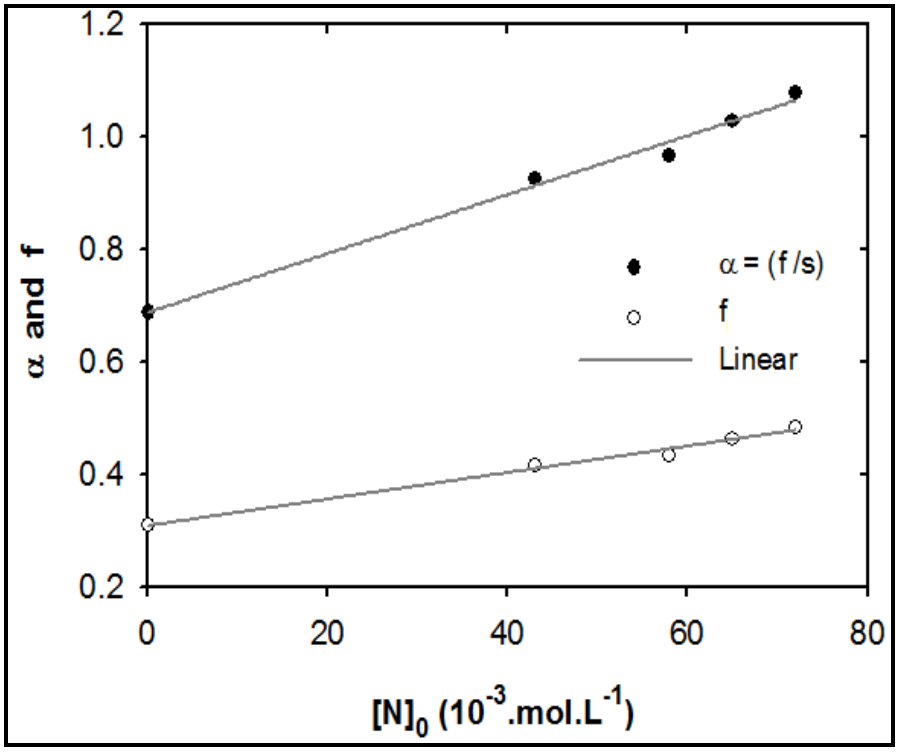


Figure 2b.

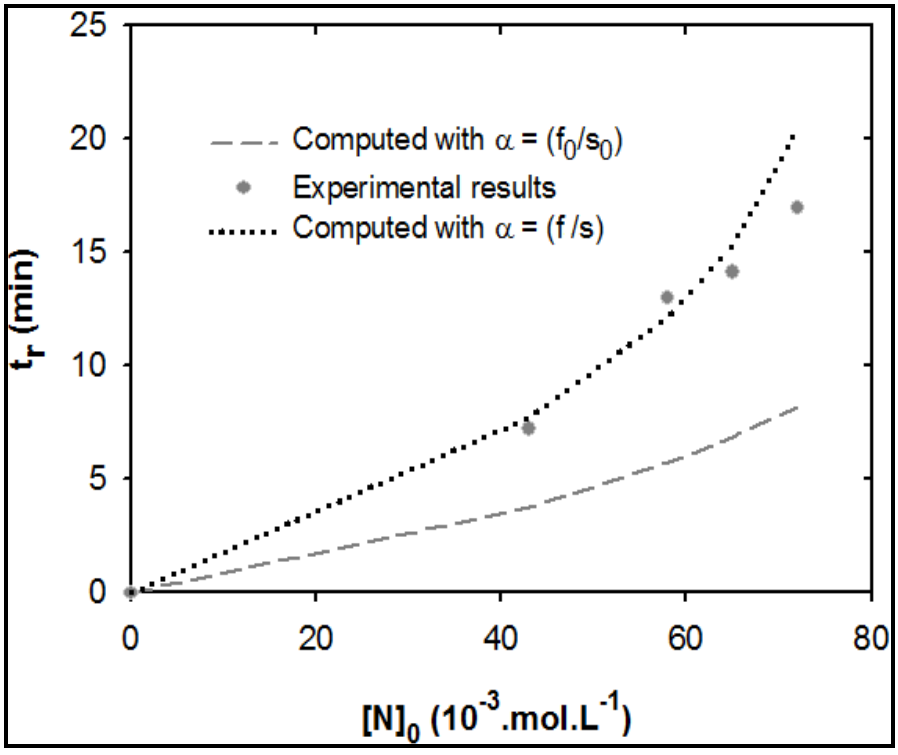


Figure 2. Dependence of the initiator efficiency and scorch time on TEMPO concentration. T=160℃

a) The linear lines are the best fit of experimental data according to Equ 19 (c_1 = 5.2 and α_0 = 0.69) and Equ 20 (c_2 = 2.34 and f_0 = 0.31). Here 'α' is efficiency ratio and '*f*' is initiator efficiency.

b) Comparison of computed and experimental values of the scorch time: Dashed line α = f/s according to Equ 19; Dotted line α = constant =f_0/s_0

Figure 2a shows the dependence of *α* on $[N]_0$ from the experimental variation of t_r at T=160℃. The results shown in Figure 2a prove that *α* is not constant but linear-dependent on the amount of TEMPO. Consequently, the linear extrapolation of the values obtained for r = 1.2, 1.6, 1.8 and 2 (see Table 1) allows us to determine the dependence of *α* on the initial concentration of TEMPO:

$$\alpha = c_1 * [N]_0 + \alpha_0 \tag{19}$$

Where, $\alpha_0 = 0.69$ and c_1 = 5.2 ($mol^{-1}.L$).

According to Equ 19 and initial conditions ($[DCP]_0=36 \times 10^{-3}$ $mol.L^{-1}$ and f_0 = 0.31 [7] for r = 0 (TEMPO free)), the inhibitor efficiency *s* must be equal to 0.45. Subsequently, from Equ 19 and with the calculated value for *s*, the dependence of *f* on the initial concentration of TEMPO can be predicted by the following equation:

$$f = c_2 * [N]_0 + f_0 \tag{20}$$

Where f_0 = 0.31 and c_2 = 2.34 $mol^{-1}.L$.

As a result, Figure 2a shows that initiator efficiency increases from 0.31 to 0.485 with $[N]_0$ (TEMPO concentration, see Table 1). This result is in agreement with the experiment results of Zhang and Ray [22]. Indeed, these authors proved that addition of stable radicals can boost the initiator efficiency.

Moreover, Figure 2b shows the TEMPO concentration dependence of t_r at T=160℃. The experimental results do not agree well with the linear relation of t_r *vs* $[N]_0$; i.e., the experimental scorch time is higher than the predicted one from of Equ 11 (with $f = f_0$, s_0 = 0.21 according to our previous work [7]). However, Figure 2b shows that the predicted times t_r are in close agreement with experimental results using Equ 11 with α= *f/s* as defined in Equ 19.

Table 1. Comparison between the experimental and the calculated values of scorch time, efficiency of TEMPO and initiator.

$[N]_0$ (10^{-3}.mol.L^{-1})	*r*	$t_{r,exp}$ (min)	$t_{r,cal}$ (min)	$\alpha=f/s$	*f*	$[R_{cc}]$ mol.m^{-3}	μ [a)] mol.m^{-3}
0	0	0	0	0.689	0.31	11.1	10.1
43	1.2	7.2	7.7	0.926	0.417	5.07	5.6
58	1.6	13	12.2	0.966	0.435	2.96	4
65	1.8	14.1	15.3	1.029	0.463	1.97	2.6
72	2.0	16.9	20.4	1.078	0.485	1.02	1.6

NB: $[R_{cc}]$ is the total concentration of crosslinked bonds when the reaction is completed. Initial concentration of DCP: $[DCP]_0 = 36 \times 10^{-3}$ mol.L^{-1} and T=160℃.

[a)] is retrieved from ref. [7]

4.2. Determination of k_{cc} using anisothermal DSC data

During crosslinking reaction the long chains of the polymer chemically crosslink. Each covalent C-C bond formed between the macromolecular chains of polymer releases a quantum of energy. One of the methods mostly used in the literature to determine the enthalpy and kinetic parameters of this crosslinking reaction is thermal analysis by differential scanning calorimetry (DSC) at anisothermal mode [23]. The dynamic mode allowed us to estimate k_{cc} as a function of the temperature. Indeed, reaction rate depends on time and temperature. Kissinger [24] was one of the first

researchers who evaluated the kinetic parameters of a chemical reaction from the anisothermal DSC using peak temperature-heating rate data, with the following equation:

$$Ln\left(\dot{T}/T_{peak}^{2}\right)=\frac{E_{ac}}{R}\left(\frac{1}{T_{peak}}\right)-Ln\left(\frac{A_{0c}R}{E_{ac}}\right) \tag{21}$$

Where $\dot{T}$ is heating rate and R is the ideal gas constant. The kinetic parameter A_{0c} represents collision frequency factor and E_{ac} is activation energy for the bimolecular termination reaction (crosslinking reaction). Kissinger's method assumes that the maximum reaction rate occurs at peak temperatures (T_{peak}). Therefore, by plotting $Ln(\dot{T}/T^2_{peak})$ versus $1/T_{peak}$ according to Equ 21, E_{ac} can be then obtained from the slope of the corresponding straight line and A_{0c} corresponds to the ordinate at origin.

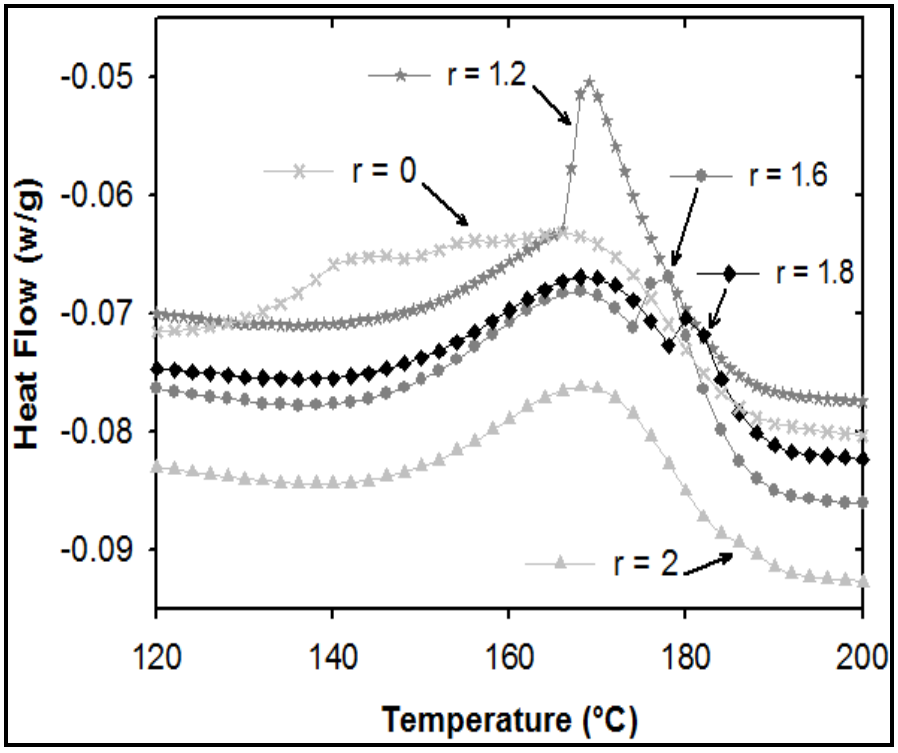


Figure 3. DSC curves showing the total heat of crosslinking reaction obtained for various values of *r* at a heating rate of 2.5 ℃.min $^{-1}$. Where *r* = [TEMPO]/[DCP].

The anisothermal DSC scans of (PDMS/DCP/TEMPO) curing system at different amount of TEMPO (r=0, 1.2, 1.6, 1.8 and 2) are shown in Figure 3. Confirming our last original results with isothermal mode [7], these dynamic DSC kinetics allowed us to separate exothermic peak of C-C bonds creation from the other reactions like the homolytic decomposition of the initiator (DCP) and its addition on the polymer chains. Furthermore, the addition of TEMPO in the PDMS/DCP system results in a secondary exothermic peak, as shown in Figure 3. This peak is assigned to C-C bonds creation. This hypothesis is validated by comparison of the rheological and DSC results in anisothermal mode for r =1.2 as shown in Figure 4. The end of the inhibition phase is observed by both techniques; i.e., strong variation of the complex shear modulus and evidence of a second exothermic peak. As a result, this peak temperature corresponds exactly to the network formation through the chemical crosslink reaction between PDMS polymer chains.

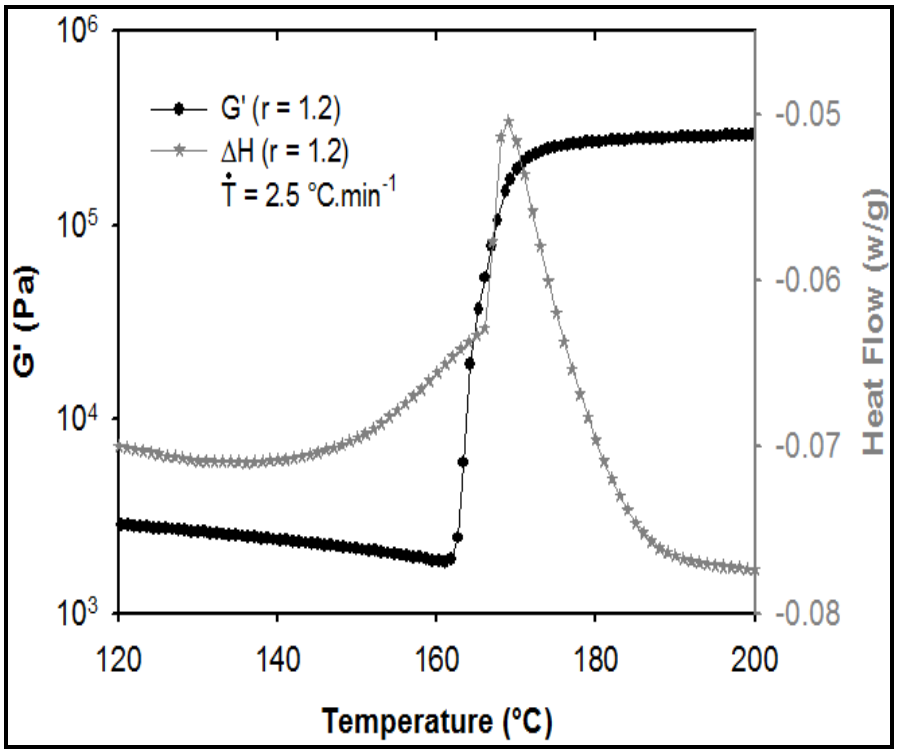


Figure 4. Comparison of the variation of the storage modulus and enthalpy of the reaction (r =1.2) under anisothermal condition $\dot{T}$ = 2.5 °C.min $^{-1}$.

Experimentally, the peak temperature of the termination reaction shifts to higher temperatures with increasing the heating rate. This is probably because the reaction takes place very rapidly at higher curing temperatures. More precisely, the dependence of $Ln(\dot{T}/T^2_{peak})$ on $(1/T_{peak})$ is plotted and the linear variation of T_{peak} with the heating rate is observed to be in agreement with the Kissinger assumption based on the linear relation between peak temperature and heating rate. Consequently, E_{ac} and A_{0c} were calculated according to Equ 21. The dependence of k_{cc} on the temperature can be expressed using the Arrhenius law:

$$k_{cc} = A_{0c} Exp\left(-E_{ac}/RT\right) \tag{22}$$

Where, $A_{0c} = 2.68 \times 10^{10}$ s^{-1} and $E_{ac} = 87300$ $J.mol^{-1}$.

4.3. Kinetics of chemical network growth

The influence of the experimental conditions ($[DCP]_0$, $[N]_0$, α and T) on the cross-linking reaction kinetics and network growth, has been studied at the molecular scale according to this newly developed kinetic model. Note that in the following part equations 19 and 20 were used to derive *α* and *f* respectivly for use in Equ 14, 16 and 17.

According to Equ 14 (T = 160 ℃), the time-concentration variation of a ctive PDMS carbon-centered radicals $[R_p^{\bullet}(t)]_{act}$ is plotted in Figure 5a. Without TEMPO (r=0), the initiation reaction occurs instantaneously and PDMS macro-radicals concentration increases to an optimal value followed by continuous decrease as the termination reaction is faster than initiation. In the presence of TEMPO, scorch time is highlighted and increases with increasing the TEMPO concentration (i.e. the ratio *r*). From a modelling point of view, the active chains are created and instantaneously inactivated by TEMPO addition reaction during this inhibition phase. The residual concentration of

DCP after the complete consumption of TEMPO can initiate other polymers chains so that the generation of $[R_p^{\bullet}(t)]_{act}$ can be observed as shown in Figure 5a.

Figure 5a

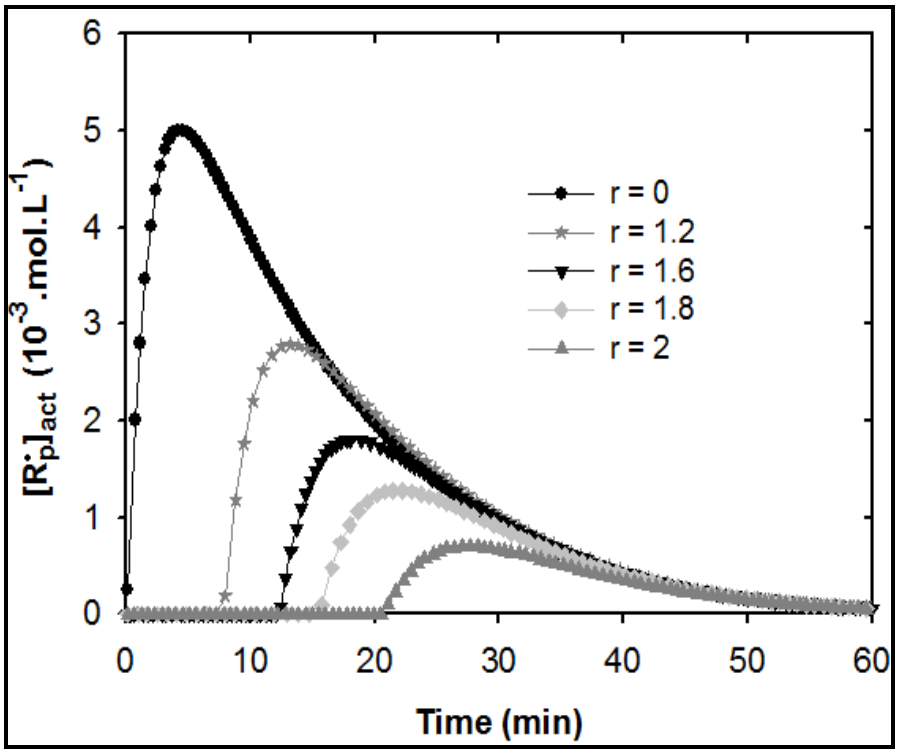


Figure 5b

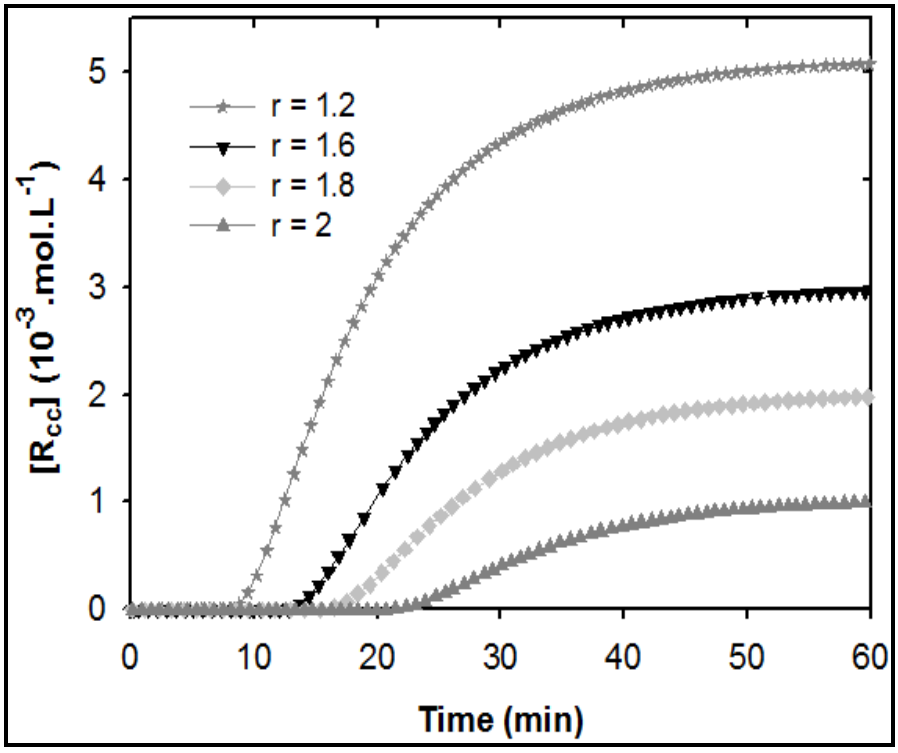


Figure 5c

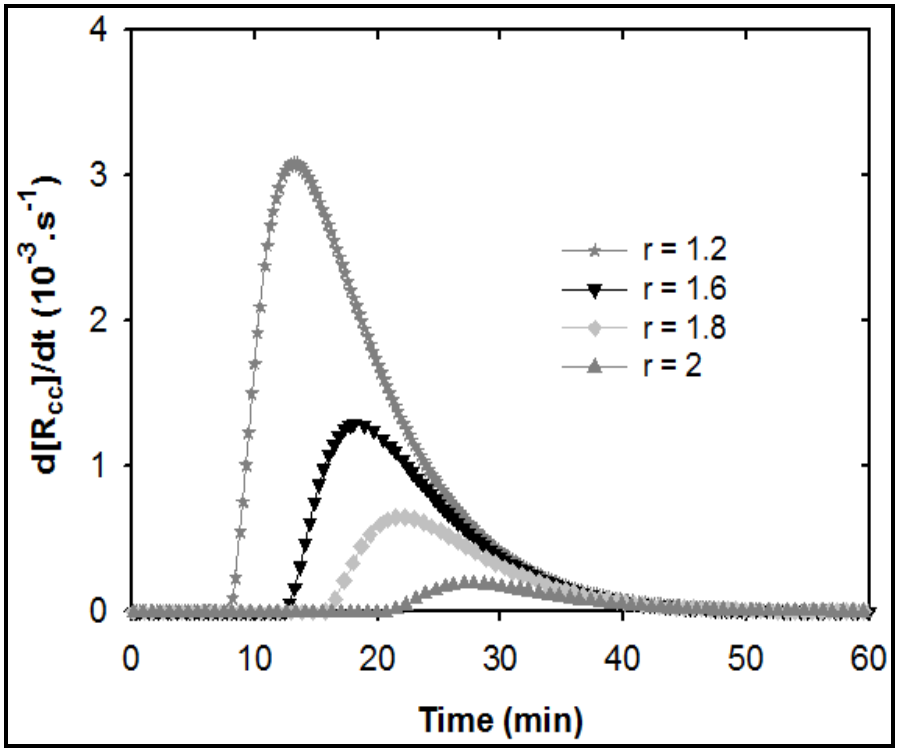


Figure 5. Time dependence of PDMS crosslinking reactions for various values of r=[TEMPO]/ [DCP]. T= 160℃; $[DCP]_0 = 36\times10^{-3}$.mol.$L^{-1}$

a) Variation of active carbon-centered radicals

b) Variation of crosslinked bonds concentration versus crosslinking time

c) Variation of crosslinking rate

On the other hand, the optimal $[R_p^{\bullet}(t)]_{act}$ values for $t > t_r$ decrease with increasing the initial TEMPO concentration. Actually, this result was expected from our previous work [7]. We proved that the crosslinling delayed action in the presence of TEMPO is the result of trapped carbon-centered polymer radicals by nitroxides. Furthermore, TEMPO interacts with the macro-radicals from vinyl-PDMS during scorch phase to produce non-reactive species. Consequently, the bimolecular termination reaction is completely prevented ($[R_p^{\bullet}(t < t_r)]_{act}= 0$). One TEMPO has completely reacted, the macro-radicals coupling (crosslink formation) starts in respect of the residual concentration of $[R_p^{\bullet}(t > t_r)]_{act}$.

To show the key effect of TEMPO on the curing process, Figure 5b compares the concentration variation of the crosslinking covalent bonds $[R_{cc}(t)]$ with the reaction time (according to Equ 17 at T= 160℃) for different initial concentrations of TEMPO. It can be clearly seen how the TEMPO influences the scorch time, the crosslinking reaction rate and final concentrations of crosslinking bonds ($[R_{cc}]$).

During the inhibition stage, TEMPO inactivate the primary PDMS macro-radicals and prevent the radical coupling $[R_{cc}(t < t_r)] = 0$. Therefore, if we accept that the TEMPO is completely consumed during the scorch period and that the crosslinking reaction does not begin until the TEMPO is totally consumed, the bimolecular termination reaction starts but it is slows down due to lower concentration of initiator. Kinetically, the reduction in the concentration of active PDMS macro-radicals shown in Figure 5a by TEMPO slows down the crosslinking rate ($d[R_{cc}(t)]/dt$) according to Equ 5. According to these results, Figure 5b demonstrated that TEMPO is a very powerful inhibitor for free-

radical crosslinking of PDMS and that the crosslinking kinetics are entirely in agreement with the kinetic scheme in Figure 1.

According to Figure 5c, the rate of the crosslinking reaction $d[R_{cc}(t)]/dt$ predicted from Equ 5 may be very low initially. This results explain the difference between kinetics of $[R_p^{\bullet}(t)]_{tot}$, $[R_p^{\bullet}(t)]_{act}$ and $[R_{cc}(t)]$ at the beginning of the macro-radicals coupling phase. It should be noted that $k_d = 2.3 \times 10^{-3}\ s^{-1}$ and $k_{cc} = 0.8\ (L.mol^{-1}.s^{-1})$ at T=160℃, and the slow kinetic start of the chains recombination may be the result of the competition between the initiation and the bimolecular termination reactions. Thereafter, $d[R_{cc}(t)]/dt$ gradually increases to a maximum rate before decreasing with the decrease of $[R_p^{\bullet}(t)]_{act}$ at the end of crosslinking phase. Interestingly, we obtain the maximal values of $[R_{cc}] = 0.5 \times [R_p^{\bullet}]_{tot}$ at the end of the numerical computations (see Table 1), such as $[R_p^{\bullet}]_{tot} = 22.2 \times 10^{-3}.mol.L^{-1}$ and $[R_{cc}] = 11.1 \times 10^{-3}.mol.L^{-1}$ for r = 0 at T= 160 ℃.

Furthermore, the comparison of the predicted final $[R_{cc}]$, i.e. when the reaction is completed, with our last results of μ (density of chemical crosslink bonds) [7] computed by using Pearson and Graessley model (presented in Table 1) shows a very satisfactory agreement which validates our kinetic hypothesis. On the other hand, the dependence of the computed final concentrations of crosslinking bonds $[R_{cc}]$ and total macro-radicals $[R_p^{\bullet}]_{tot}$ versus $[N]_0$ at T = 160℃ is shown in Figure 6. It can be observed that optimal values of $[R_p^{\bullet}]_{tot}$ and $[R_{cc}]$ are linearly dependent on the initial TEMPO concentration. According to linear extrapolation of $[R_{cc}]$, the total amount of TEMPO necessary to totally prevent the crosslinking reaction ($[R_{cc}] = 0$) is then equal to $79 \times 10^{-3}.mol.L^{-1}$. Translating this value in terms of [TEMPO]/[DCP] ratio leads to r = 2.2. This result is in agreement with the value observed from rheological measurement r = 2.4 for which no crosslinking reaction was observed. In addition, these numerical results confirm our prediction using the DSC technique in the last experimental work [7].

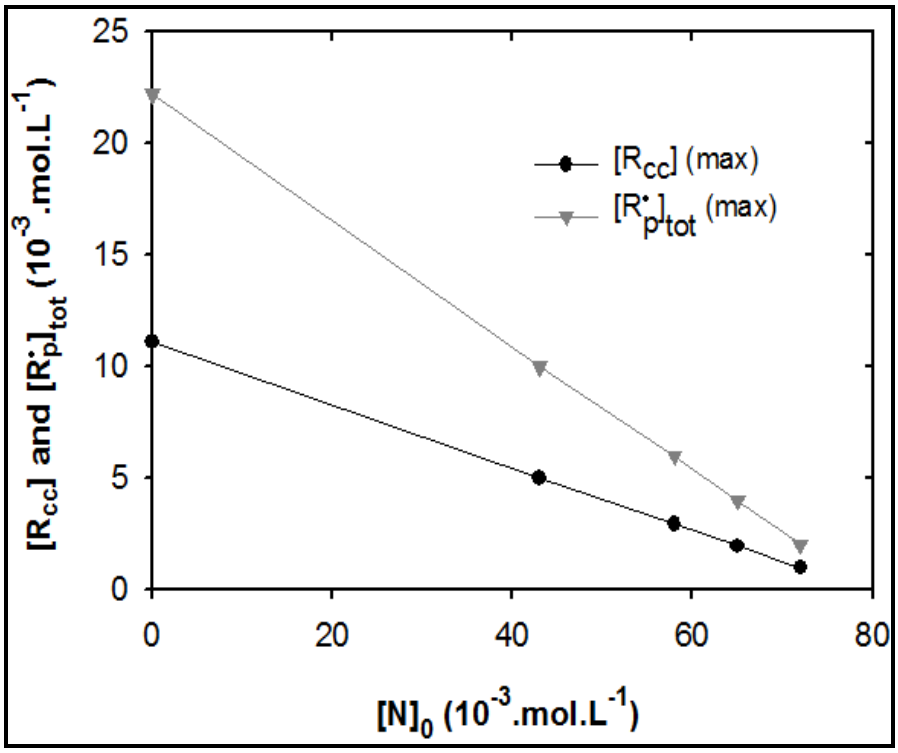


Figure 6. Dependence of the final concentrations of crosslinking bonds, $[R_{cc}]$, and total macro-radicals, $[R_p^{\bullet}]_{tot}$ on the initial concentration of TEMPO at T=160℃.

Finally, it can be concluded from the variation of k_d and k_{cc} with temperature that our model is able to predict the variation of $[R_{cc}(t)]$ (including inhibition time) for any temperatures and any ratio. However, this temperature dependence is not plotted here for brevity and clarity. The temperature dependence will be checked in the next part on the variation of the viscoelastic properties versus time for different values of *r*.

4.4. Rheo-Kinetic modelling

The main objective of this work is to predict the changes of viscoelastic properties of PDMS during a free-radical crosslinking process controlled by the addition of TEMPO. We have established in the previous part that the kinetic model is capable to predict peroxide decomposition [DCP(t)], active PDMS carbon-centred radicals $[R_p^{\bullet}(t)]_{act}$, and crosslink formation $[R_{cc}(t)]$. Then, rheo-kinetic modelling aims to predict the time

variations of the complex shear modulus ($G'(t)_\omega$ and $G''(t)_\omega$). This can be achieved from the variation in crosslinking bonds formation [$R_{cc}(t)$] derived from Equ 17. However, at present we cannot theoretically predict the relationship between complex shear modulus and [$R_{cc}(t)$]; excepted when the reaction is completed (prediction of the equilibrium modulus). As far as we know, such kind of work for free-radical crosslinking process has never been reported in the literature from the standpoint of quantitative analysis. We solved this task by carrying out some experiments of crosslinking with different initial concentrations of DCP and TEMPO at T=160 ℃. Furthermore, combining Equ 17 (kinetic model) and the experimental variation of complex shear modulus with the reaction time, we can experimentally express the variation of complex shear modulus versus radical coupling [$R_{cc}(t)$] through a master curve.

From a numerical point of view, kinetic model was implemented through Matlab Figure 7 plots the variation of the complex shear modulus versus the crosslinking bond concentration [$R_{cc}(t)$] for r = 1.2 at T = 160 ℃, by using experiment al variation of complex shear modulus and kinetic equation 17. We used this curve as reference and the time dependence of complex shear modulus was predicted for any temperature and any initial DCP or TEMPO concentrations.

Figure 8 shows the prediction of storage modulus $G'(t)_\omega$ for different [TEMPO]/[DCP] ratio at T=160℃. As expected, the addition of TEMPO results in the increase of the predicted scorch time t_r. In addition, all simulations exhibit a plateau after a long period of time which expresses the completion of crosslinking reaction. The frequency sweep experiment proved that this plateau is the equilibrium modulus G_e. However, it is clear that the time needed by the modulus to reach a plateau gets longer as TEMPO concentration increases. Furthermore, it can be seen that the rheo-kinetic model predicts a decrease in equilibrium storage modulus (G_e) as TEMPO input increases. As far as we know, such kind of results has never been reported in the literature from a quantitative viewpoint.

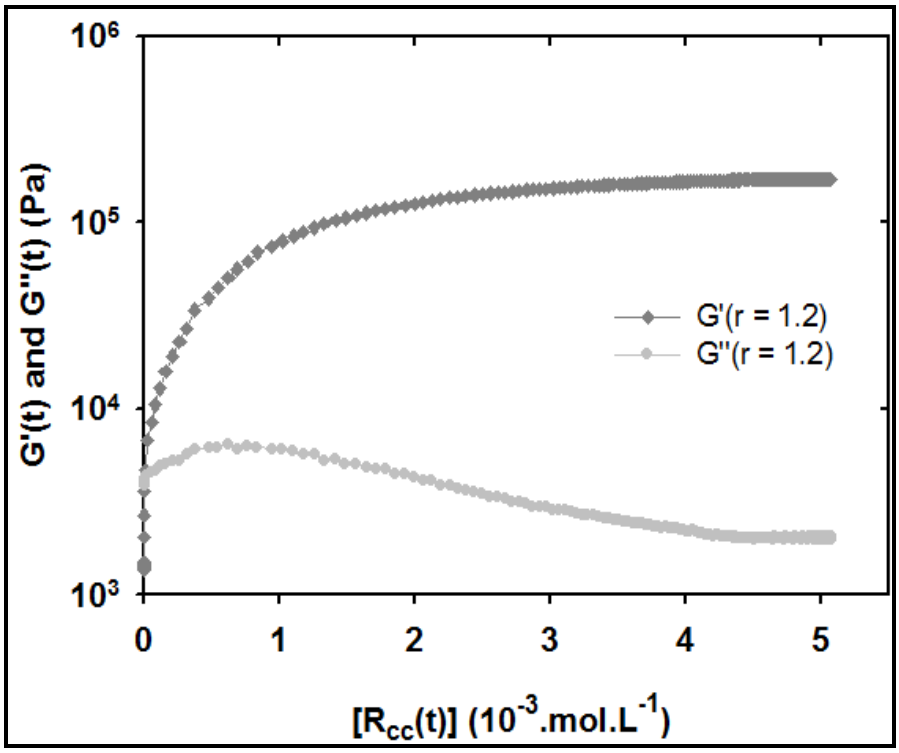


Figure 7. Variation of the complex shear modulus versus the effective concentration of crosslinking bonds [R_{cc}] at T = 160 ℃. This curve was used as reference f or modelling developments.

However, Figure 8 shows that the model slightly overestimates the equilibrium storage modulus for r =1.8 and 2. This result can be explained by the fact that the Rheo-kinetic model overestimates the effect of physicals entanglements for lower equilibrium storage modulus. Actually the time variation of complex shear modulus for r = 1.2 was used as reference curve. So the rheological model includes the trapped physical entanglements. Nevertheless, the probability of such trapping is expected to decrease with decreasing the crosslinking density; whereas the model takes into account a constant probability whatever the final crosslinking density. Moreover, Figure 8 shows a slowly decrease of the experimental storage modulus at the earlier stage of reaction. This phenomenon is clearly shown for r=2. This significant decrease in complex modulus may be attributed to PDMS degradation in the presence of TEMPO nitroxide. This behaviour can not be

predicted here because the complex degradation mechanism (detailed in our previous work [7]) was not investigated in the present kinetic model.

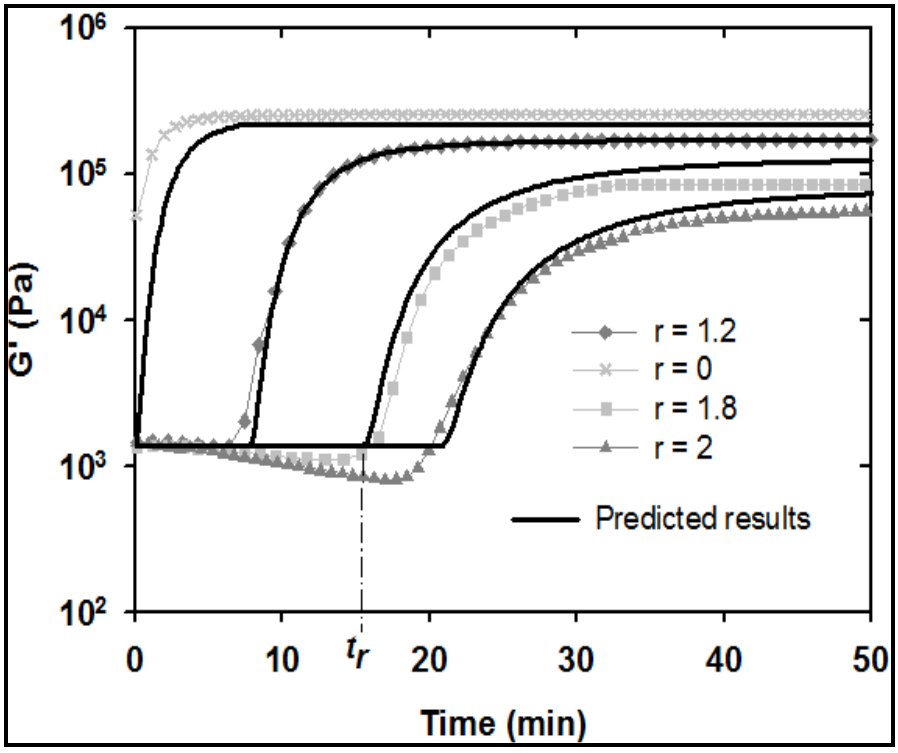


Figure 8. Modelling of the time variations of storage modulus for different ratios: r = 0, 1.2, 1.8, 2. (T=160℃). Solid curves are obtained f rom simulations, while patterned lines are drawn from experimental data.

Comparison of the predicted storage and loss modulus with rheometer data for different [TEMPO]/[DCP] ratio at T=160℃ is shown i n Figure 9a and b. From a qualitative point of view, the viscoelastic variation of $G'(t)_\omega$ and $G''(t)_\omega$ was remarkably predicted by the rheo-kinetic model. Interestingly, Figure 9b shows that at higher amount of TEMPO (r=2.4), the rheo-kinetic model predicted that the crosslinking reaction was totally prevented.

Figure 9a.

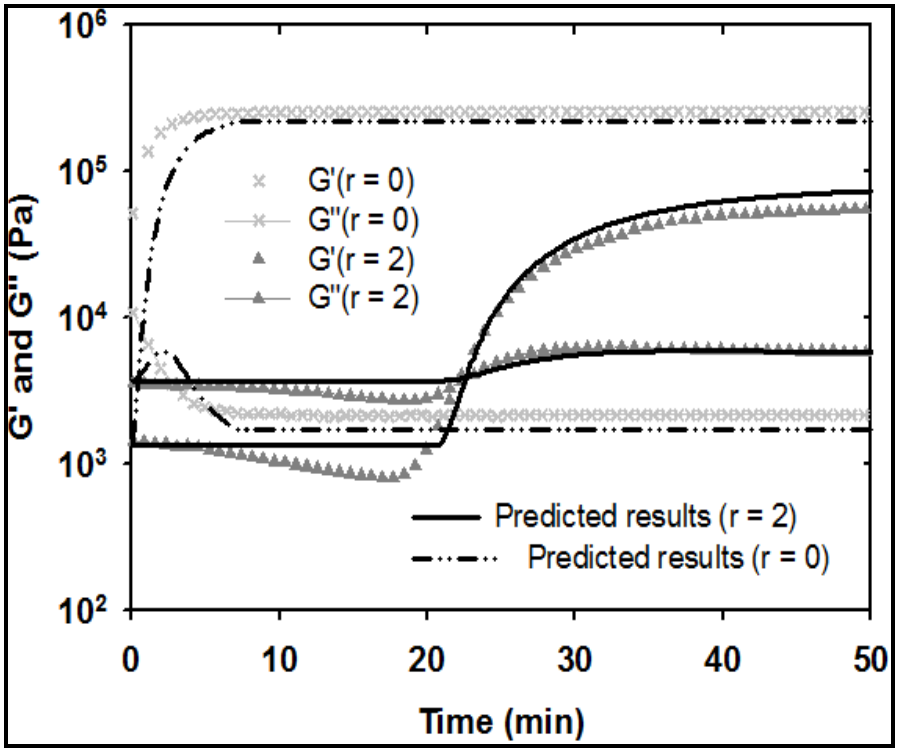


Figure 9b.

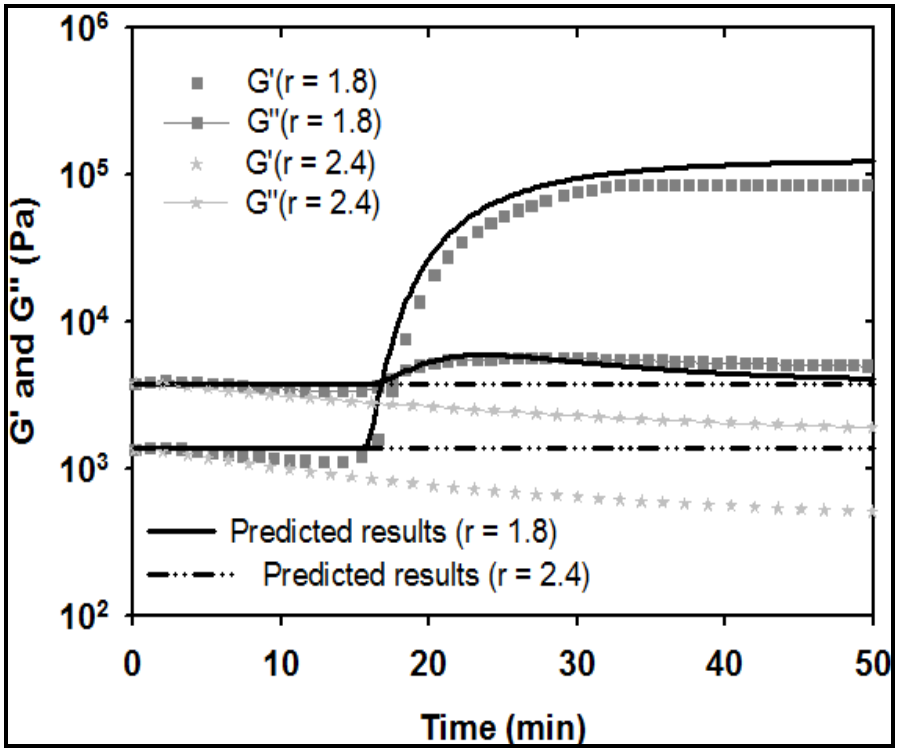


Figure 9. Modelling of the time variation of the complex shear modulus for different [TEMPO]/[DCP] ratios (T = 160 ℃): Solid curves are obtained from simulations, while patterned lines are drawn from experimental data. a) r = 0 and r=2.0, b) r=1.8 and r=2.4

Finally, Figure 10 shows that the rheo-kinetic model predicts well the variation of storage modulus versus time at different temperatures (T=160, 180, and 200℃) for r=1.6. As experimentally observed, the rheo-kinetic model predicts that the scorch time decreases with the increase in temperature. For example, the model predicts that t_r shifted from 12.2 min at 160 ℃ to 2.2 min at 180 °C and crosslinking becomes "instantaneous" at 200 ℃. Finally, as expected fro m our hypothesis, the model predicts that the equilibrium modulus does not depend on the temperature. This behaviour is not observed for the experimental variation due to side reactions which can occur at the higher temperatures (T> 170℃) according to Mskani et al [15].

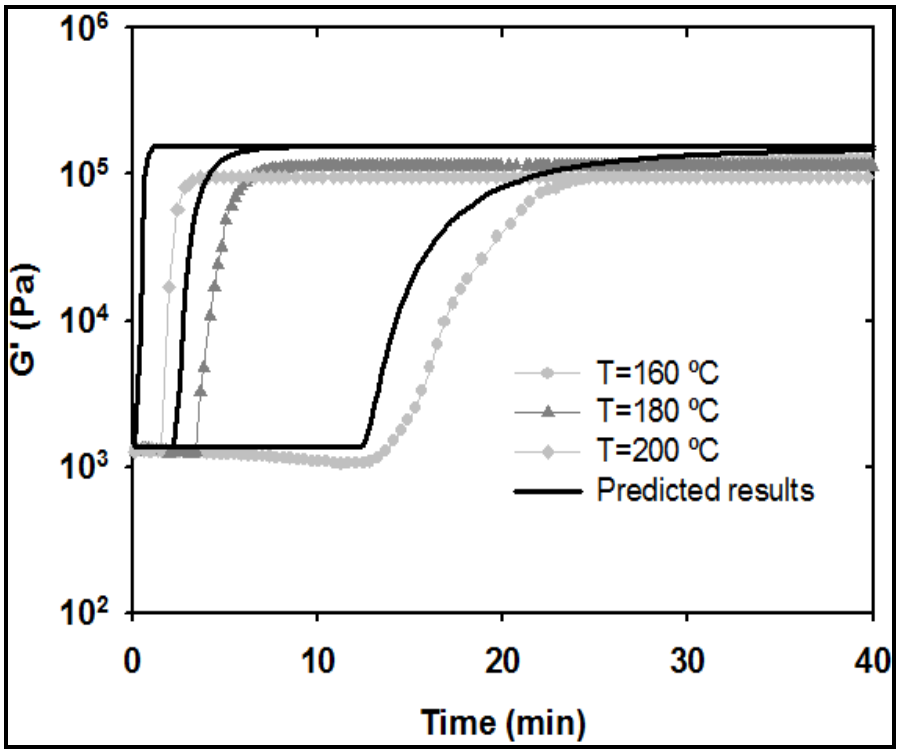


Figure 10. Modelling of the time variation of the storage modulus for different temperatures at r = [TEMPO]/[DCP] = 1.6. Solid curves are obtained from simulations, while patterned lines are drawn from experimental data.

5. Conclusion

In this study, a new rheological modelling method was developed to predict the variation of complex shear modulus for PDMS network formation under free radical crosslinking reaction controlled by TEMPO. This new method is based on the relationship between the kinetic of the macro-radicals coupling [$R_{cc}(t)$] derived from a fundamental kinetic model and the viscoelastic variation of complex shear modulus ($G'(t)_\omega$ and $G''(t)_\omega$). Owing to the complexity of crosslinking chemistry, a simplified reactions scheme was used to establish the fundamental kinetic model.

First of all, a kinetic model was derived in order to predict the crosslinking process including decomposition of the peroxide [DCP(t)], active PDMS carbon-centered radicals $[R_p^\bullet(t)]_{act}$ creation, inhibition reaction time t_r and the crosslinking bonds formation [$R_{cc}(t)$]. The influence of formulation conditions such as ($[DCP]_0$, [TEMPO]/[DCP] and Temperature) on the crosslinking reaction kinetics and the network growth, has been studied at the molecular scale according to this kinetic model. It was observed that the addition of TEMPO nitroxide can boost the initiator efficiency. On the other hand, the Kissinger DSC method was used to calculate the activation energy E_{ac} (87300 J.mol^{-1}) and the collision frequency factor A_{0c} (2.68 x 10^{10} s^{-1}) for the bimolecular termination reaction rate k_{cc}.

Finally, the rheological modelling shows that this new method precisely predicts the time variation of the complex shear modulus at any temperature and [TEMPO]/[DCP] ratio. Although, this modelling has been developed for PDMS rubber, it can easily be extended to any rubber crosslinking via radical chemistry in the presence of nitroxide.

References

[1] Yuxi, J.; Sheng, S.; Shuxia, X.; Lili, L.; Guoqun, Z. Polymer 2002, 43, 7515-7520.

[2] Blaz, L.; Matjaz, K. Polym. Eng. Sci. 2008, 49, 60-72.

[3] Yuxi, J.; Sheng, S.; Lili, L.; Yue, M.; Lijia, A. Acta. Materialia 2004, 52, 4153-4159.

[4] Baquey, G.; Moine, L.; Degueil-Castaing, M.; Lartigue, J.C.; Maillard, B. Macromolecules 2005, 38 (23), 9571–9583.

[5] Dorn, M. Adv. Polym. Technol. 1985, 5, 87-91.

[6] Chaudhary, B.I.; Chopin, L.; Klier, J. J. Polym. Sci. 2007, 47, 50-61.

[7] Mani, S.; Cassagnau, P.; Bousmina, M.; Chaumont, P. Macromolecules 2009, 42, 8460-8467.

[8] Langley, N.R., J.D. Macromolecules 1968, 1, 348-352.

[9] Dossin, L.M.; Graessley, W.W. Macromolecules 1979, 12, 123-130.

[10] Robert, P.M. EP 0,837,080, A1; 1997.

[11] Esseghir, M.; Chaudhary, B. I.; Cogen, Jeffrey M.; Klier, J.; Jow, J.; Eaton, R. F.; Guerra, S. M. U. S Patent 7, 465, 769 B2; 2008.

[12] Ciullo, P. A.; Hewitt, N. 'The rubber formulary'', New York, 1999.

[13] Dluzneski, P. R. Rubber Chem. Technol. 2001, 74, 451-492.

[14] Kurdikar D. L.; Peppas, N. A. Macromolecules 1994, 27, 4084-4092.

[15] Msakni, A.; Chaumont, P.; Cassagnau, P. Rheol. Acta. 2007, 46, 933-943.

[16] Flat, J. J. Private communication. Internal report from Arkema Company 2004.

[17] Russell, K. E. Prog. Polym. Sci. 2002, 27, 1007-1038.

[18] Zhou, W.; Zhu, S. Macromolecules 1998, 31, 4335-4341.

[19] Berzin, F.; Vergnes, B.; Dufosse, P.; Delamare, L. Polym. Eng. Sci. 2000, 40, 2, 344-356.

[20] Bamford, C. H.; Tipper, C. F. H. "Free-radical polymerisation-Comprehensive chemical kinetics", Vol. 14A, New York, Elsevier 1976, Chap.1, p.7.

[21] Han, C. D.; Lee, D. S. J. Appl. Polym. Sci. 1987, 34, 793-813

[22] Zhang, M.; Ray, W. H. J. Appl. Polym. Sci. 2002, 86, 1630-1662.

[23] Yousefi, A.; Lafleur, P. G. Polym. Comp. 1997, 18 (2), 157-168.

[24] Kissinger, H. E. Anal. Chem.1957, 29, 1702-1706.

Chapter 4

Morphology Development in Novel Composition of Thermoplastic Vulcanizates Based on PA12/PDMS Reactive Blends

Abstract

The main objective of the present work was to tailor a new thermoplastic vulcaniste (TPV) composed of Polyamide 12 (PA12) as the thermoplastic phase and Polydimethyl-vinylmethyl-siloxane (PDMS) as the rubber phase. The PDMS was crosslinked by dicumyl peroxide (DCP). Interestingly, addition of 2,2,6,6-tetramethylpiperidinyloxyl

(TEMPO) to the TPV provided the compatibilization of the PA12/PDMS blend in the dynamic process and gave a new material with control structure and morphology. The Electron microscopy (SEM and TEM) studies revealed that adding silica nanoparticles and Lotader in PA12 and PDMS phases, respectively, led to a drastic reduction in R_v of the PDMS particles from 16.5 µm (virgin blend) to nearly 0.6 µm for the PA12/PDMS reactive blend. Therefore, a stable co-continuous morphology was obtained for the new TPV based on 60-40 wt.-% of PDMS-PA12 blend.

This chapter 4 was published in ***Macromolecular Materials and Engineering Journal 2011, 296, 1-12.***

1. Introduction

The development of new thermoplastic vulcanizates (TPVs) [1-3] has been a very active area in the field of polymer processing, because dynamic vulcanization [4] can be used to obtain desired thermoplastic/rubber blends with controlled structure and morphology. Depending on the structure and the nature of the dispersed phase, one may tailor a wide spectrum of TPV material properties [5]. Furthermore, TPVs have several advantages over the traditional crosslinked elastomers, since functional performances similar to those of thermoset elastomers can be obtained using the classical processing tools of polymer melts, while being at the same time recyclable as thermoplastics [6]. However, conventional TPV based on polypropylene (PP) matrix and a vulcanized ethylene propylene diene monomer (EPDM) rubber phase have found limited use in automotive underhood applications that require continuous use temperatures exceeding 135℃ and oil resistance [7]. To satisfy these needs, Dow Corning developed in early 2004 a new family of TPV called “Super-TPV” based on vulcanized silicone rubber particles dispersed in a variety of engineering-thermoplastic matrixes [8]. The Super-TPV class designed to replace higher-cost thermoset rubbers and upgrade the performances of conventional TPVs in more extreme applications, notably in automotive underhoods and industrial parts subjected to high temperatures (135 to 170℃) in the presence of oils and greases. Recently, Super-TPV class was broadened by the introduction of new members from Zeon Chemicals and DuPont Engineering Polymers [9]. These new Super-TPVs are based on a continuous morphology of polyamide thermoplastic matrix and dynamically vulcanized polyacrylate (ACM) elastomer [10]. In this context, blends of thermoplastic polymers with polydimethylsiloxane (PDMS) silicone rubber are of particular interest and a new Super-TPV with some synergism of physico-chemicals and mechanical properties can be obtained.

Indeed, PDMS is widely used in a variety of industrial niches because of its well known unique properties [11]. Its structure is composed of highly flexible O-Si-O bonds in the main chain, with methyl groups attached to a silicon atom [12]. Hence, their

physical and chemical properties combine both inorganic and organic characteristics. Because of this peculiar molecular architecture, PDMS has excellent low and high temperature retention of mechanical properties, excellent aging, dielectric properties, and thermal stability [13], but it has low resistance to oil and solvents [14]. In the present investigation, a blend of PDMS and Polyamide 12 (PA12) has been chosen to prepare a new Super-TPV material with controlled dispersed or co-continuous morphology. PA12 has excellent solvent and oil resistance, in particular acid and alkali resistance, and excellent environmental stress cracking resistance at elevated temperatures [15]. However, the PDMS low solubility parameter makes it highly immiscible and incompatible with the majority of organic polymers such as PA12 [16]. This immiscibility leads to a PA12/PDMS blend with coarse morphologies, causing fast deterioration of the blend properties due to thermodynamically driven phase separation. Moreover, PDMS tends to migrate toward the surface due to its low surface free energy (around 19 mN/m at 20 ºC). This effect results in a surface covered by a hydrophobic liquid PDMS that causes undesired adsorption of hydrophobic contaminants and poor surface properties [17].

Usually, a high interfacial tension [18] between the phases in immiscible polymer blends leads to coarse and unstable morphologies [19], which can be overcome by addition or in-situ formation of compatibilizers that act as interfacial agents [20]. The physical and mechanical properties of the blends can be greatly improved by using such compatibilizers, which reduce the interfacial tension between the two phases, increase the surface area of the dispersed phase, promote adhesion between the phase components, and stabilize the dispersed phase morphology [21]. Likewise, a new concept of compatibilization by using solid nanoparticles has been recently introduced. The work of Bousmina and coworkers [22-28] summarizes well the questions that arise when trying to identify the mechanisms involved in the refinement of the morphology by nanofillers. Actually, several phenomena can lead to morphology changes: (i) reduction in the interfacial energy, (ii) inhibition of coalescence by the presence of a solid barrier around the minor polymer drops, (iii) changes in the viscosity of the phases due to the uneven distribution of the filler, (iv) immobilization of the dispersed drops (or of the

matrix) by the creation of a physical network of particles when the concentration of the solid is above the percolation threshold, and (v) the strong interactions of polymer chains onto the solid particles inducing steric hinderance. For instance, Elias et al. [29] have investigated the role of hydrophobic and hydrophilic silica nanoparticles on the morphology stabilization in immiscible PP/PS blend and concluded that the mechanism of morphology stabilization of PP/PS blend by hydrophilic silica was the reduction in the effective interfacial tension, whereas hydrophobic silica particles act as a rigid layer preventing the coalescence of PS droplets. Martin et al. [30] investigated the influence of silica nanoparticles on the uncrosslinked PP/EPDM blends and showed that silica nanoparticles stabilized the blends morphology and affected their relaxation behaviour. In the same line, Maiti et al. [31] studied the distribution of silica nanoparticles in nitrile rubber (NR) and epoxidized natural rubber (ENR) blends and found that silica nanoparticles migrated preferentially to the ENR phase and stabilized the blend morphology by preventing the coalescence of the droplets, making this morphology thermo-mechanically stable. It was argued that the reasons for the preferential migration of silica to ENR phase included the low viscosity of the ENR and physical interactions between the epoxide group of ENR and the silanol group of silica. Another study by Thareja and Velankar [32] showed that the addition of fumed silica nanoparticles in PDMS/PIB blends can induce clustering of the drops and consequently stabilize droplets coalescence. Actually, the mechanism by which silica nanoparticles stabilize the morphology against coalescence is not fully understood yet. Most of the authors concluded that the fillers act as physical barriers due to their accumulation at the interface, which prevent the coalescence of the dispersed phase [33]. More recently, Fenouillot et al. [34] investigated theoretically the competition between thermodynamic wetting of the silica nanoparticles by the polymeric phases and kinetic control of the filler localization and linked the effect of the filler particles to the rate of the mixing process. This aspect is believed to be a specificity of filled polymer blends and is known to have a drastic and sometimes predominant effect on particle localization and therefore finely tuned morphologies in immiscible polymer blends can be obtained, where the particles do not occupy their equilibrium position.

On the other hand, only few studies have addressed the compatibilizion of PDMS based blends. Kole et al. [35] showed that the incompatible nature of 50/50 silicone PDMS and EPDM rubber blends was overcome by the introduction of silane-grafted ethylene-propylene copolymer (EPR), which interacts with both components. In such ternary blends (matrix, dispersed phase and compatibilizer), a core-shell morphology can be observed [36]. For example, PP and polyamide 6 (PA6) (70-30 wt%) blend showed very coarse morphology and poor mechanical properties, but by using the reactive compatibilizer, SEBS-g-MA, PA6 was encapsulated by SEBS-g-MA and the final mechanical properties were enhanced [37]. Maric et al. [38] attempted to exploit amine/anhydride, amine/epoxy and carboxylic acid/epoxy reactions to compatibilize PDMS blends with both PA6 and polystyrene (PS). Recently, Santra et al. [39] showed that EMA can compatibilize the low-density polyethylene (LDPE) and PDMS rubber blend. They also showed [14] that blends of ethylene-methyl-acrylate (EMA) copolymer and PDMS rubber are miscible throughout the composition range. The miscibility has been inferred to a specific chemical reaction between the pendant vinyl group of the PDMS rubber and the α-H of the ester group of the EMA copolymer. To the best of our knowledge, no work has been reported in the open literature on PDMS rubber and PA12 polymer blends.

In addition to the PA12/PDMS incompatibility, free-radical crosslinking of PDMS by organic peroxide suffers from premature crosslinking at high temperatures, which is called scorching [40], due to a fast decomposition of peroxide at elevated temperatures [41]. This renders the dispersion of PDMS rubber within the PA matrix difficult to obtain due to the fast crosslinking of PDMS that segregates in large elastic phase, that makes the dispersion and compatibilzation quite impossible and one obtains a phase separation and degradation of the PDMS in the form of a macroscopic powder at the beginning of the compounding process.Thus, the control of cross-linking reaction at the mixing step and at higher temperatures cannot be overemphasized. A tricky route to overcome the difficulties is to control and delay the peroxide decomposition kinetics by using peculiar specific species used in controlled radical polymerisation process. In fact, in our previous experimental and modeling studies [41, 42], the effect of 2,2,6,6-

tetramethylpiperidinyloxyl (TEMPO) on the control of the free-radical kinetics of vinyl-PDMS rubber crosslinking initiated by dicumyl peroxide (DCP) at high temperatures was investigated. The results showed that trapped PDMS macro-radicals in the presence of a radical scavenger such as TEMPO can be a novel route for controlling the kinetics of PDMS crosslinking after its adequate dispersion within the PA matrix. Consequently, we decided to add TEMPO in order to make the PDMS crosslinking kinetics compatible with the melting temperature of PA12 (T=180℃) and with the mixing process time to tailor a new TPV with a controlled network morphology of the rubber phase.

Obviously, the complex nature of TPV process requires a fundamental understanding of the mechanisms that govern the chemical reactions in polymeric melt phases and the role of the key process parameters on the final properties of the developed TPV [43, 45]. Additionally, understanding the relationships between morphology and blend composition is therefore quite important to control the final mechanical properties of the tailored TPV [46]. Accordingly, the main objective of the present work is to investigate the state of dispersion/distribution of PDMS rubber particles in PA12 thermoplastic matrix for the development of a new TPV material with controlled structure and morphology.

2. Experimental section

2.1 Materials

Polymers: PA12 homopolymer was used as thermoplastic phase and PDMS of high molar mass (PDMS gum) containing 0.2 mol-% of vinyl groups was used as rubber phase. The molar mass of molecular segment between two consecutive reactive sites, i.e. between two vinyl sites is therefore: $M_0 = 13,000 g.mol^{-1}$. Finally, the terpolymer (*Lotader 3410)* of ethylene (E), butyl acrylate (BA) and maleic anhydride (MAH) was used as compatibilization agent of the PA12/PDMS blend. This terpolymer contains 18% of BA and 3% of MAH as potential functional groups. The main characteristics of these polymers materials are reported in Table 1.

Free-Radical Crosslinking: DCP was used as the free-radical initiator of the crosslinking reaction and the nitroxide 2,2,6,6-tetramethylpiperidinyloxyl (TEMPO) was used as the inhibitor. Both products were purchased from Aldrich Chemicals and used without any further purification. All experiments were carried out with identical concentration of DCP: $[DCP]_0 = 36 \times 10^{-3}$ (mol.L^{-1}). The concentration of TEMPO was calculated in order to have the following molar ratio (r = [TEMPO]/[DCP] = 1.6) [41,42].

Table 1. Some characteristics of the formulation components.

Material	*Trade Name*	*T_m (°C)*	*T_g (°C)*	*$M_n x10^3$ (g.mol^{-1})*	*η_0(180°C) (Pa.s)*	*Density (g.cm^{-3})*	*Supplier*
Silicone rubber	PDMS gum	-42	-123	300	5700	0.98	ABCR
Polyamide PA 12	Rilsan 12	180	39	25	11000	1.01	Arkema
Compatibilizing agent	Lotader 3410	91	-50	290	1720	0.94	Arkema
Hydrophilic Silica	Aerosil A 200					2.2	Degussa Corp.

2.2. Compounding Process

The blends made of polymers, Lotader and silica nanoparticles, were prepared using a Haake Plasticorder fitted out with an internal mixer (Haake Rheomix R600 of 50 cm^3) fitted with two contra-rotating rotors. The mixing chamber can be regulated in temperature and the rotor speed can be well controlled. The thermocouple located in the mixing chamber indicates the temperature of the molten blend. Consequently, the variation of both the torque and the melt temperature during the TPV processing can be monitored in real time during mixing.

The following processing conditions were used: Polyamide 12 (or filled PA12 with Silica) was kept molten for 3 min in the internal batch mixer at 180℃ and 85 rpm. PDMS and Lotader were then added and mixed. The Lotader concentration was varied from 0 to 6.-wt%. For the reactive blends (with DCP and TEMPO), the PDMS was mixed at room temperature with the initiator and the inhibitor before its addition to the molten PA12. The blend was then removed from the chamber and the samples were then compression molded into 1.5 mm-thick sheets for 3 min at 200℃ and then left to cool to room temperature. All samples were stored at room temperature prior to testing. The same operating conditions were also used for the new tailored PA12/PDMS (40/60 wt.-%) TPV. Table 2 sums up the seven most relevant blends which have been studied in this work.

2.3. Morphology

The morphology of the blends was first observed using a Hitachi S800 Scanning Electron Microscope (SEM). The samples were cryo-fractured in liquid nitrogen to avoid any plastic deformation and morphology alteration. The PDMS phase was selectively extracted in solvent for 7 days at room temperature. The fractured surfaces were then sputter-coated with thin gold conductive layer. The morphology was also examined by transmission electron microscopy (TEM) using a Philips CM120 microscope. Samples, taken in triplicate throughout the whole material, were ultra-microtomed into 50-100 nm thin films at -110℃ using a crystal blade to ensur e that no phase deformation occurred (as these sample preparations were realised below both the PA12 and PDMS glass transition temperatures).

The droplet size was determined by using digital image analysis. The radius of each droplet (R_i) was calculated from the corresponding area (A_i) taking approximately 100 particles for each analyzed sample. The 3D average particle size was obtained by performing the Schwartze-Saltikov correction method [47]. The correction was done by first dividing the particle size into 15 linear size ranges and by characterizing each size

Table 2. Blend designations and compositions.

Blend	PA12 Wt-.%	PDMS Wt-.%	Lotader wt-.%	Silica wt-.%	*r* = ([TEMPO] /[DCP])	Preparation
1	80	20	0	0	0	Virgin blend
2	80	20	0	6	0	Non reactive blend of PA12 (pre-mixing with 6 wt-.% of Silica) and PDMS
3	80	20	3	0	0	Non reactive blend of PA12 and PDMS (pre-mixing with 3 wt-.% of Lotader)
4	80	20	3	6	0	Non reactive blend of PA12 (pre-mixing with 6 wt-.% of Silica) and PDMS (pre-mixing with 3 wt-.% of Lotader)
5	80	20	3	6	1.6	Reactive blend of PA12 (pre-mixing with 6 wt-.% of Silica) and PDMS (pre-mixing with 3 wt-.% of Lotader and r=1.6 of [TEMPO]/[DCP] molar ratio)
6	40	60	6	10	0	Reactive blend of PA12 (pre-mixing with 10 wt-.% of Silica) and PDMS (pre-mixing with 6 wt-.% of Lotader and 1wt-.% of DCP)
7	40	60	6	10	1.6	Reactive blend of PA12 (pre-mixing with 10 wt-.% of Silica) and PDMS (pre-mixing with 6 wt-.% of Lotader and r=1.6 of [TEMPO]/[DCP] molar ratio)

range with midpoint of the range. The particle size was then multiplied by a matrix of coefficients resulting from a set of equations to get the real particle size distribution in three dimensions. The number average radius (R_n) and the volume average radius (R_v) were calculated based on the real particle size distribution by Equ 1 and 2, respectively:

$$R_n = \frac{\sum_i (N_v)_i R_i}{\sum_i (N_v)_i} \quad (1)$$

$$R_v = \frac{\sum_i (N_v)_i R_i^4}{\sum_i (N_v)_i R_i^3} \quad (2)$$

with $(N_v)_i$ is the number of particles having radius R_i. Finally, the size polydispersity d was characterized by $d = R_v/R_n$.

3. Results and discussion

3.1 Nonreactive Blends

Thermoplastic vulcanizates are complex systems that, when formulated and processed correctly, result in materials that show significant processing advantages over thermoset rubber. The first key requirement that has been identified in the preparation of the new silicone-based TPV is that PA12/PDMS blend should be compatibilized. Furthermore, the morphology shown in Figure 1 and 2a, clearly shows that the PDMS disperses coarsely in the PA12 phase. The volume droplet radius of the PDMS particles is about 16.5 μm (see Table 3). From a qualitative point of view, samples 1 and 2 (7 and 10 min of mixing) showed PDMS drops dispersed in PA12 matrix. According to the compositions of these blends, this trend is in total agreement with all semi empirical models predicting the morphology of two immiscible polymers blends [48]. For longer times of mixing (15 and 25 min of mixing, after the torque stabilization), the morphology is characterized by a mixture of larger droplets and domains with irregular shapes due to coalescence of the PDMS particles.

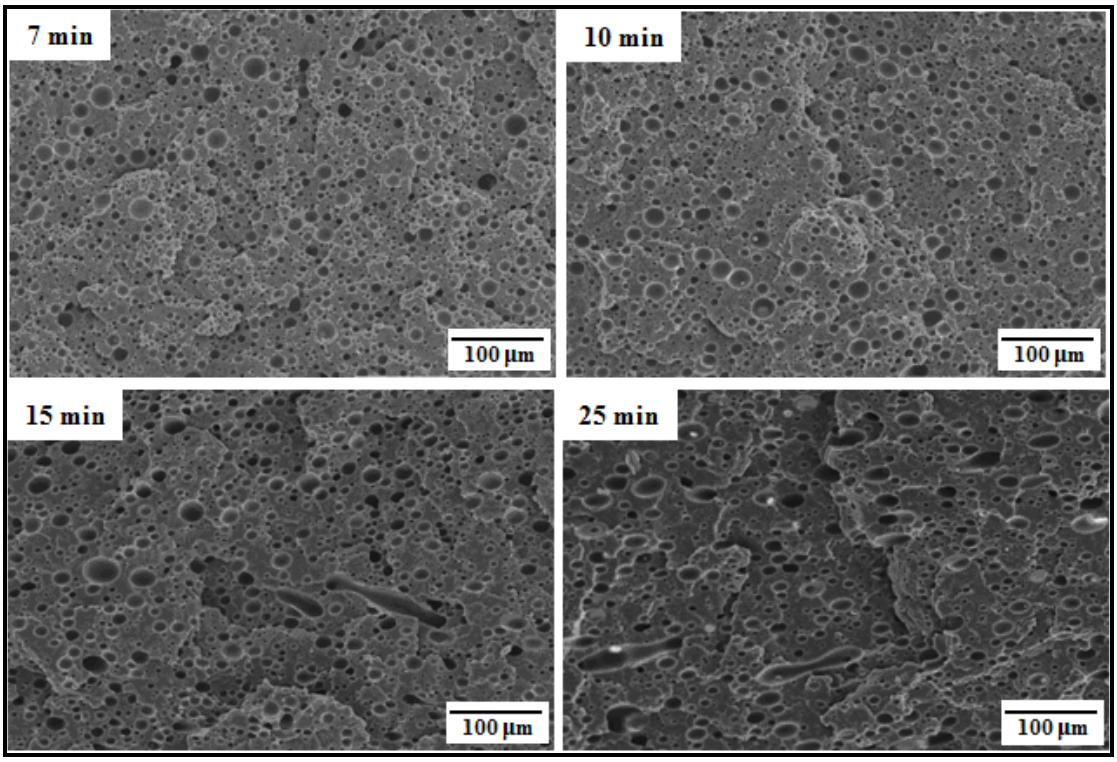


Figure 1. Change of the two-phase blend morphology versus times of mixing for the Blend 1 (PA12/PDMS: 80/20) mixed at T =180℃ and 85 rpm.

Table 3. Average radius (R_n and R_v) and size polydispersity (d) of PDMS droplets in PA12 matrix.

PA12/PDMS (80/20 wt.-%)	R_n (µm)	R_v (µm)	d
Blend 1 (Fig. 2a)	8	16.5	2
Blend 2 (Fig. 2b)	7	15	2.1
Blend 3 (Fig. 2c)	7.5	16	2.1
Blend 4 (Fig. 2d)	4.5	5.5	1.2
Blend 5 (Fig. 4)	0.45	0.6	1.3

Another interesting observation is that addition of silica nanoparticles or Lotader separately does not affect the blend morphology, with an average PDMS particles size of about 15 µm similar to the virgin blend mixed under the same conditions (see Table 3). However, when both silica nanoparticles and Lotader are added altogether in the non reactive PA12 and PDMS phases, respectively, the coalescence is inhibited and the average particle size was divided by approximately a factor 3, shifting from 15 to 16 µm to 5.5 µm with a narrower size distribution (see Table 2). Obviously, only the combined addition of silica with the terpolymer is at the origin of this fine morphology. In this first part, the objective was to investigate how the presence and the localization of silica and Lotader in this biphasic blend influence the morphology development. Thereafter, we use this novel composition to develop a new PA12/PDMS-based TPV with controlled morphology.

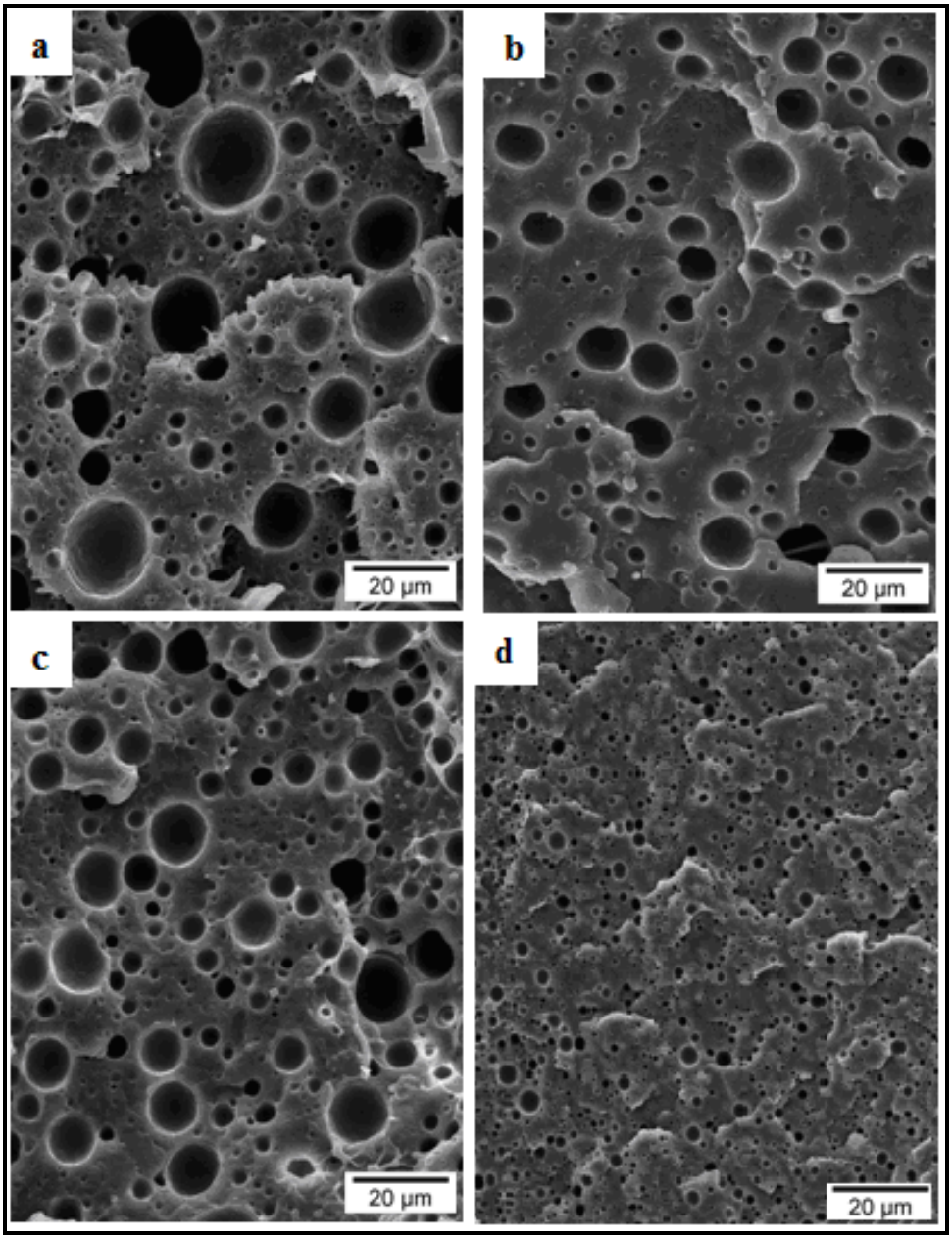


Figure 2. SEM micrographs of the cryofractured surfaces of the non-reactive blends (PA12/PDMS: 80/20) mixed at T =180℃ and 85 rpm. a) Blend 1, b) Blend 2, c) Blend 3, d) Blend 4. See Table 2.

3.2 PA12/PDMS Reactive Blends: Towards TPVs

Keeping in mind that the new TPV is obtained via a dynamic vulcanization process, the selective cross-linking of the PDMS rubber phase must be achieved only after a well-mixed and compatibilized PA12/PDMS blend with high rubber content. In fact, the reactive mixture cannot be processed without adding a crosslinking inhibitor. Actually, the radical crosslinking kinetics of the PDMS phase at high temperature (T=180℃) is faster than the PDMS/PA blending kinetics. In our previous experimental and modeling work [41,42] the effect of TEMPO nitroxide for the control of the free-radical kinetics of vinyl-PDMS rubber crosslinking initiated by DCP at high temperatures was investigated. The results revealed that in presence of inhibitor molecules like TEMPO nitroxide, the PDMS macro-radicals are rapidly trapped by a grafting reaction before they are able to form crosslinks.

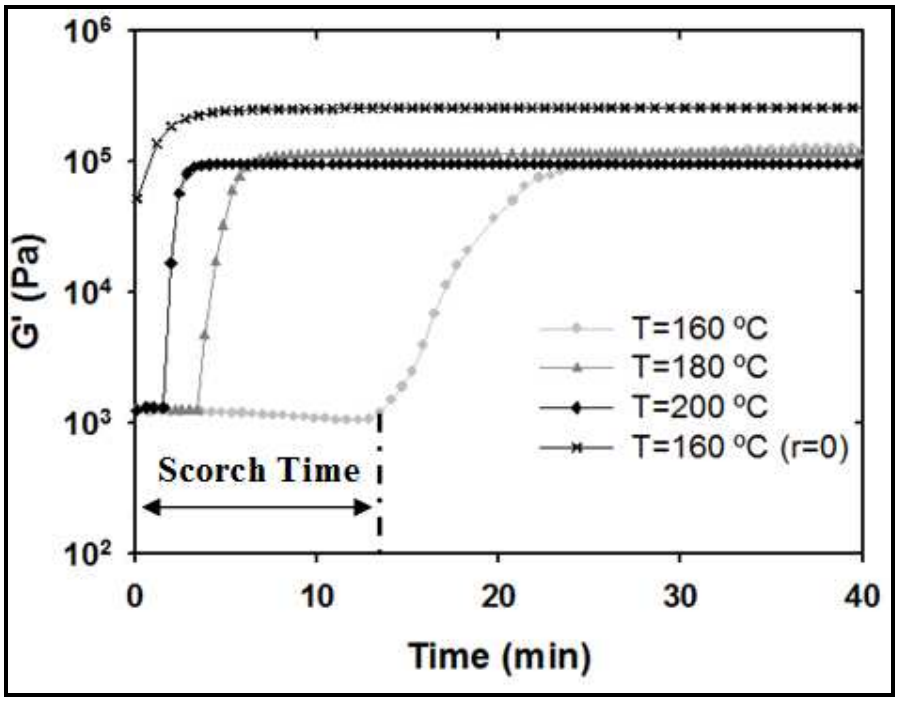


Figure 3. Temperature dependence (T = 160, 180, and 200 ℃) of the PDMS cross-linking reaction: Variation of the storage modulus versus time for r = [TEMPO]/[DCP] = 1.6 and r = 0.

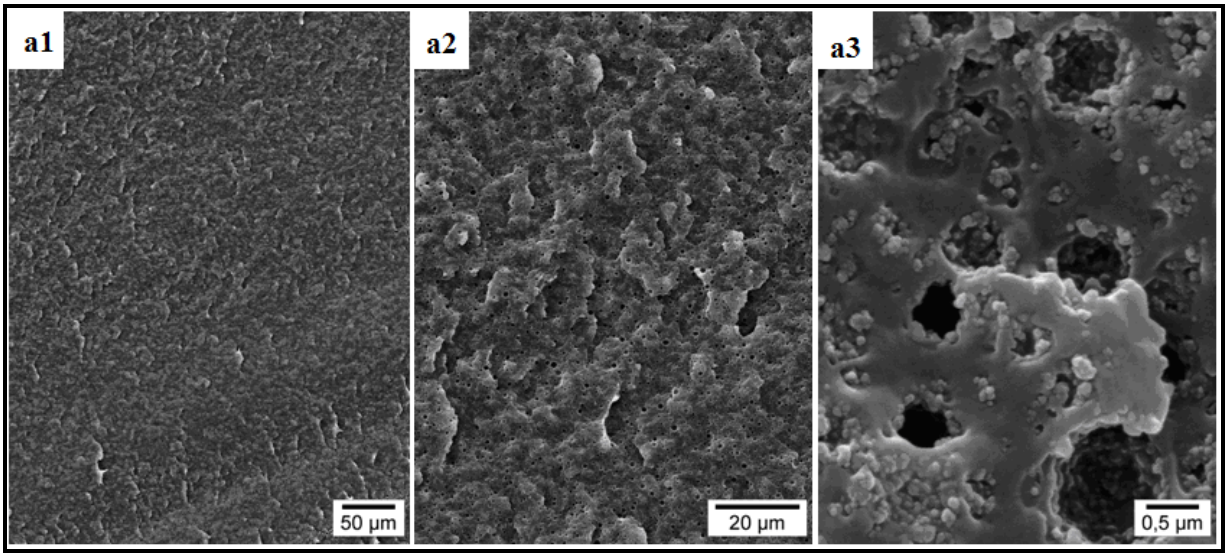
According to a free radical crosslinking mechanism [41], primary and secondary alkoxyamines (-C-O-N-) was formed between the nitroxyl and carbon-centered radicals (inactive PDMS macro-radical). Furthermore, polymeric radicals are rapidly trapped by a grafting reaction with TEMPO before they are able to form crosslinks by recombination. As a result, a remarkably scorch delay and crosslinking density control have been found with varying the molar ratio [TEMPO]/[DCP] in the range r =0 to 2.4.

From a qualitative point of view, Figure 3 (r=1.6 for illustrative example) shows that the cross-linking process is delayed by few minutes at high temperatures. The addition of TEMPO results in an increase of the scorch time from 0 min for r = 0 (Tempo free) [42] to 13 min at 160℃, 3.4 min at 180℃ and to 1.5 min at 200℃ for r = 1.6. Moreover, Figure 3 shows that the steady-state value of the complex shear modulus (G') does not seem to depend on the temperature (r=1.6). Therefore, the temperature can be considered to have not effect on the final cross-linking density in presence of the inhibitor. The addition of TEMPO to the PA12/PDMS reactive blend (at 180℃) favors the mixing and the compatibilization of the blend during the inhibition step (scorch delay). Thereafter, cross-linking of the PDMS can occur under intensive blend mixing (curing process). The concentrations of the inhibitor (TEMPO) and the crosslinking agents (DCP) added in the reactive mixtures were optimized according to our previous works (r=[TEMPO]/[DCP]=1.6) [41,42].

Subsequently, we used this strategy for the PA12/PDMS reactive blend. Figure 4 shows that the reactive blend is characterized by a fine morphology with crosslinked PDMS rubber particles dispersed in the PA12 matrix. SEM and TEM images (Figure 4.a, b, respectively) show a core-shell morphology, with a PDMS dark core phase (extracted phase) encapsulated by the silica nanoparticles (shell). SEM micrographs (Figure 4.a)) show that the sharp interface between PA12 and PDMS has been replaced by a thick PA12/Silica/PDMS interphase of about hundred of nanometers in dimensions. Interestingly, adding silica nanoparticles and Lotader in PA12 and PDMS phases respectively, lead to a drastic reduction in R_v of the PDMS particles to about 0.6 µm

(Table 3). This occurs only by the combined addition of silica and Lotader in the present reactive system.

a) SEM micrographs



b) TEM micrographs

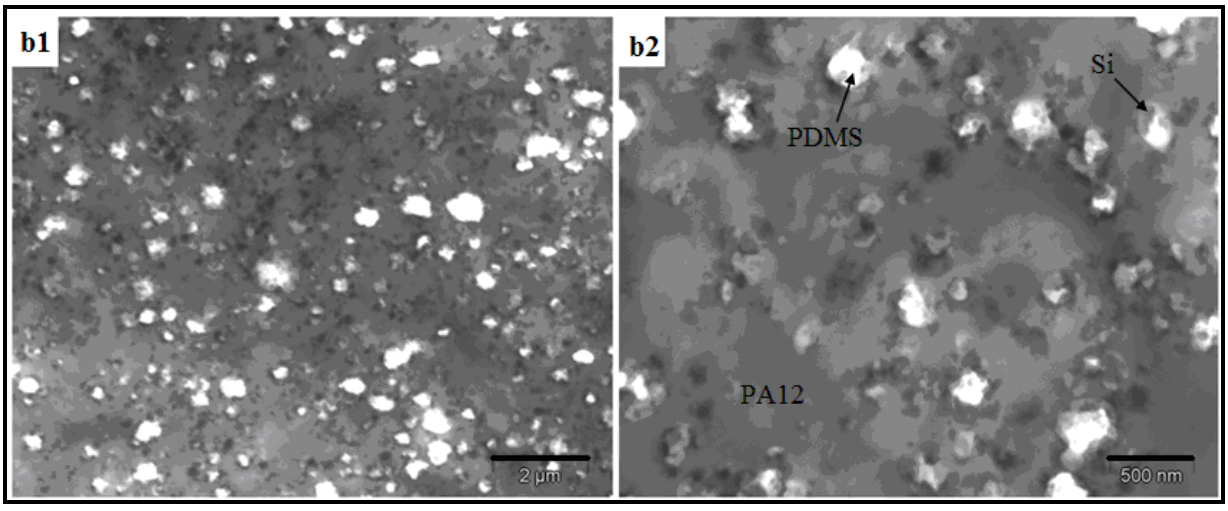


Figure 4. Morphology of the Blend 5 mixed and sheared at T =180℃ and 85 rpm.
a) SEM micrographs, b) TEM micrographs.

To understand the effects of Lotader and silica nanoparticles on this PA12/PDMS reactive blend compatibilization, we studied each system mechanism separately.

3.2.1 Role of the Silica Nanoparticles: Wetting Coefficient Analysis

At equilibrium, the localization of the silica particles is governed by thermodynamics. Silica particles can be distributed non-homogeneously and two situations are to be distinguished: (i) the particles are distributed mainly and homogeneously in one of the two phases and (ii) the particles are confined at the interface between the two polymers. This distribution can be predicted qualitatively by comparing surface tension of the three components. Difference between interfacial tensions imposes the place where the silica will be localized after stopping the mixing. According to Young's equation, it is possible to find the equilibrium position of the filler by evaluating the wetting coefficient ω_1 [49], defined as follows:

$$\omega_1 = \frac{\gamma_{Si-2} - \gamma_{Si-1}}{\gamma_{12}} \quad (3)$$

Where γ_{Si-i} is the interfacial tension between the silica particle and the polymer *i* and γ_{12} is the interfacial tension between the two polymers. When $\omega_1 > 1$, the silica is present only in polymer 1. For value of $\omega_1 < -1$, the particles are only found in polymer 2. For other values of ω_1, the silica is concentrated at the interface between the two polymers.

The interfacial tension can be evaluated from the surface tensions of the components. Two main approaches can be used depending on the type of surfaces: the harmonic mean or well-known the Wu equation, and the geometric mean or well-known the Owens and Wendt [50] equation. The Wu equation (Equation 4) is valid between low-energy materials and the Owens and Wendt equation (Equation 5) is valid between a low-energy material and a high energy material. The Wu equation:

$$\gamma_{12} = \gamma_1 + \gamma_2 - 4\left(\frac{\gamma_1^d \gamma_2^d}{\gamma_1^d + \gamma_2^d} + \frac{\gamma_1^p \gamma_2^p}{\gamma_1^p + \gamma_2^p}\right) \quad (4)$$

And the Owens and Wendt equation:

$$\gamma_{12} = \gamma_1 + \gamma_2 - 2\sqrt{\gamma_1^d \gamma_2^d} - 2\sqrt{\gamma_1^p \gamma_2^p} \quad (5)$$

Where the exponents *d* and *p* stand for the dispersive and the polar contributions, respectively. The blends have been prepared at 180°C. As surface tension is temperature dependent, a way to estimate γ at other temperature is the application of the relationship suggested by Guggenheim [51]:

$$\gamma = \gamma(0)(1 - T / T_{cr})^{11/9} \quad (6)$$

The values of *γ(0)* and T_{cr} have been taken from literature. According to Equation 6, the surface tension decreases with temperature. The calculation of the interfacial tension requires the values of the polar and the dispersive contributions to the surface tension. These are commonly given in the literature at room temperature. Assuming that the temperature dependence of each contribution follows the same law as for the surface tension; it is then possible to use Equation 6 to estimate γ^d and γ^p at the temperature of mixing (T=180℃). For silica particles, the surface tension was estimated at 180℃ using the rate dγ/dT which is assumed to be constant in the interval of the used temperature [29].

The values of the surface energy of polymers in the melt state have been extrapolated from literature values at 20℃ as detailed below [52,53] and are summarized in Table 4, with the simplifying hypothesis that the polarity is independent of temperature. The computed interfacial tensions at 180 ℃ were evaluated based on the Equation (4 and 5) and given in Table 5.

Table 4. Surface tension data of the components of the blends at 20℃.

Material	*Dispersive surface Energy* γ_d *(mN.m^{-1})*	*Polar surface Energy* γ_p *(mN.m^{-1})*	*Total surface Energy* γ *(mN.m^{-1})*	*γ(0) (mN.m^{-1})*	*Temperature coefficient dγ/dT (mN.mK^{-1})*
PA12	35.9	4.9	40.8	59.8	-0.065
PDMS	19	0.8	19.8	33.9	-0.048
Hydrophilic silica A200	29.4	50.6	80	109.3	-0.1

According to results shown in Table 5, the PA12/PDMS blend has a high interfacial tension, which is responsible for the immiscibility of the components.

Table 5. Interfacial tensions and wetting coefficient at 180 ℃ calculated using harmonic and geometric mean equations.

Material	*Interfacial tension according to harmonic mean equation (mN.m^{-1})*	*Interfacial tension according to geometric mean equation (mN.m^{-1})*
PA12/PDMS	8.4	4.6
PA12/A200	41.4	25.9
PDMS/A200	48.4	38.8
ω_{PDMS}	-0.83	-0.67

For this PA12/PDMS blend and at the temperature T = 180℃, we then found ω_{PDMS} value between -1 and 1. According to this result, the silica should be located at the

interface between PA12 and PDMS and in the PA12 matrix at the thermodynamic equilibrium.

These results are in agreement with the morphologies showed in Figure 4. Actually, image analysis of the micrographs in Figure 4 proves that the hydrophilic silica is located in the PA12 phase and at the interface between PA12 and PDMS phases (interphase thickness 100-200 nm). In addition, the presence of silica nanoparticles reduces significantly the coalescence phenomena and the PDMS domain size is decreased by approximately ten times (see micrographs in Figure 2b and 4b). The existence of the silica layer interphase stabilizes the blend morphology due to inhibition coalescence by the solid shell surrounding the individual PDMS drops. This assumption agrees with the work of Vignati and Piazza [54], Vermant et al. [55] and Sinha-Ray et al. [22-28] who argued that leaving steric hindrance or surface rheology effect is the most probable mechanism of morphology stabilization.

3.2.2 Role of the Lotader copolymer

A proposed chemical mechanism has been reported in Figure 5. Maleic anhydride from Lotader reacts with the amine (NH_2) end group of PA12 [56] forming PA12-grafted-Lotader copolymer (STEP 1) and reduces the interfacial tension between PDMS and PA12. On the other hand, the Lotader and the PDMS rubber have been found by Santra et al. [14, 39] to be miscible throughout the composition range. Indeed, the formed PA12-grafted-Lotader preferentially situated between the PA12 and the PDMS phase, reacts with the PDMS (STEP 2) and reduces the interfacial tension in the polymer blend.

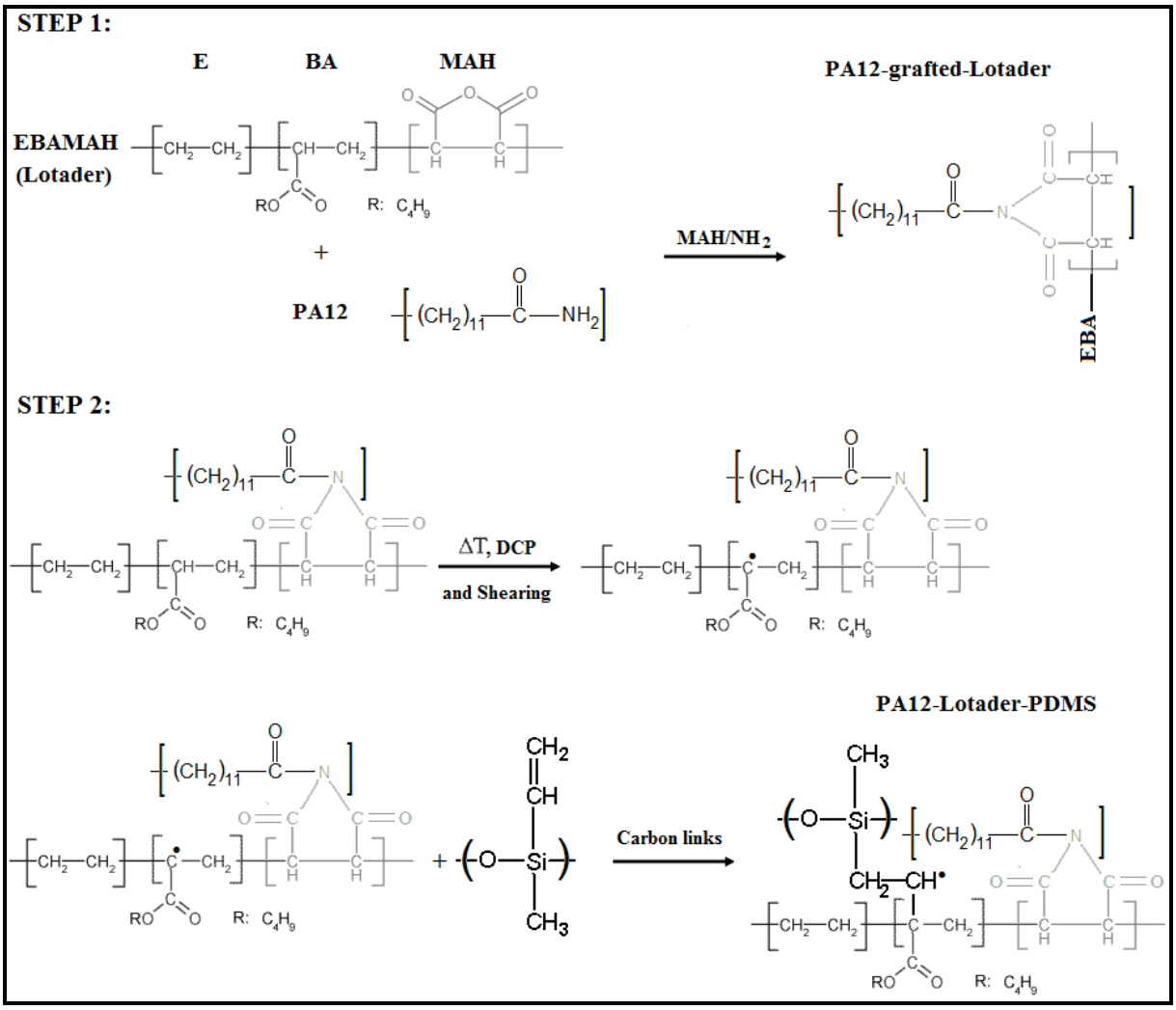


Figure 5. The reaction scheme for the Lotader effect in PA12/PDMS blends compatibilization.

3.3 Tailoring a new TPV

According to the above studies, the formulation of PA12/PDMS blend containing 60 wt.-% of PDMS rubber have been developed. Figure 6 shows the variation of the torque versus the time of mixing for the new TPV (Blend 7), compared with the reactive formulation without TEMPO (Blend 6). From a qualitative analysis, it is clear that the

curves for Blends 6 and 7 show different behaviours. Without TEMPO, the curve for the blend 6 shows instantaneous increases of the torque after the addition of PDMS to the molten PA12 phase. In fact, the rapid process of PDMS crosslinking at this temperature (T = 180 ℃) leads to a significant elasticity of the PDMS phase before its mixing and compatibilization with the PA12 phase. As a result, the mechanical degradation of the PDMS in the form of a macroscopic powder is observed.

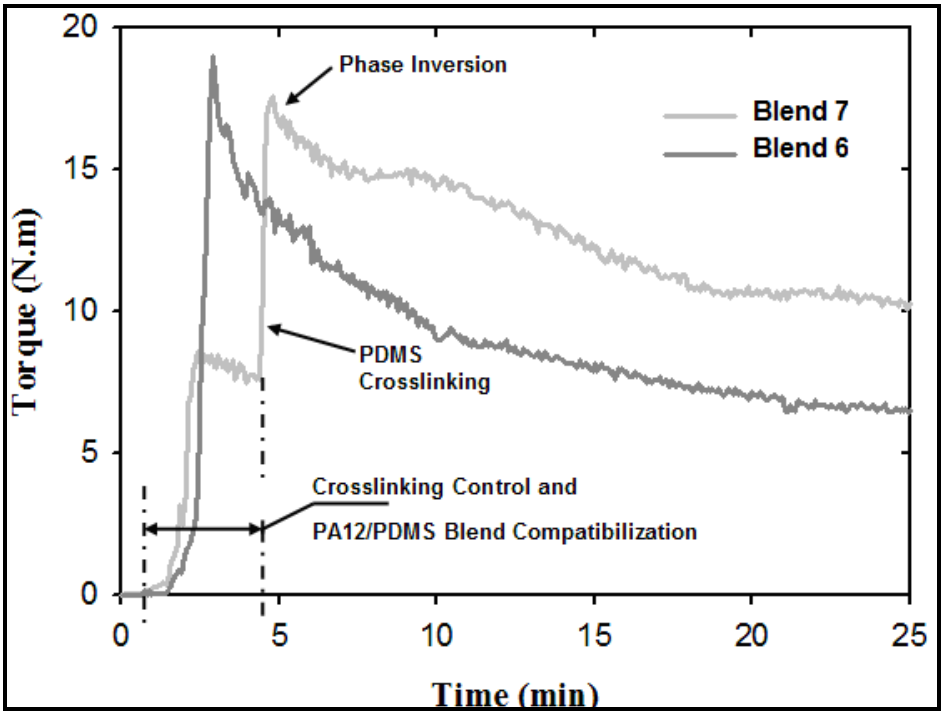


Figure 6. Variation of the torque versus mixing time for Blend 6 and Blend 7 at T=180℃ and 85 rpm.

The addition of TEMPO in the PA12/PDMS leads to a quite different process and consequently a different material. The curve for the blend 7 shows that the crosslinking of the PDMS phase is delayed by few minutes (≈3 min). Interestingly, this delay time is close to the scorch time obtained for r = 1.6 at 180 ℃ in our previous work [41]. Consequently, the addition of TEMPO to the PA12/PDMS reactive blend (at 180℃) ensures the good mixing and compatibilization of the blend during the scorch period prior the crosslinking reaction.

It is also worth to notice that the torque curve passes by an maximum, generally associated with the phase inversion in the case of the TPV formulation [46]. This is in fact induced by the increase in the elasticity of the PDMS major phase, which considerably changes the blend viscoelasticity. Such phase inversion corresponds to the moment when the two phases interpenetrate to form a co-continuous morphology [43]. Finally, a stable co-continuous morphology was obtained for the new TPV as shown in Figure 7.

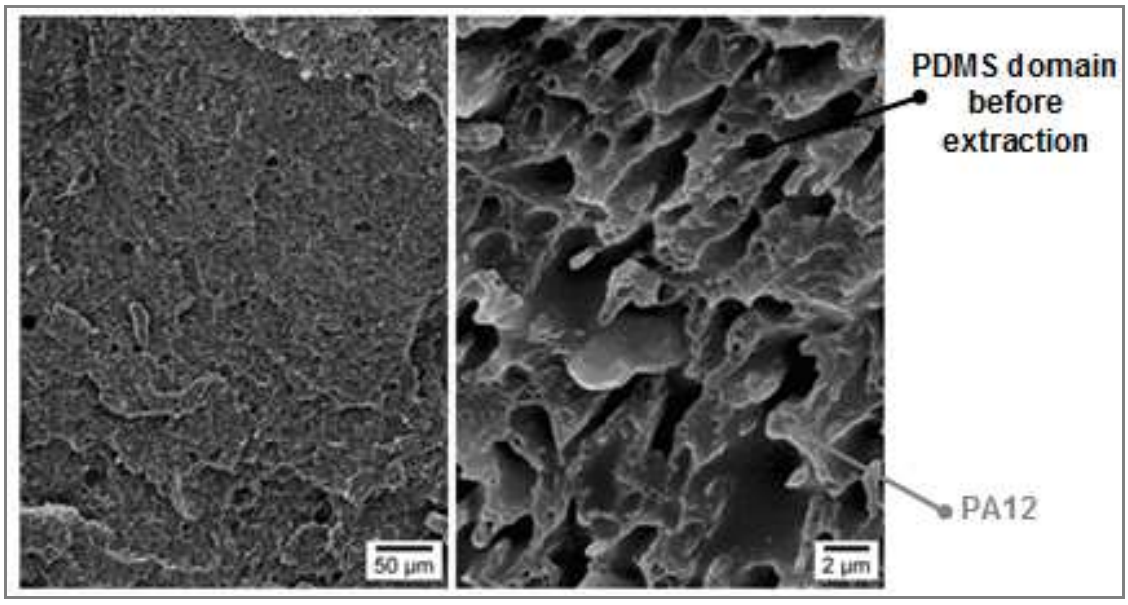


Figure 7. Morphology of the new TPV tailoring in the internal mixer at T=180℃ and 85 rpm, correspond to the Blend 7 in Figure 6. SEM micrographs.

The general mechanical properties obtained for this new TPV are encouraging. For example, the elongation at break for such TPV is close to 100%. Furthermore, the mechanical properties could be improved in a second step with optimization of the mixing process conditions, the extent of crosslinking and the time of mixing.

4. Conclusion

In this study a new TPV based on PDMS and PA12 blend (Super-TPV) compatiblized by Lotader and silica nanoparticles, was prepared by dynamic vulcanization. First, we investigated non-reactive and reactive blends of PA12 (80 wt.-%) as the matrix component and PDMS (20 wt.-%) as the dispersed phase. In the reactive case, PDMS was crosslinked by DCP. Interestingly, the addition of TEMPO to the PA12/PDMS reactive blend (at 180 ℃) delayed the crosslinking reaction for about 3 min, period of time during which the mixing and the compatibilzation processes may be completd before the crosslinking of the PDMS phase. Therefore, an in situ chemical reaction at the interface reduced the size of the PDMS dispersed drops. Furthermore, reaction between maleic anhydride and amine end group occured readily during mixing of the Lotader and PA12. Therefore, and as expected the in situ-formed PA12-grafted-Lotader copolymer plays a role in reducing the PA12/PDMS interfacial tension. However, the reduction in the dispersed phase particles size cannot be explained only by this grafting reaction. The fine morphology comes from the miscibility between Lotader and PDMS, combined with the morphology stabilization by the silica nanoparticles. Typically, the volume droplet radius significantly decreases from 16.5 µm (virgin blend) to nearly 0.6 µm for the PA12/PDMS filled reactive blends (80-20 wt.-%).

Actually, it is shown that addition of hydrophilic silica nanoparticles prevents the coalescence of the PDMS droplets imparting the blend with a core-shell morphology containing PDMS droplets (core) encapsulated by silica nanoparticles (shell) in PA12 matrix. Depending on the mixing strategy, the Silica nanoparticles are either at least partially located at the interface between the two polymers and in the PA12 phase. The localization of the silica nanoparticles is determined by the interactions between the filler and the polymers. In addition, SEM and TEM micrographs analysis proved that the hydrophilic silica is located at the interface between PA12 and PDMS phases. For the latter case, electronic microscopy micrographs showed that the interface between PA12 and PDMS has been changed by thick PA12/Silica/PDMS interphases of about hundred

of nanometers. Finally, in the case of TPV formulation based on 60 wt.-% PDMS, the addition of TEMPO led to a stable and fine co-continuous morphology.

References

[1] Drobny, J. G. “Handbook of Thermoplastic Elastomers” 2007, chap. 6, p. 179.

[2] Oderkerk, J.; Groeninckx, G. Polymer 2002, 43 (8), 2219-2228

[3] Holden, G; Kricheldrof, H. R.; Quirk, R. P. “Thermoplastic Elastomers” Hanser 2004, chap. 9, p. 217.

[4] White, J.; De, S. K.; Naskar, K. “Rubber Technologist’s Handbook Volume 2” 2009, chap. 7, p. 219.

[5] Bousmina, M.; Muller, R. Rheol. Acta. 1996, 35, 369-381.

[6] Abdou-Sabet, S.; Puydak, R. C.; Rader, C.P. “Rubber Chemistry and Technology” 1996, 69 (3).

[7] Cail, B. J.; Demarco, R. D. “New Heat and Oil Resistant (TPV) for Demanding Under Hood Applications” Zeon Chemicals 2003, (01-0942).

[8] Chorovath, I.; and al. Dow Corning Corp. PCT 2001, WO 01/72903, A2.

[9] Leaversuch, R. “Super-TPVs The New Challenge to Rubber” 2009, www.PTOnline.com

[10] Dickerhoof, J. E.; Cail, B. J; Harber, S. C. “150°C Heat- and Oil-Resistant TPVs” Zeon Chemicals 2004, Technical Product Data Sheet.

[11] Chang, C. L.; Don, T. M.; Lee, H. S. J.; Sha, Y. O. Polym. Degrad. 2004, 85, 769-777.

[12] Hardan, B.; Torkelson, A. “Encyclopedia of Polymer Science and Engineering” 1989, 15, p. 204.

[13] Mark, J. E.; Allcock, H. R.; Wesr, R. “Inorganic Polymers, Second Edition” 2005, Chap.4, p. 172.

[14] Santra, R. N.; Mukunda, P. G.; Nando, G. B.; Chaki, T. K. Thermochimica Acta. 1993, 219, 283-292.

[15] ARKEMA, “Market Research Showed That Rilsan PA11 and Rilsan PA12 Are Highly Valued By major car OEMs”, www.arkema.com.

[16] Munoz, MA. P.; Werlang, M. M.; Yoshida, I. V. P.; Mauler, R. S. J. Appl. Polym. Sci. 2002, 83, 2347-2354.

[17] McManus, N. T.; Zhu, S. H.; Tzoganakis, C.; Penlidis, A. J. Appl. Polym. Sci. 2006, 101, 4230-4237.

[18] Xing, P.; Bousmina, M.; Rodrigue, D.; Kamal, M. R. Macromolecules 2000, 33, 8020-8034.

[19] Sundararaj, U.; Macosko, C. W. Macromolecules 1996, 28, 2647-2657.

[20] Robeson, L. M. “Polymer blends: A comprehensive review” 2007, Chap.3, p. 65.

[21] Utracki, L. A. Polym. Eng. And Sci. 1983, 23, 602-609.

[22] Ray, S. S; Pouliot S, Bousmina M, Utracki LA. Polymer 2004, 45, 8403-8413.

[23] Ray, S. S; Bousmina M. Macromol Rapid Commun 2005, 26, 1639-1646.

[24] Ray, S. S; Bousmina M, Maazouz A. Polym Eng Sci 2006, 46, 1121-1129.

[25] El-Mabrouk, K.; Bousmina M. J. Nanoscience and Nanotechnology 2006, 6, 472-282.

[26] Ray, S. S; Bousmina M. Macromol Rapid Commun 2005, 26, 450-455.

[27] EL-Mabrouk, K.; Vaudreuil S.; Zeghloul A.; Bousmina M. J. Nanoscience and Nanotechnology 2008, 8, 1895-1900.

[28] Ray, S. S; Bandyopadhyay J.; Bousmina M. Macromol. Mat & Eng. 2007, 292, 729-747

[29] Elias, L.; Fenouillot, F.; Majesté, J. C.; Alcouffe, P.; Cassagnau, P. Polymer 2007, (48), 6029-6040.

[30] Martin, G.; Barres, C.; Sonntag, P.; Garois, N.; Cassagnau, P. Mat. Chem. And Phys. 2009, 113, 889-898.

[31] Maiti, S.; De, S.; Bhowmick, A. K. Rubber. Chem. Technol. 1992, 65(2), 293-302.

[32] Thareja, P.; Velankar, S. Rheol. Acta. 2007, 46, 405-412.

[33] Elias, L.; Fenouillot, F.; Majesté, J. C.; Alcouffe, P.; Cassagnau, P. Polymer 2008, (49), 4378-4385.

[34] Fenouillot, F.; Cassagnau, P.; Majesté, J.C. Polymer 2009, 50, 1333-1350.

[35] Kole, S.; Bhattacharya, A. K.; Tripahathy, D. K.; Bhowmick, A. K. J. Appl. Polym. Sci. 1993, 48, 529.

[36] Luzinov, I.; Xi, K.; Pagnoulle, C.; Huynh-Ba, G.; Jérôme, R. Polymer 1999, 40, 2511-2520.

[37] Sierra, C. A.; Galan, C.; Fatou, J. G.; Parellada, M. D.; Barrio, J. A. Polymer 1997, 38, 4325.

[38] Maric, M.; Ashurov, N.; Macosko, C. W. Polym. Eng. And Sci. 2001, 41, 4, 631-642.

[39] Santra, R. N.; Samantaray, B. K.; Bhowmick, A. K.; Nando, G. B. J. Appl. Polym. Sci. 1993, 49 (7), 1145-1158.

[40] Dorn, M. Adv. Polym. Technol. 1985, 5, 87-91.

[41] Mani, S.; Cassagnau, P.; Bousmina, M.; Chaumont, P. Polymer 2010, 51 (17), 3918-3925.

[42] Mani, S.; Cassagnau, P.; Bousmina, M.; Chaumont, P. Macromolecules 2009, 42, 8460-8467.

[43] Joubert, C.; Cassagnau, P.; Michel, A.; Choplin. L. Polym. Eng. And Sci. 2002, 42 (11), 2, 2222-2233.

[44] Machado, A. V.; Duin, M., V. Polymer 2005, 46, 6575-6586.

[45] Harrats, C.; Thomas, S.; Groeninckx, G. “Micro-and Nanostructured Multiphase Polymer Blend Systems: Phase Morphology And Interfaces” CRC Press 2006, chap. 9, p. 295.

[46] Verbois, A.; Cassagnau, P.; Michel, A.; Guillet, J.; Raveyre, C. Polym. Int. 2004, (53), 523-535.

[47] Saltikov, SA. In: Elias H, editor. Stereology. Proceedings of the second international congress for stereology. New York: Springer-Verlag; 1967, p. 163-173.

[48] Omonov, T. S.; Harrats, C.; Moldenaers, P.; Groenickx, G. Polymer 2007, 48, 5917.

[49] Wu, S. Polymer interface and adhesion 1982, Marcel, New York: Dekker Inc.

[50] Owens, D. K.; Wendt, R. C. J. Appl. Polym. Sci. 1969, 13 (8), 1741-1747.

[51] Guggenheim, E. A. J. Chem. Phys. 1945, 13, 253-261.

[52] www.surface-tension.de/solid-surface-energy.htm.

[53] Bismarck, A.; Kumru, M. E.; Springer, J. Journal of Colloid and Interface Science 1999, 217, 377-387.

[54] Vignati, E.; Piazza, R. Langmuir 2003, 19, 6650-6656.

[55] Vermant, J.; Cioccolo, G.; Golapan Nair, K.; Moldenaers, P. Rheol. Acta. 2004, 43, 529-538.

[56] Majumdar, B.; Keskkula, H.; Paul, D. R. Polymer 1994, 35 (7), 1386-1398.

Summary

Survey of the available literature reveals that free-radical crosslinking of rubbers and/or thermoplastics by organic peroxide suffer from premature crosslinking at high temperatures. High temperatures lead to the faster decomposition of peroxide. Indeed, several solutions have been discussed in literature to prevent scorching. Nevertheless, the control of free-radical crosslinking of the PDMS rubber materials has never been resolved. Consequently, the molecular understanding of the network topology–crosslinking kinetics relationships still remains incompletely understood. This is primarily because conventional rubbers formed by random cross-linking methods have very obscure structure with a broad network strand length distribution and an unknown number of dangling chains.

Therefore, the basic aim of the investigations described in this thesis is to find a novel way to control free-radical crosslinking chemistry and topological parameters of final networks such as the length of the network strands, functionality of cross-links, the amounts of entanglements and dangling chains. Moreover, the PDMS will be crosslinked by Dicumyl peroxide (DCP). The advantage of this free radical crosslinking reaction that it is can be well controlled at the mixing step and at higher temperatures using an appropriate inhibitor. Furthermore, addition of inhibitor to a new biphasic material such as PA12/PDMS blend type TPV (Thermoplastic Vulcanizated) provided the compatibilization in the dynamic process and gives a new material having a controlled structure and morphology.

A general introduction is given in Chapter 1. Various topics and aspects which are relevant for the work described in this thesis are introduced. Free radical crosslinking of polymers and the control at high temperatures of this complex chemical process are reviewed in this chapter. The PDMS rubbers and their typical end-use applications are also touched upon.

The work is primarily focused on the extensive study of the crosslinking control of PDMS rubber at high temperatures. Therefore, the roles of nitroxides such as TEMPO in scorch delay and cross-linking control of free-radicals cross-linking process have been investigated in Chapter 2. A remarkably scorch delay has been found with varying the molar ratio [TEMPO]/[DCP] in the range r=0-2.4. First of all, rheological measurements were carried out in order to determine the linear viscoelastic properties of the PDMS networks. The scorch and gel times, the equilibrium modulus (G_e), and the soluble PDMS chains fraction were found to be a function of the concentration of TEMPO. Furthermore, the characterization of the network features based on the phenomenological model of Langley and Dossin and Graessley provided that the control of the network topology can be achieved by using nitroxide TEMPO. In agreement with rheological measurements, NMR microstructural studies revealed that the cross-linking delayed action in the presence of TEMPO is the result of trapped carbon-centered polymer radicals by nitroxides. As a result, once the TEMPO is totally consumed, the cross-linking can proceed as usual. Furthermore, DSC was used to characterize the effect of TEMPO in cross-linking reaction at the molecular scale. An original result has been shown using this technique by varying the molar ratio [TEMPO]/[DCP]. Correlation between DSC and rheometry experiments proved that the secondary exothermic enthalpy corresponds to the covalent bonds formation between only carbon-centered polymer radicals and thus the network formation. According to this result, we developed an original method to determine the chemical cross-link density in the case of complex cure reaction system which has multiexothermal heat reaction. The predicted chemical cross-link densities are in close agreement with those calculated using the phenomenological model of the viscoelasticity.

The work specified in this thesis is therefore directed to find a proper [TEMPO]/[DCP] ratio for PA12/PDMS biphasic material, in order to maximize the degree of PDMS crosslinking and the scorch delay. For this purpose, in Chapter 3 we introduced a new rheological modelling method developed to predict the variation of complex shear modulus for PDMS network formation under free-radical crosslinking reaction controlled by TEMPO. This new method is based on the relationship between the kinetics of macro-radicals coupling [$R_{cc}(t)$] derived from a fundamental kinetic model and the viscoelastic variation of complex shear modulus ($G'(t)_\omega$ and $G''(t)_\omega$). Owing to the complexity of crosslinking chemistry, a simplified reactions scheme was used to establish the fundamental kinetic model. First of all, a kinetic model was derived in order to predict the crosslinking process including decomposition of peroxide [DCP(t)], active PDMS carbon-centred radicals $[R_p^{\bullet}(t)]_{act}$ creation, inhibition reaction time t_r and the crosslinking bonds formation [$R_{cc}(t)$]. The influence of formulation conditions such as ($[DCP]_0$, [TEMPO]/[DCP] and Temperature) on the crosslinking reaction kinetics and network growth, has been studied at the molecular scale according to this kinetic model. It was observed that the addition of TEMPO nitroxide can boost the initiator efficiency. On the other hand, the Kissinger DSC method was used to calculate the activation energy E_{ac} (87,300 J.mol^{-1}) and the collision frequency factor A_{0c} (2.68 x 10^{10} s^{-1}) for the bimolecular termination reaction rate k_{cc}. Finally, the rheological modelling shows that this new method precisely predicts the time variation of the complex shear modulus at any temperature and [TEMPO]/[DCP] ratio. Although this modelling has been developed for PDMS rubber, it can easily be extended to any rubber crosslinking via radical chemistry in the presence of nitroxide.

Interestingly, addition of TEMPO to the TPV novel composition provided the PA12/PDMS blend compatibilization in the dynamic process and gives a new material having a controlled structure and morphology. A better insight in understanding the blend composition and the morphology development relationships is aimed at in Chapter 4. Furthermore, we investigated non reactive and reactive blends of PA12 (80 wt%) as the matrix component and PDMS (20 wt%) as the dispersed phase. In the reactive case, the PDMS was crosslinked by Dicumyl peroxide (DCP). Interestingly, the

addition of TEMPO to the PA12/PDMS reactive blend (at 180 ℃) delayed the crosslinking reaction for about 3 min and provided to mix and compatibilize the blend during the inhibition phase. Therefore, an in-situ chemical reaction at the interface reduced the volume droplet radius of the PDMS dispersed phase. Furthermore, reaction between Maleic Anhydride and Amine end group occurs readily during mixing of the Lotader and PA12. Therefore, the in situ-formed PA12-grafted-Lotader copolymer played a role in reducing of the PA12/PDMS interfacial tension and increasing the depressiveness of PDMS. Nevertheless, the size reduction of the dispersed phase cannot be explained solely by this grafting reaction. The miscibility between Lotader and PDMS, in addition with the morphology stabilization by the silica nanoparticles, may yield to the fine morphology. Typically, the volume droplet radius significantly decreases from 16.5 µm (virgin blend) to nearly 0.6 µm for the PA12/PDMS filled reactive blends (80-20 wt%). In fact, it is shown that addition of hydrophilic silica nanoparticles suppresses the PDMS droplets coalescence. The blend showed a core-shell morphology containing PDMS droplets (core) encapsulated by silica nanoparticles (shell) in PA12 matrix. Depending on the mixing strategy, the hydrophilic Silica nanoparticles are either at least partially located at the interface between the two polymers and in the PA12 phase. The localization of the silica nanocharges is determined by the interactions between the filler and the polymers. In addition, SEM and TEM micrographs analysis proved that the hydrophilic silica was located at the PA12/PDMS interface. For the latter case, electronic microscopy micrographs showed that the interface between PA12 and PDMS has been changed by PA12/Silica/PDMS interphases of a hundred of nanometers thick. We then concluded that silica nanoparticles act as a rigid layer preventing the coalescence of PDMS droplets. The above studies (containing 20 wt% of PDMS) allowed to optimize the formulation of a reactive blend and to develop the new TPV. The phase inversion seems to take place at a gel content of around 60% wt of PDMS, and a stable co-continuous morphology was obtained for the new TPV based on 60 wt% of PDMS and 40 wt% of PA12. Accordingly, thermoplastic/Rubber blends stabilized by solid particles open interesting technological perspectives.

Finally, while TEMPO has been extensively studied as an initiator for living free radical polymerizations, the use of TEMPO in this thesis to control free radical crosslinking of PDMS rubber and that control of macromolecular architecture to the development of new PA12/PDMS biphasic polymeric materials with controlled structure and morphology has been an original way in TPV tailoring. The findings of this thesis will be an important impact in polymer science from both an academic and an industrial viewpoint. This interest is governed by the need to control the network architecture in order to develop new class of rubbers formulations with a rich variety of topological characteristics improved and/or new mechanical and physical properties.